「理論懇シンポジウム」 2010.12.20-22

# 初代天体・銀河形成論

梅村　雅之

筑波大学　計算科学研究センター

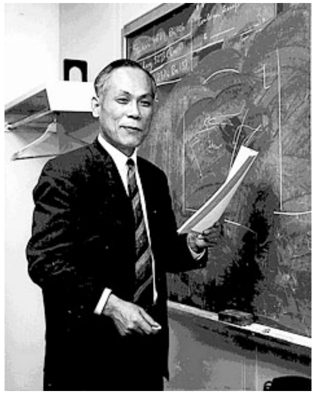

林忠四郎(1920-2010)

坂下志郎(1933-2006)

池内了

## 坂下志郎

- Sakashita, S., Ono, Y., Hayashi, C. 1959, PTP, 21, 315-323
  The Evolution of Massive Stars. I. $M=15.6M_\odot$
- Sakashita, S., Hayashi, C. 1959, PTP, 22, 830-834
  Internal Structure and Evolution of Very Massive Stars $M=46.8M_\odot$
- Sakashita, S., Hayashi, C. 1961, PTP 26, 942-946
  Internal Structure of Very Massive Stars $M=46.8M_\odot$

Sakashita, Hanami, Umemura, 1984, 1985 (Bipolar outflow in SF)

## 池内了

Umemura & Ikeuchi 1984, 1985, 1986a, 1986b, 1987, Ikeuchi & Umemura, 1984
(Galaxy Formation in DM Univ.)

「宇宙流体力学」（坂下 志郎 , 池内 了 (著), 培風館）

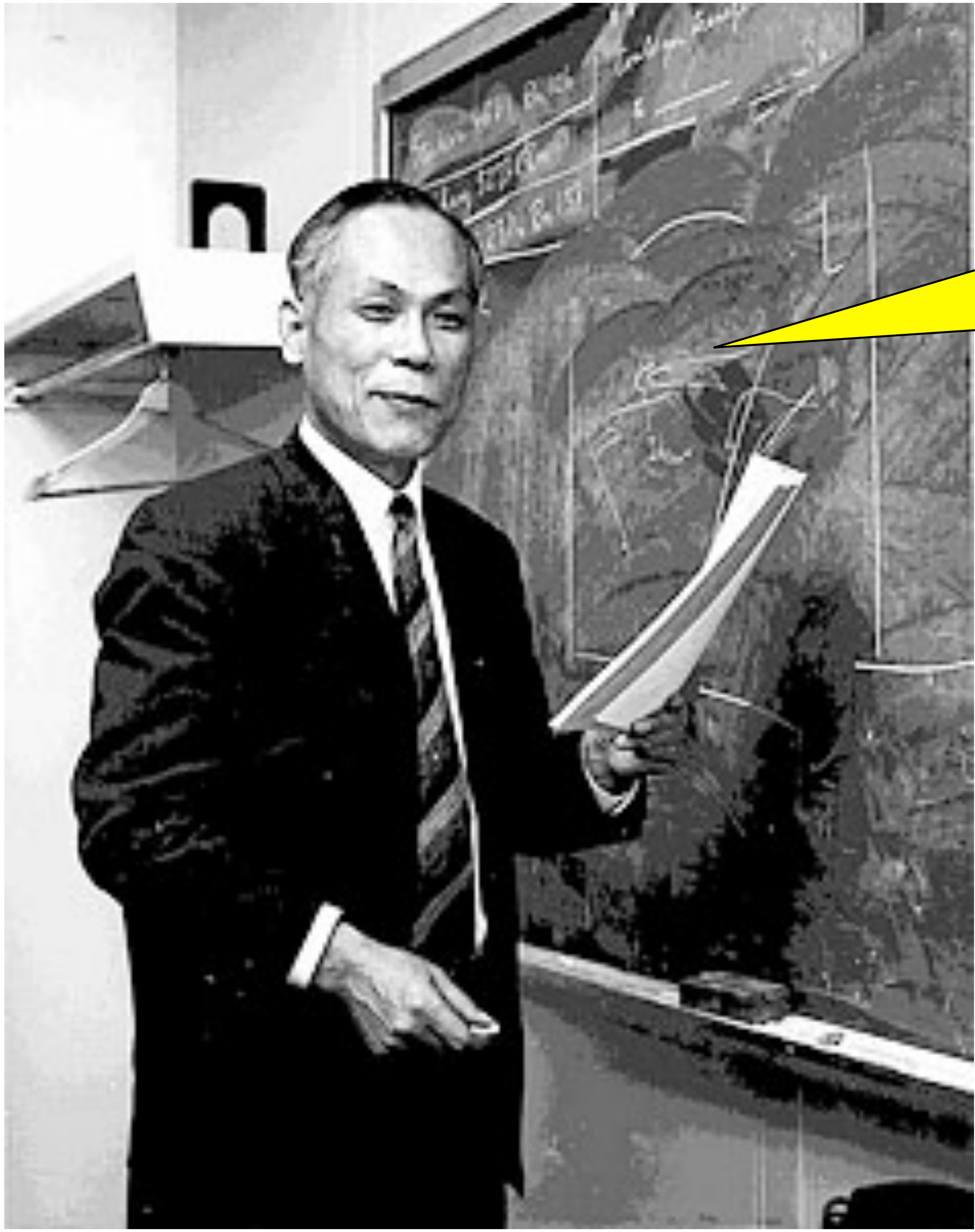

銀河はまだ早い

池内さん談
（1980年代）

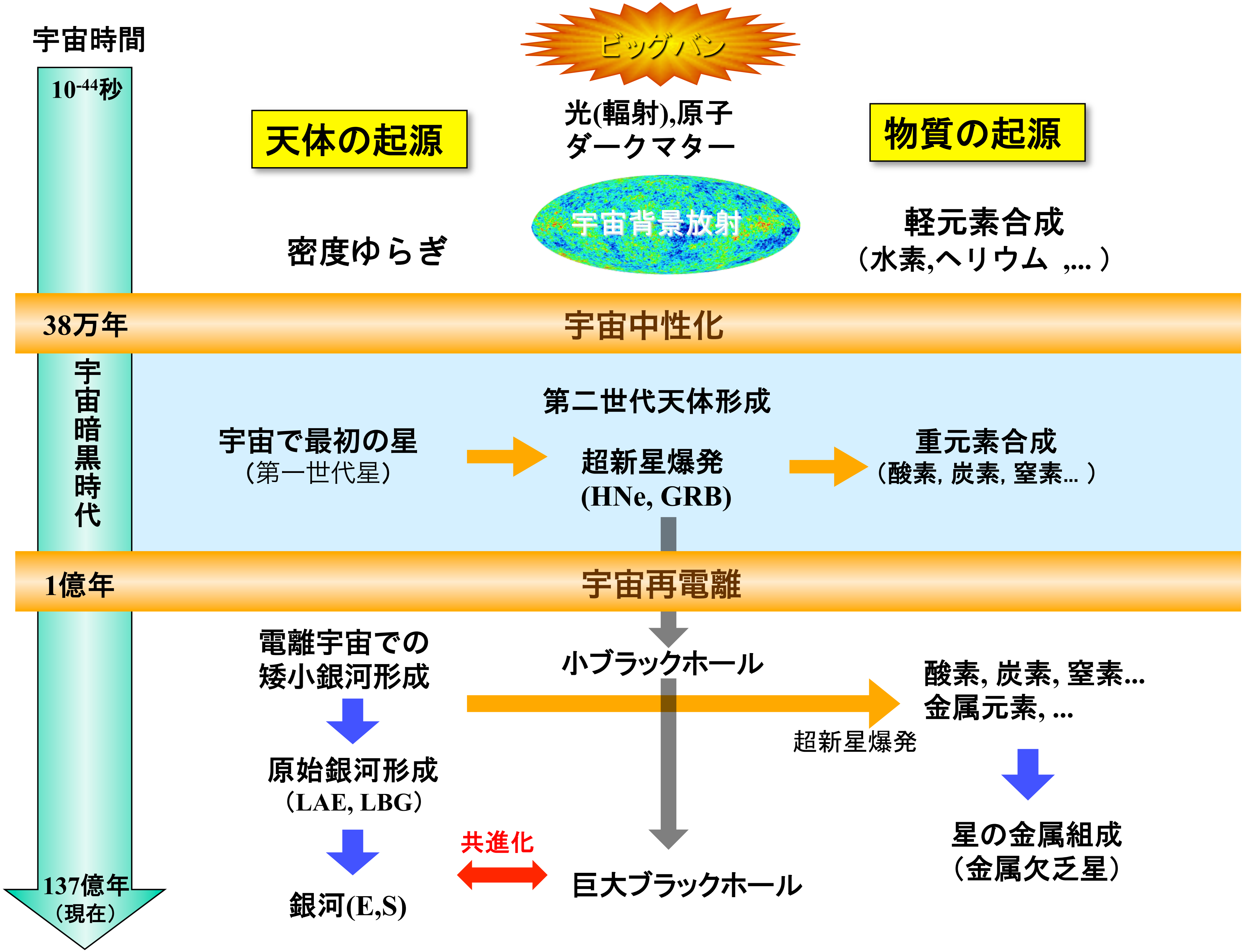

宇宙時間
10-44秒
ビッグバン
天体の起源
光(輻射),原子
ダークマター
物質の起源
宇宙背景放射
密度ゆらぎ
軽元素合成
（水素,ヘリウム ,... ）
38万年
宇宙中性化
宇宙暗黒時代
第二世代天体形成
宇宙で最初の星
（第一世代星）
超新星爆発
(HNe, GRB)
重元素合成
（酸素, 炭素, 窒素... ）
1億年
宇宙再電離
電離宇宙での
矮小銀河形成
小ブラックホール
酸素, 炭素, 窒素...
金属元素, ...
超新星爆発
原始銀河形成
（LAE, LBG）
共進化
星の金属組成
（金属欠乏星）
137億年
（現在）
銀河(E,S)
巨大ブラックホール

# Contents

◆初代天体

◆宇宙再電離

◆銀河形成

◆巨大ブラックホール形成

# 初代天体

## Pop III.1 (1st generation Pop III)

- first collapse
- core fragmentation
- binary formation
- magnetic fields

## Pop III.2 (2nd generation Pop III)

- UV feedback
- Pop III star formation in pre-ionized gas (HD cooling)

## Pop II.1 (1st generation Metal Poor Star )

- metal/dust cooling

# H2 Formation

Reaction 1: $e^- + H \rightarrow H^- + h\nu \Rightarrow H^- + H \rightarrow H_2 + e^-$ (z<100)

Reaction 2: $p + H \rightarrow H_2^+ + h\nu \Rightarrow H_2^+ + H \rightarrow H_2 + p$ (z>100)

Matsuda, Sato, & Takeda (1969, Prog. Theor. Phys., 42, 219)

Non-equilibrium processes

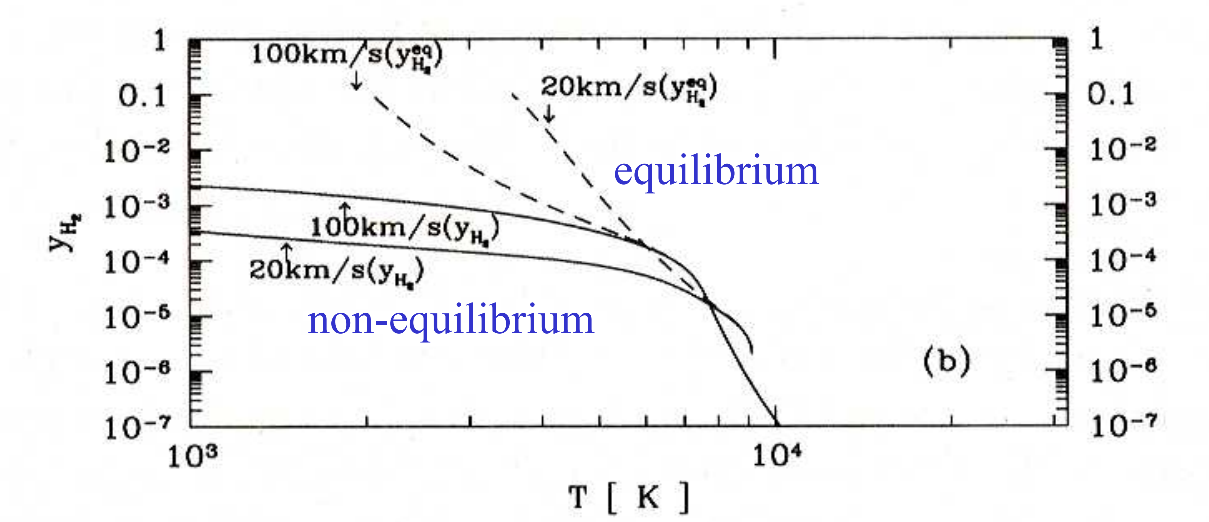


Susa et al.
(1998, PTP, 100, 63)

IGM (residual ion. $\chi_e \approx 10^{-5}$): $\chi_{H2} \approx 10^{-6}$

No shock ion. ($T_s < 10^4$K): $\chi_{H2} \approx 10^{-4} - 10^{-3}$

Shock ion. ($T_s > 10^4$K): $\chi_{H2} \approx 10^{-3} - 10^{-2}$

## ① critical density $n_{crit}$

$n < n_{crit} = 10^{3-4}\,\mathrm{cm}^{-3}$

$$n_j\left(\sum_{k<j} A_{jk} + \sum_{k\neq j} n_e C_{jk}\right) = \sum_{k>j} n_k A_{kj} + \sum_{k\neq j} n_e n_k C_{kj}$$

$$\therefore\; n_j A_{jk} = n_e n_k C_{kj} \;\Rightarrow\; \Lambda = \sum_{j\geq 2}\sum_{k<j} n\, n_k C_{kj} h\nu_{jk} \propto n^2$$

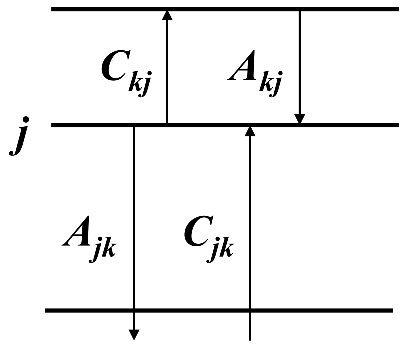


$n > n_{crit} = 10^{3-4}\,\mathrm{cm}^{-3}$

$$n_j \sum_{k\neq j} n_e C_{jk} = \sum_{k\neq j} n_e n_k C_{kj}$$

$\Rightarrow n_j$ : Local Thermodynamic Equilibrium (LTE)

$$n_j = n\, g_j e^{-h\nu_{j1}/kT} \Rightarrow \Lambda = \sum_{j\geq 2}\sum_{k<j} n_j A_{jk} h\nu_{jk} \propto n$$

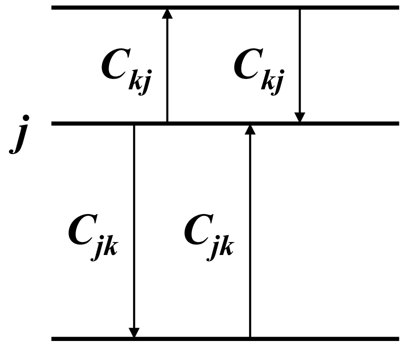


## ② three-body reaction density $n_{three}$

$\mathrm{H+H+H} \rightarrow \mathrm{H_2 + H}$

$n_{three} \sim 10^{8}\,\mathrm{cm}^{-3}$

## ③ optically-thick density $n_{thick}$

$n_{thick} \sim 10^{12}\,\mathrm{cm}^{-3}$

# Palla, Salpeter & Stahler 1983

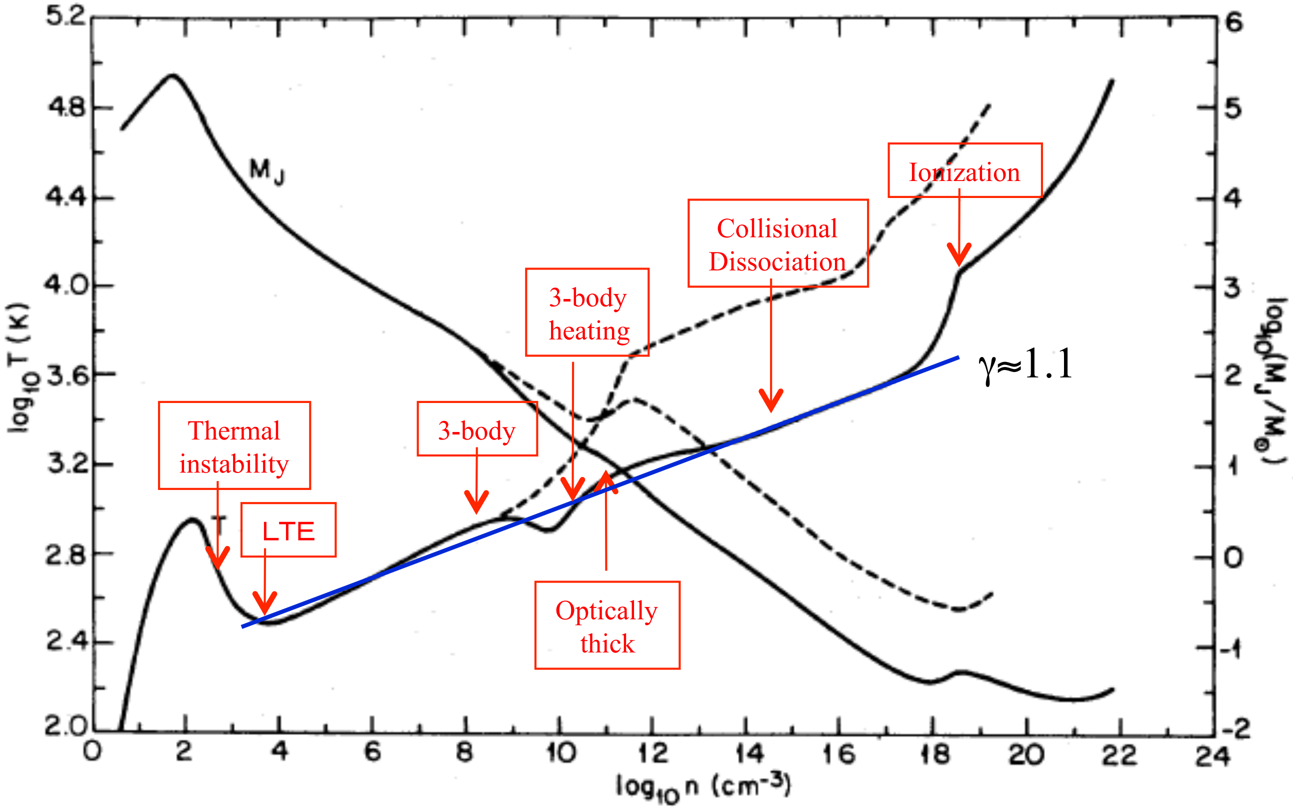


$M_{core} \approx 0.05\, M_\odot$

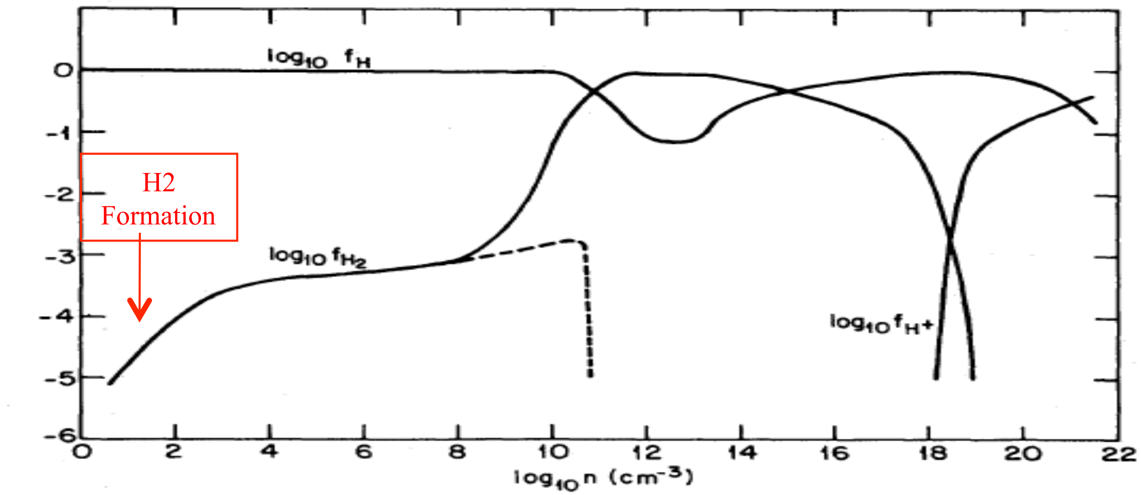

# Runaway Collapse to First Star

Omukai & Nishi 1998

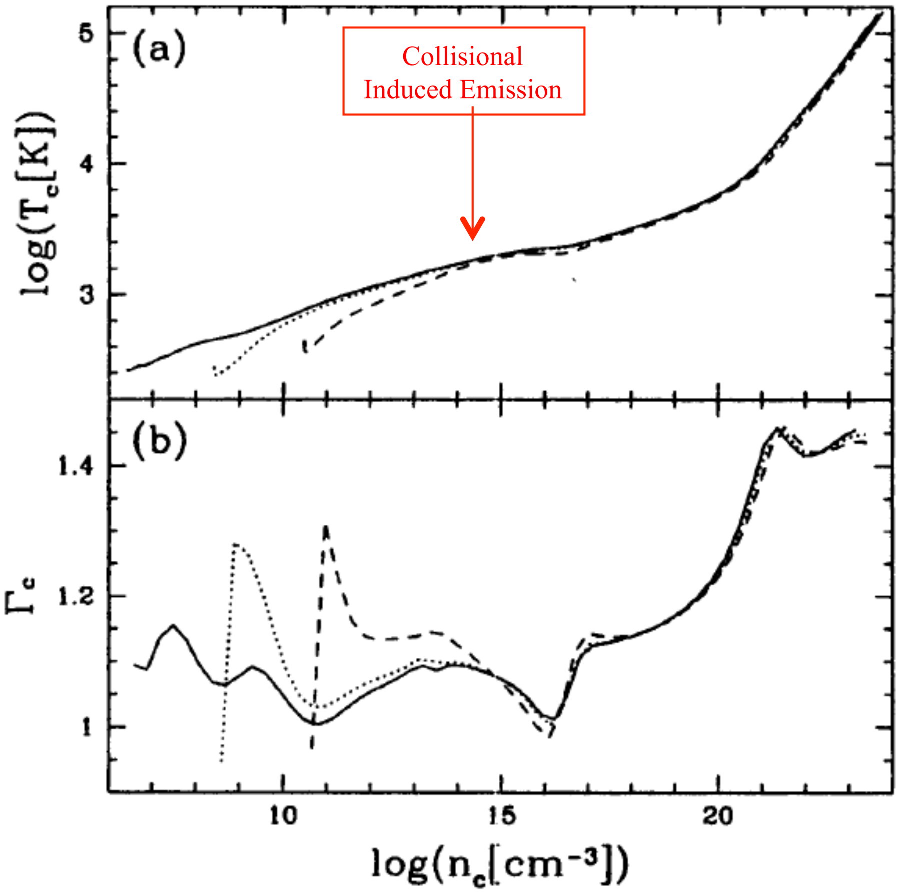


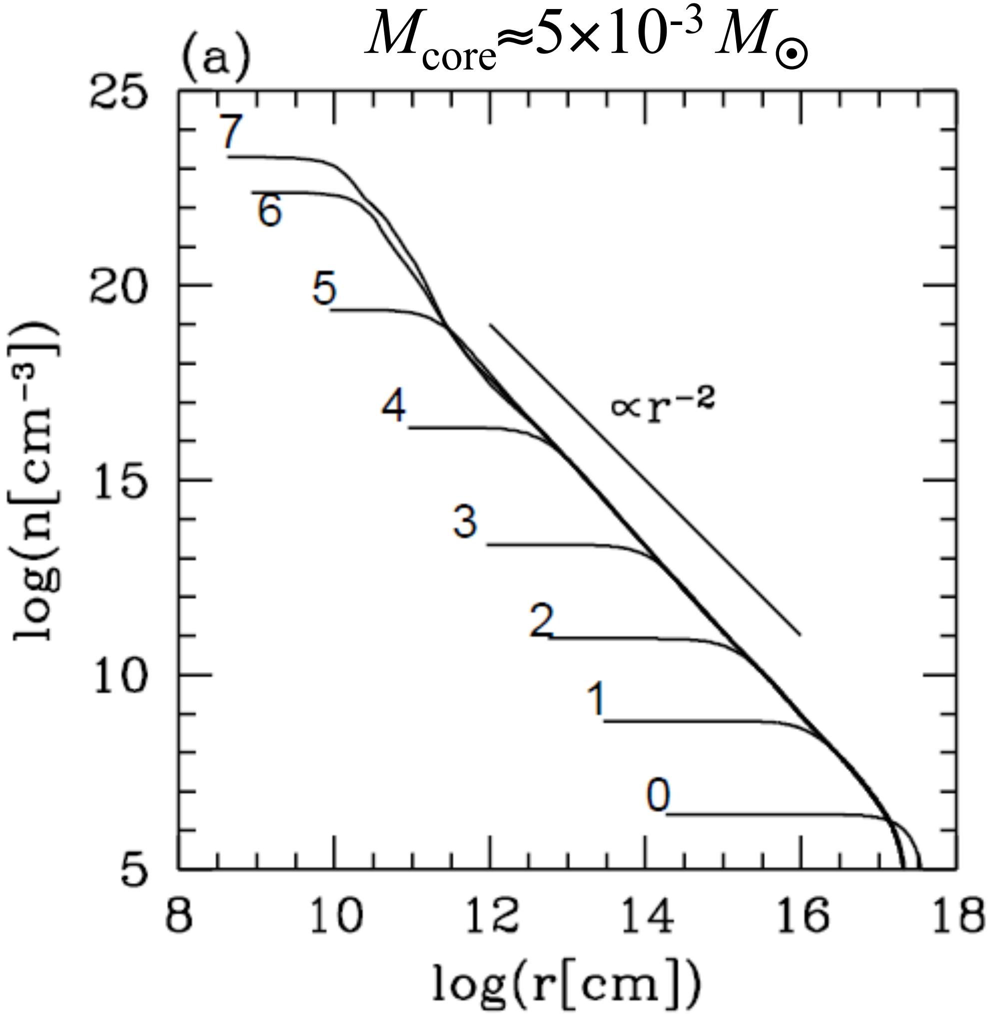

# Two Fragmentation Modes

**Nakamura & Umemura, 2001, ApJ, 548, 19**

## 1) Fragmentation at the critical density of $H_2$ for $n_{in} < n_{crit} \approx 10^4 cm^{-3}$

line density: $l = \frac{2c_s^2}{G}$

most unstable mode: $\lambda_m = 22 \frac{c_s}{(4\pi G \rho_0)^{1/2}}$

$M_{frag} = l\lambda_m = 2.8 \times 10^3 M_\odot \left(\frac{T}{300\ K}\right)^{3/2} \left(\frac{n}{10^4 cm^{-3}}\right)^{-1/2}$

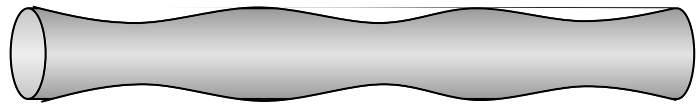

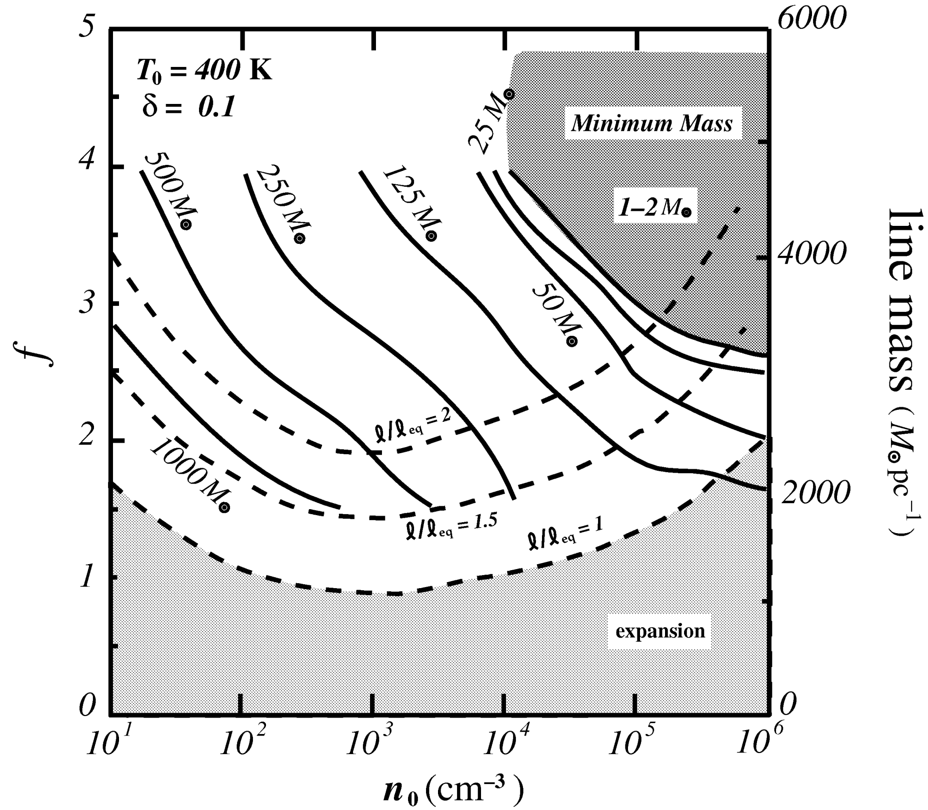


## 2) Opatically thick ($n \approx 10^{12} cm^{-3}$) fragmentation for $n_{in} > n_{crit}$

$m_{min} = 1 - 2 M_\odot$

**Rees mass**

$m_{min} \sim \alpha_c^{-1/2} \mu^{-1/4} (m_{Planck}^3 / m_p^2)$

# ガス降着による質量決定

Runaway Collapse & Accretion Rate

$$\text{core size} \approx \lambda_{\mathrm{J}} = c_{\mathrm{s}} t_{ff}$$

$$c_s = \left(\frac{kT}{\mu}\right)^{1/2}, t_{ff} = \left(\frac{1}{G\rho}\right)^{1/2}$$

$$\dot{m} \approx \frac{M_J}{t_{ff}} = \frac{\rho\left(c_s t_{ff}\right)^3}{t_{ff}} = \rho t_{ff}{}^2 = \frac{c_s{}^3}{G}$$

$$\dot{m} \approx \frac{c_s{}^3}{G} = 10^{-3}\left(\frac{T}{300K}\right)^{3/2} M_{\odot}\mathrm{yr}^{-1}$$

# Runaway (Larson-Penston collapse) vs Kelvin-Helmholtz contraction

$$t_{LP} = \sqrt{\frac{5/3}{4\pi G\rho}} < t_{KH}(m)$$

Omukai 2000, ApJ, 534, 809

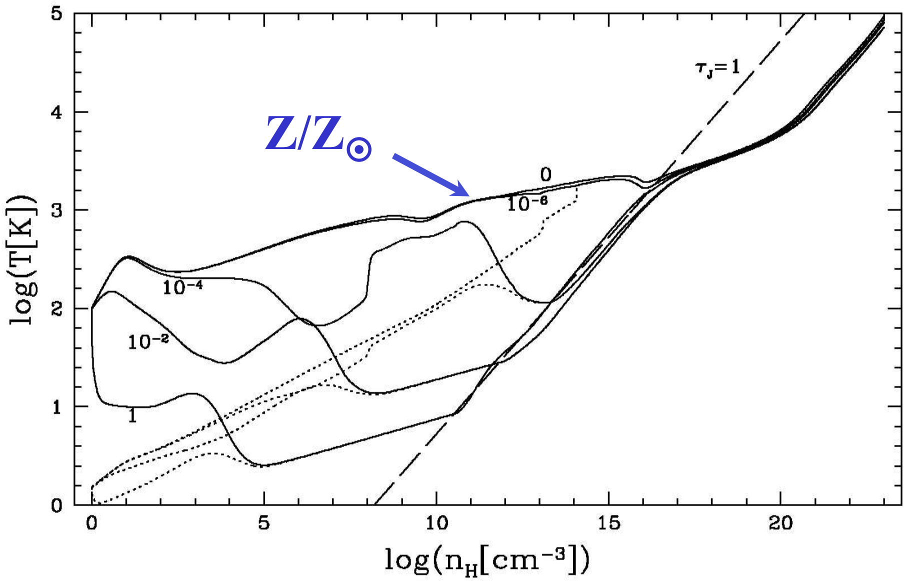


星質量の決定

$$\dot{m}\,t_{KH}(m) = m$$

$$\dot{m} \approx \frac{c_s^3}{G} = 10^{-3}\left(\frac{T}{300K}\right)^{3/2} M_\odot \mathrm{yr}^{-1}$$

**$m$=数100$M_\odot$ー1000$M_\odot$**

| Pop III | Pop I |
| --- | --- |
| $M_{core} \approx 10^{-3}\,M_\odot$ | $10^{-3}\,M_\odot$ |
| $M_{frag} \approx 10^{3}\,M_\odot$ | $>0.1\,M_\odot$ |
| $\dot{m} \approx 10^{-3}\,M_\odot$/yr | $10^{-5}\,M_\odot$/yr |

**Omukai & Nishi 1998, ApJ, 508, 141**
**Omukai 2000, ApJ, 534, 809**
**O'Shea & Norman, 2007, ApJ, 654, 66**
**Hosokawa & Omukai, 2009, ApJ, 703, 1810 (radiative feedback)**

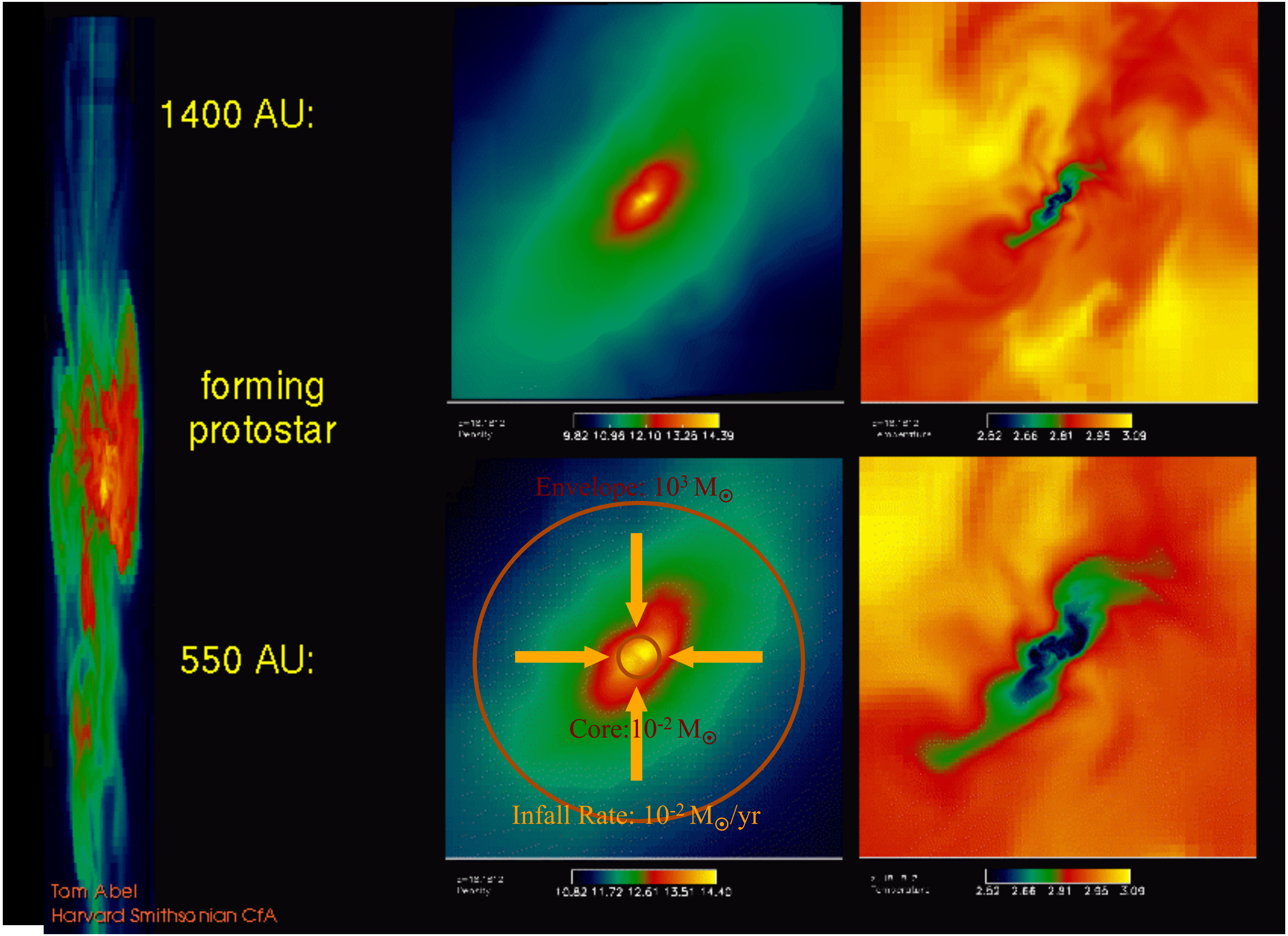
1400 AU:
forming protostar
550 AU:
Tom Abel
Harvard Smithsonian CfA
Density
9.82 10.96 12.10 13.25 14.39
2.52 2.66 2.81 2.95 3.09
Envelope: $10^3$ $M_\odot$
Core: $10^{-2}$ $M_\odot$
Infall Rate: $10^{-2}$ $M_\odot$/yr
Density
10.82 11.72 12.61 13.51 14.40
Temperature
2.52 2.66 2.81 2.95 3.09

# Cosmological Simulations

Yoshida et al. 2003, ApJ, 592, 645

**ΛCDM context**
(Yoshida et al. 2003; O'Shea & Norman 2007)

$M<M_J$ $M\approx M_J$ $M>M_J$

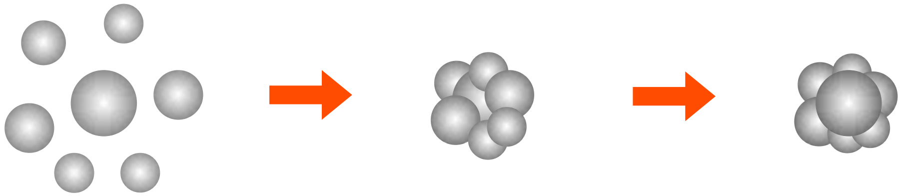

Jeans instability ($H_2$ cooling) runaway

$$M_{\rm halo,cr} \approx 7\times10^5\, M_\odot$$
$$M_{\rm b,cr} \approx 10^5\, M_\odot$$

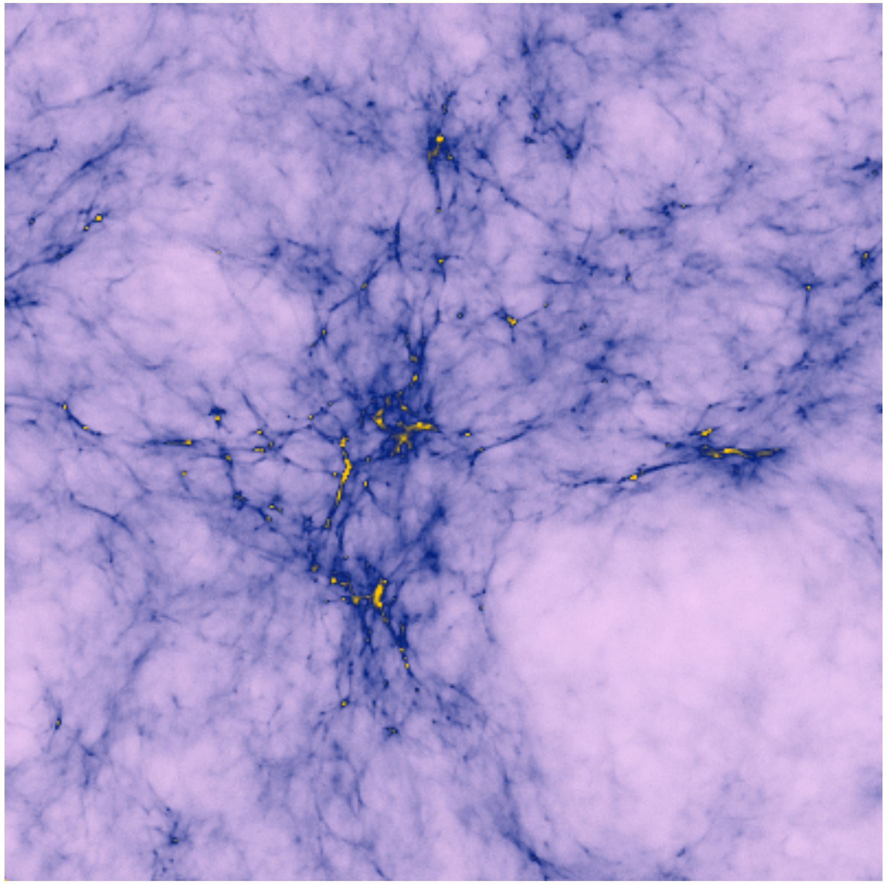

$6h^{-1}$Mpc

**mass resolution**
$m_b = 30\, M_\odot$

# Runaway Collapse by Dark Matter Cusps

Suwa, Umemura, Susa, Hasegawa, 2010 (in prep)
Umemura, Suwa, Susa, 2009

$$M_J = \rho_b \left( \frac{c_s^2}{G\bar{\rho}_{tot}} \right)^{3/2} = \rho_b \left( \frac{4\pi r^3 c_s^2}{3G\left[M_{DM}(r) + M_b(r)\right]} \right)^{3/2}$$

**Minimm mass $M_{b,min} \approx 10^3 M_\odot$**

**peak separation ≈ 50pc**

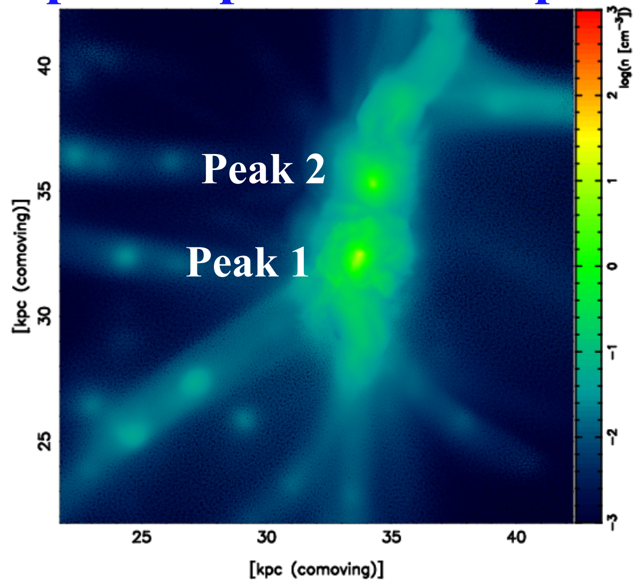


**Peak 1**

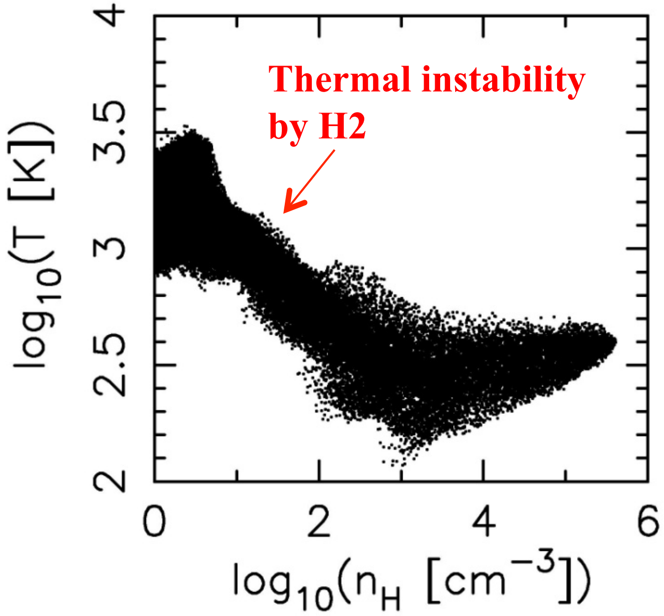


**Peak 2**

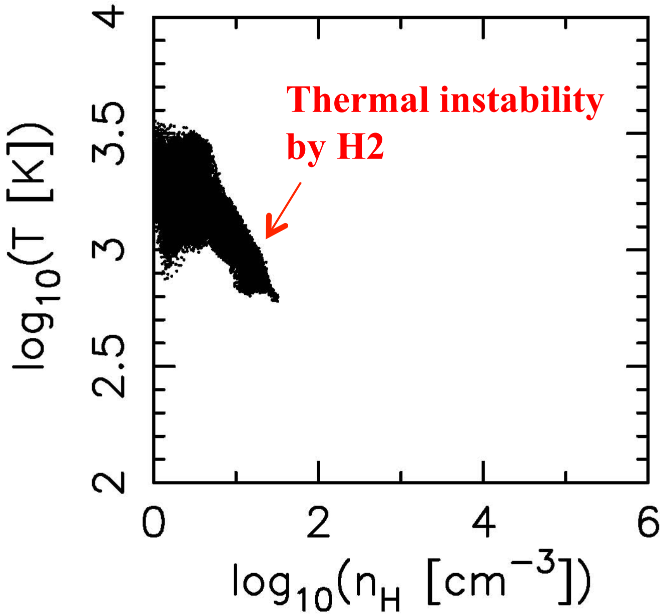

# Cosmological Simulations

Yoshida, Omukai, Hernquist
2008, Science, 321, 669

$$M_{\rm core} \approx 10^{-2} M_{\odot}$$

$$\dot{m} \approx 0.1 - 0.01 M_{\odot} {\rm yr}^{-1}$$

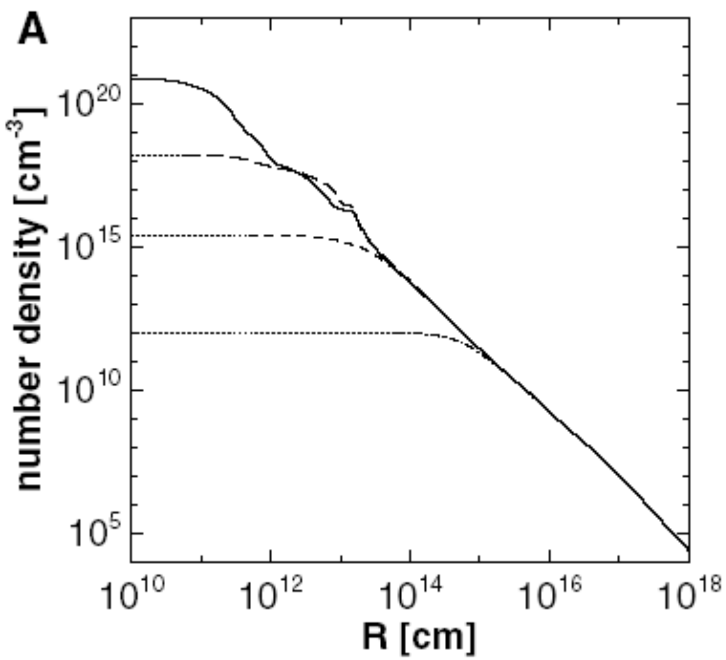


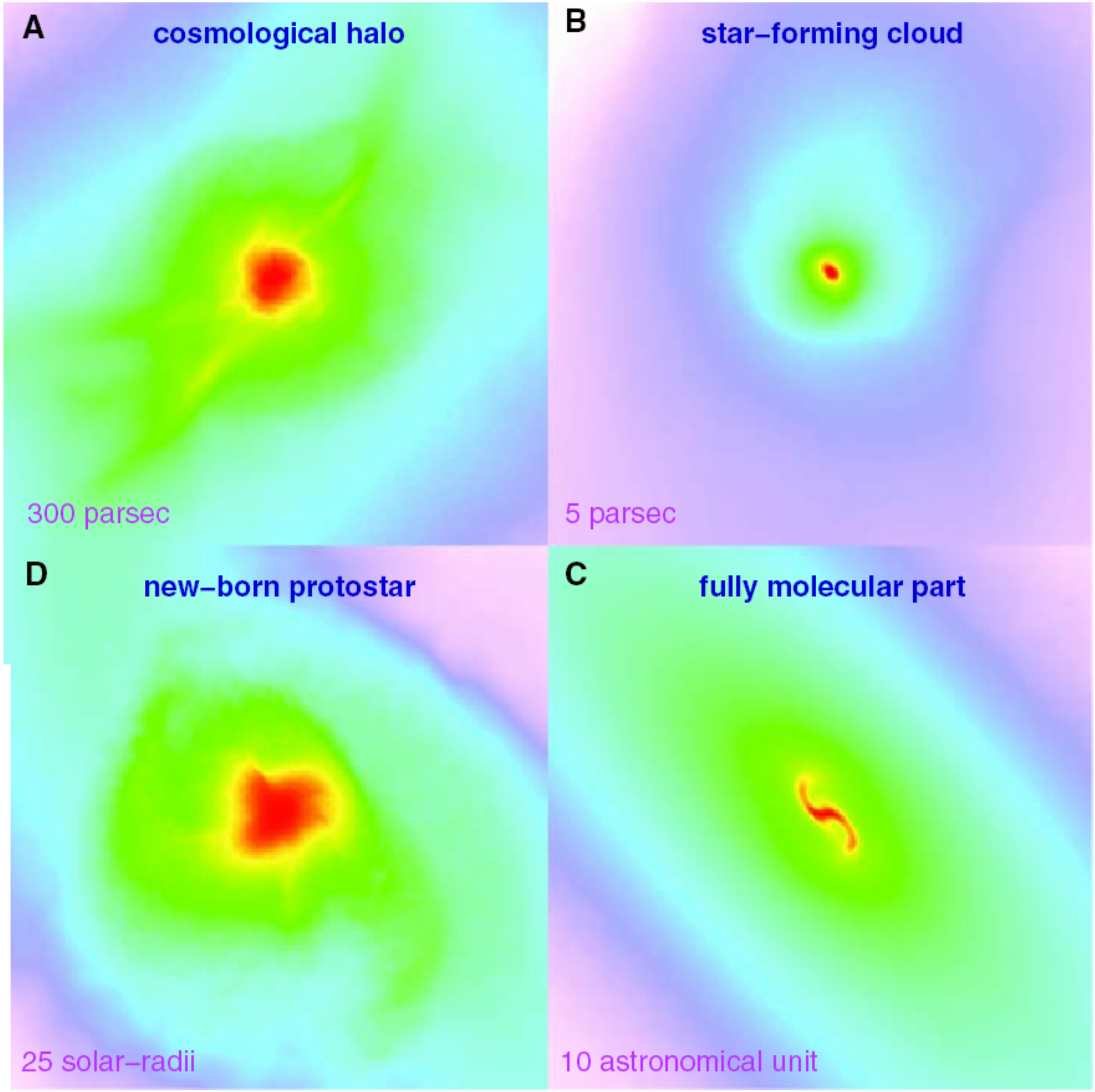


**ig. 1.** Projected gas distribution around the protostar. (**A**) The large-scale gas distribution around the osmological halo (300 pc on a side). (**B**) A self-gravitating, star-forming cloud (5 pc on a side). (**C**) The entral part of the fully molecular core (10 astronomical units on a side). (**D**) The final protostar (25 solar adii on a side). The color scale from light purple to dark red corresponds to logarithmically scaled hydrogen umber densities from 0.01 to $10^3$ cm$^{-3}$ (A), from 10 to $10^6$ cm$^{-3}$ (B), and from $10^{14}$ to $10^{19}$ cm$^{-3}$ (C). The color scale for (D) shows the density-weighted mean temperature, which scales from 3000 to 12,000 K.

# Cosmological Variance

O'Shea & Norman 2007, ApJ,654, 66

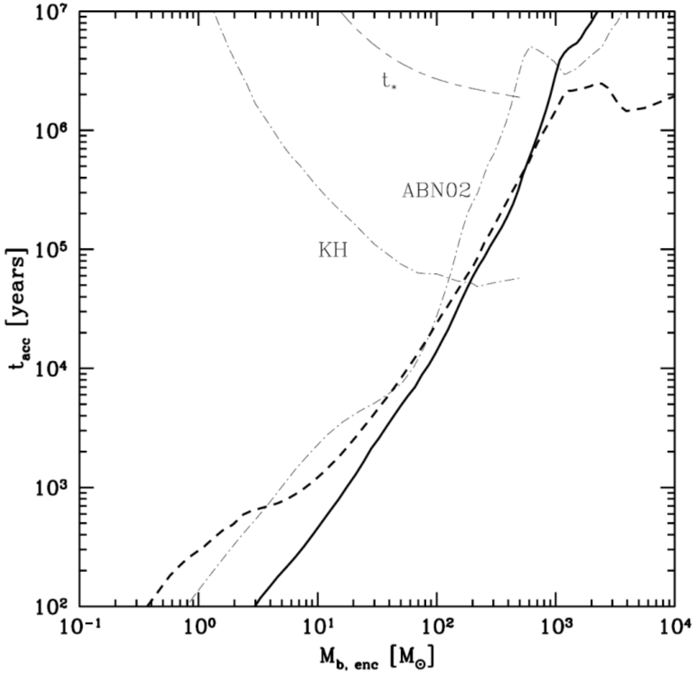


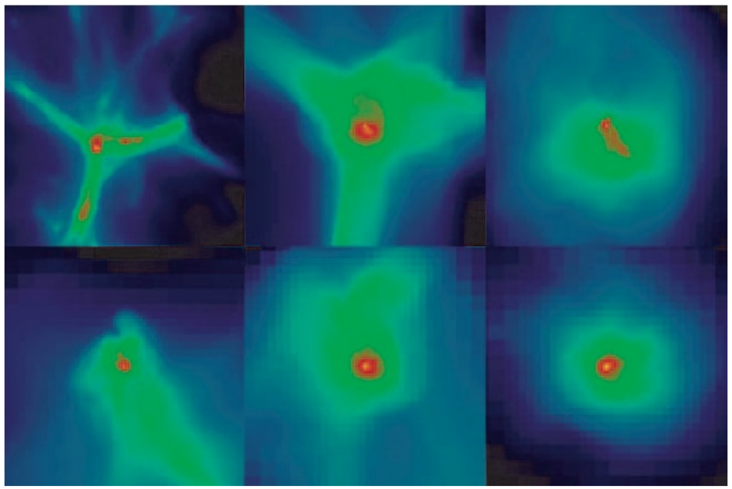

$m \sim 50M_\odot - 300M_\odot$

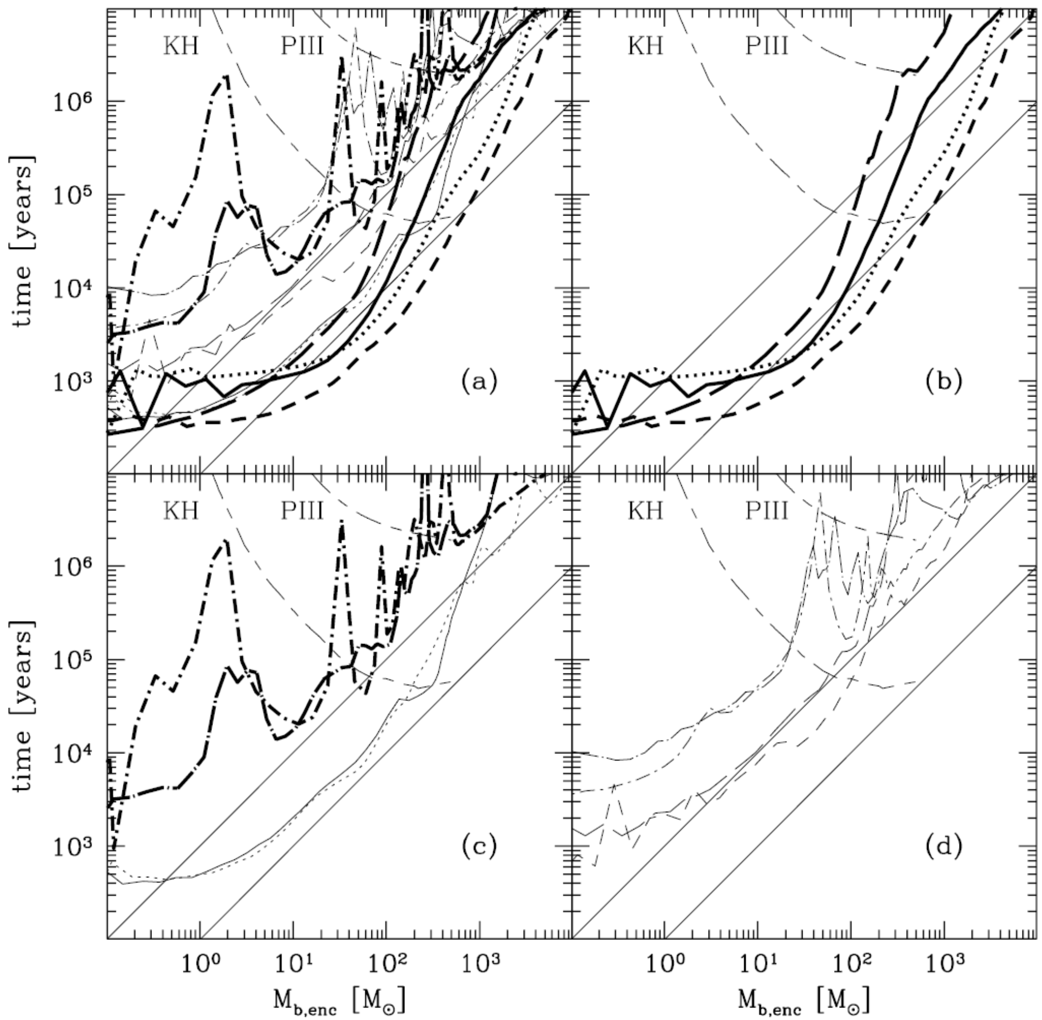

# Pop III Binary Formation

**Saigo, Matsumoto, Umemura, 2004, ApJL, 615, L65**

Low rotation case

$$\beta \equiv \frac{\text{centrifugal force}}{\text{pressure force}} = 0.1$$

**EOS (Polytrope)**
**Nested-Grid**

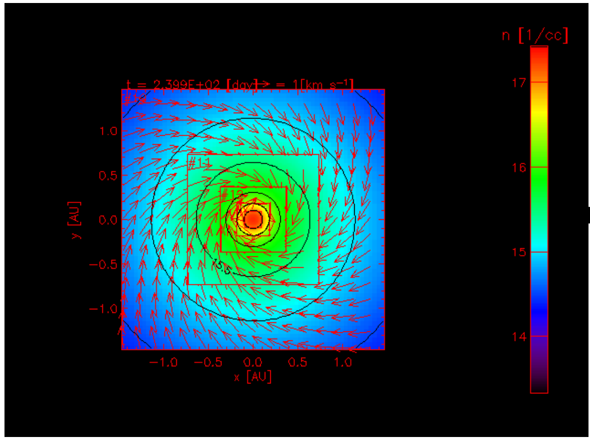


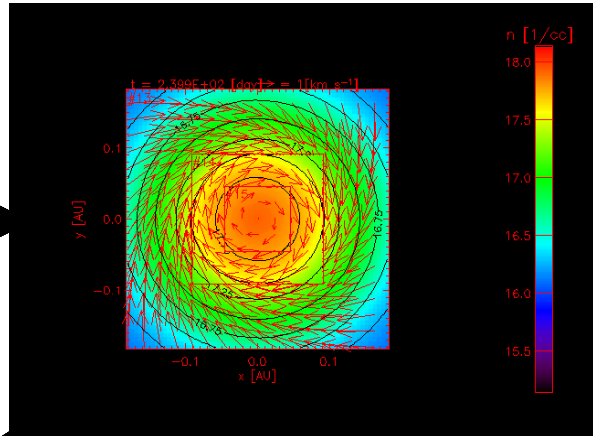


rotationally-supported disk

mass accretion

$$\frac{T_{rot}}{|W|} = 0.245$$

$< 0.27$

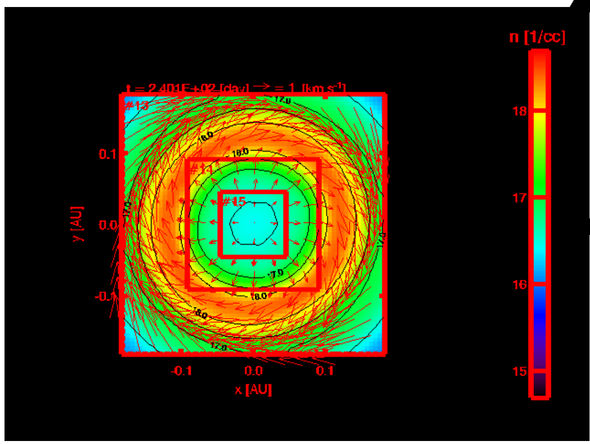


1 AU

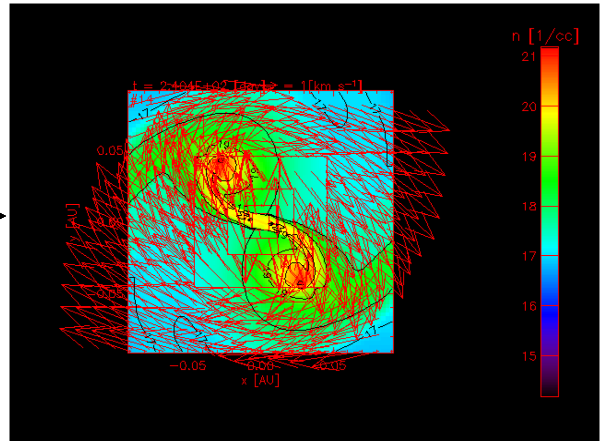


ring instability

binary formation

High rotation case

$$\beta \equiv \frac{\text{centrifugal force}}{\text{pressure force}} = 1$$

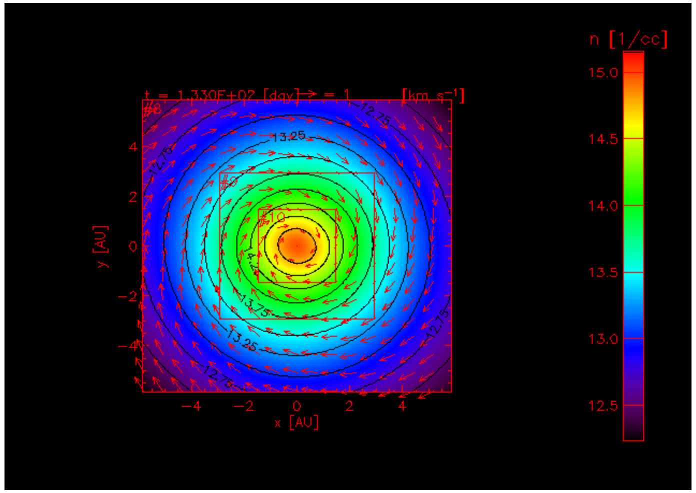


rotationally-supported disk

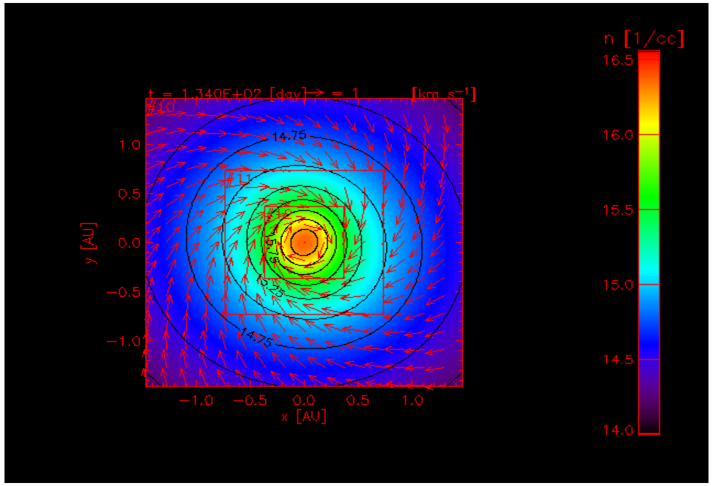


mass accretion

$$\frac{T_{rot}}{|W|} = 0.327$$

$$> 0.27$$

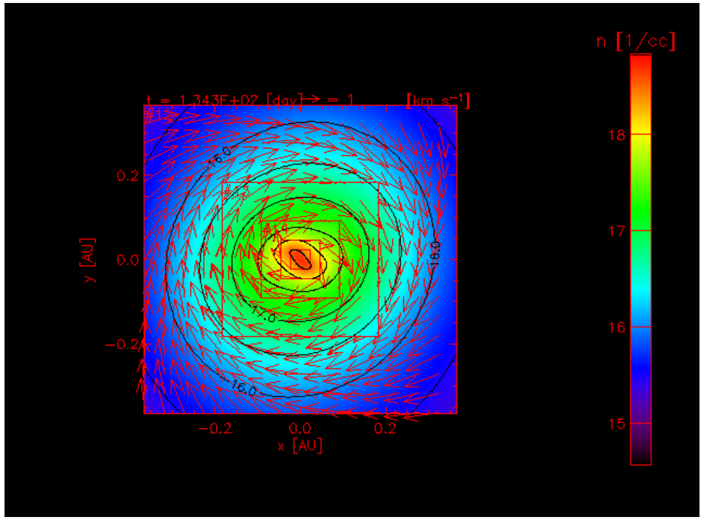


no ring

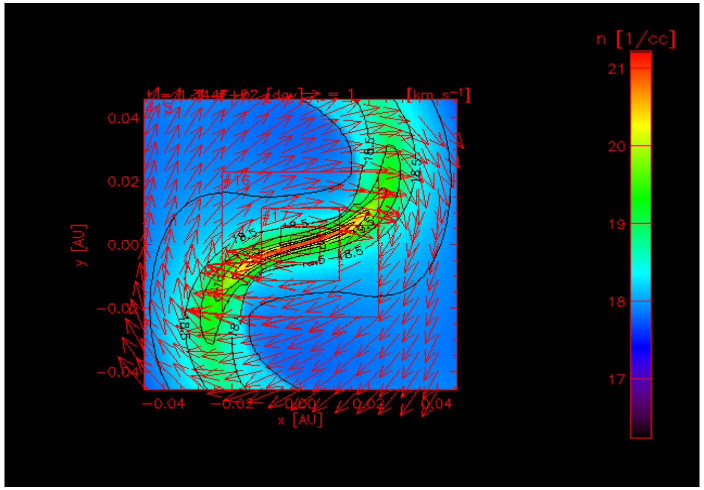


bar instability
(single star)

**Machida et al. 2008, ApJ, 677, 813**

**EOS (Polytrope)**
**Nested-Grid**

spiral → single star
bar, ring → fragmentation

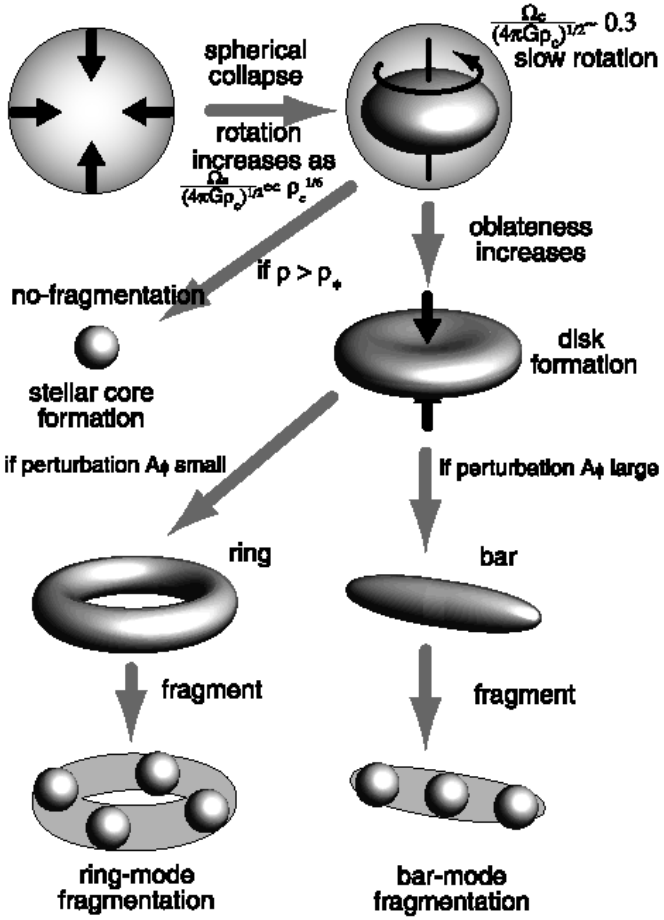


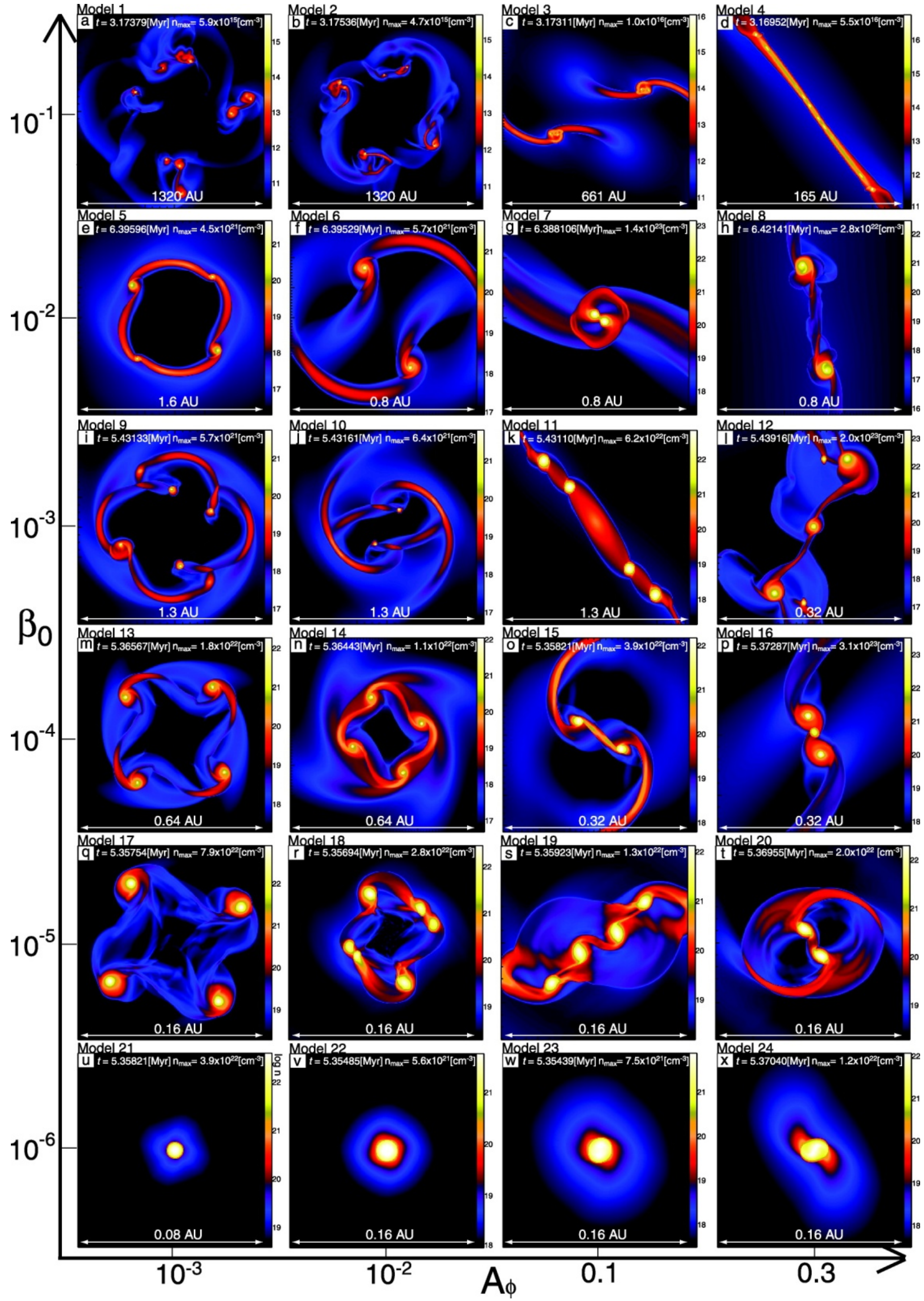

# Cosmological Simulations

Turk, Abel & O'Shea, 2009, Science, 325, 601

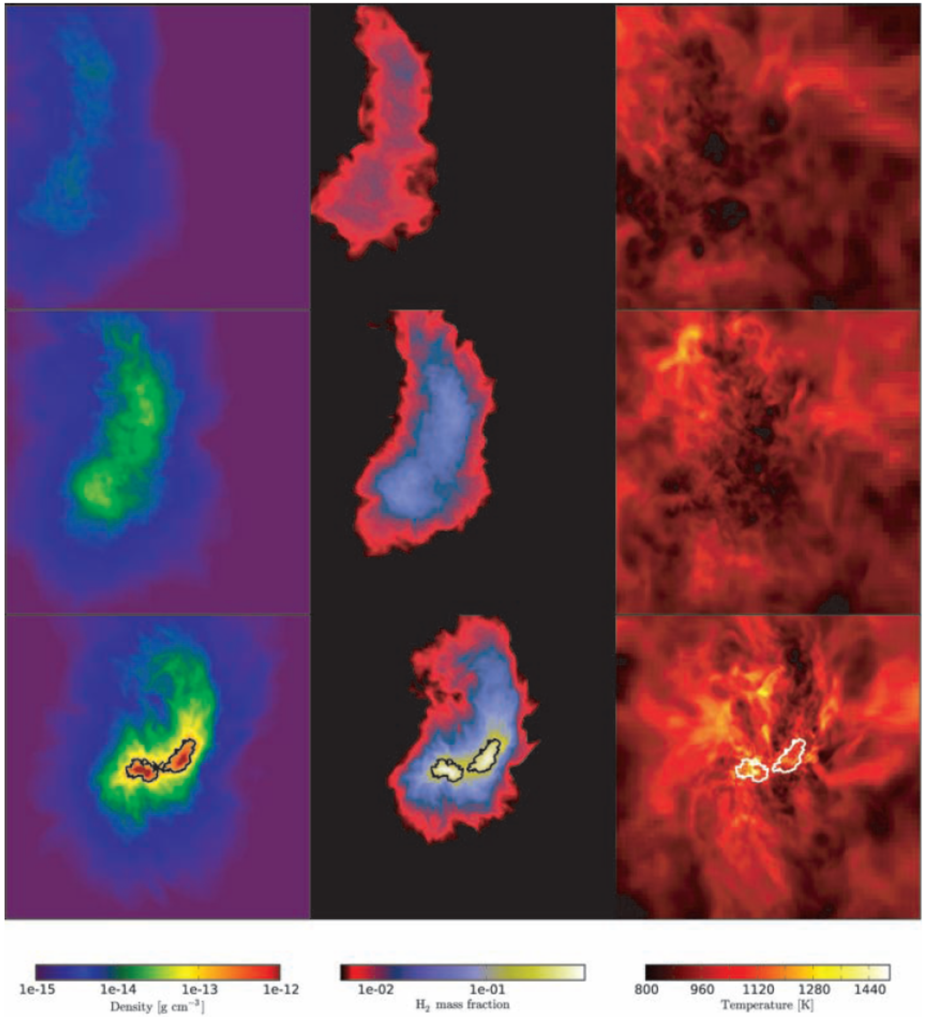


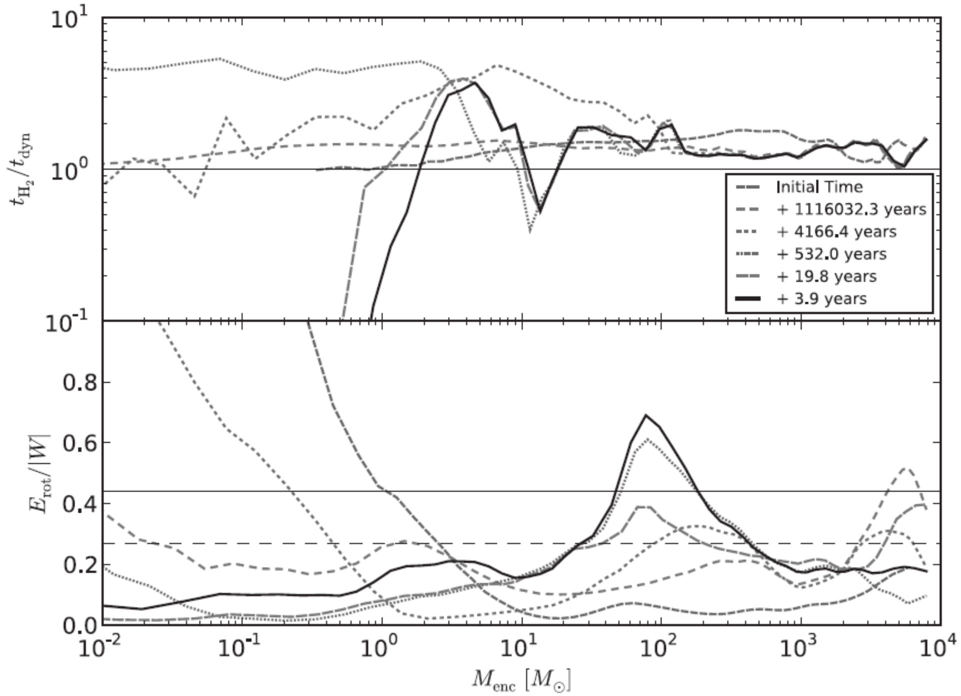


**Fig. 4.** Enclosed quantities as a function of mass enclosed, with respect to the most dense point (which is located within core A after the cloud fragments) and calculated in the rest frame of that point at different times in the simulation: the mass-weighted average ratio of the dynamical time of the gas divided by the cooling time of the molecular hydrogen, taking into account the heating from three-body formation processes (**top**) and rotational energy divided by gravitational binding energy (**bottom**). In the bottom graph, lines have been drawn to indicate ratios of 0.27 (thin dashed horizontal) and 0.44 (thin solid horizontal).

# Stacy, Greif & Bromm, 2010, MNRAS, 403, 45

GADGET 3D
100 $h^{-1}$ kpc box, $N_{SPH} = N_{DM} = 128^3$
ΛCDM cosmology
SPH refinement: $m_{SPH} = 0.015 M_\odot$
Sink particle生成: $n > n_{max} = 10^{12}$ cm$^{-3}$
longer evolution 5000 yr
*cf*. Turk, Abel & O'Shea, 2009
(Science, 325, 601) ~200 yr

- first protostarの周りに，5000年ぐらいかけてdisk形成
- 非軸対称不安定により，spiral modeが現れ，分裂する（Q ~ 0.4）
- 分裂により，binary や multiple protostar seeds が生まれる
- ~40$M_\odot$ と~ 10$M_\odot$ のbinary多く生まれる

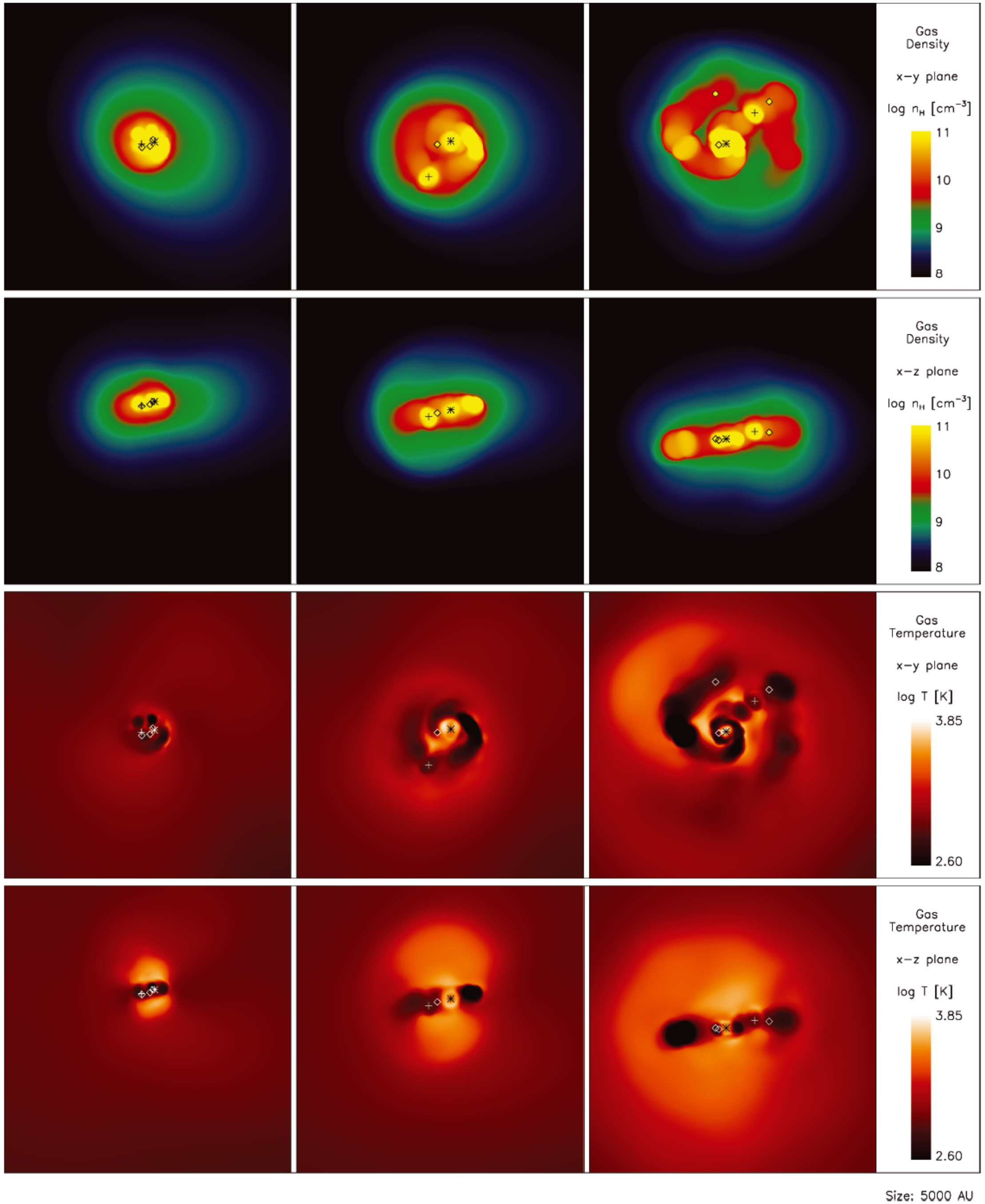


**Figure 5.** Density and temperature projections of the central 5000 au. Each row shows the projections at 1000 yr (left), 2000 yr (centre) and 5000 yr (right) after the initial sink formation. Asterisks denote the location of the most massive sink. Crosses show the location of the second most massive sink. Diamonds are the locations of the other sinks. Top row: density structure of the central region in the *x*-*y* plane. Second row: density structure of the central region in the

# Magnetic Fields in Population III Star Formation

- **Frozen-in**
  **Maki & Susa, 2004, ApJ, 609, 467**
  **2007, PASJ, 59, 787**

- ***Fundamental* 3D MHD Simulations**
  **Machida et al. 2006, ApJ, 647, L1**
  **2008, ApJ, 685, 690**

- ***Cosmological* 3D MHD Simulations**
  **Xu et al. 2008, ApJ, 688, L57**

# 磁場＋回転

$B > 10^{-9}(n_c/10^3\ \mathrm{cm^{-3}})^{2/3}$ G

Machida et al. 2006
ApJ, 647, L1; 2008, ApJ, 685, 690

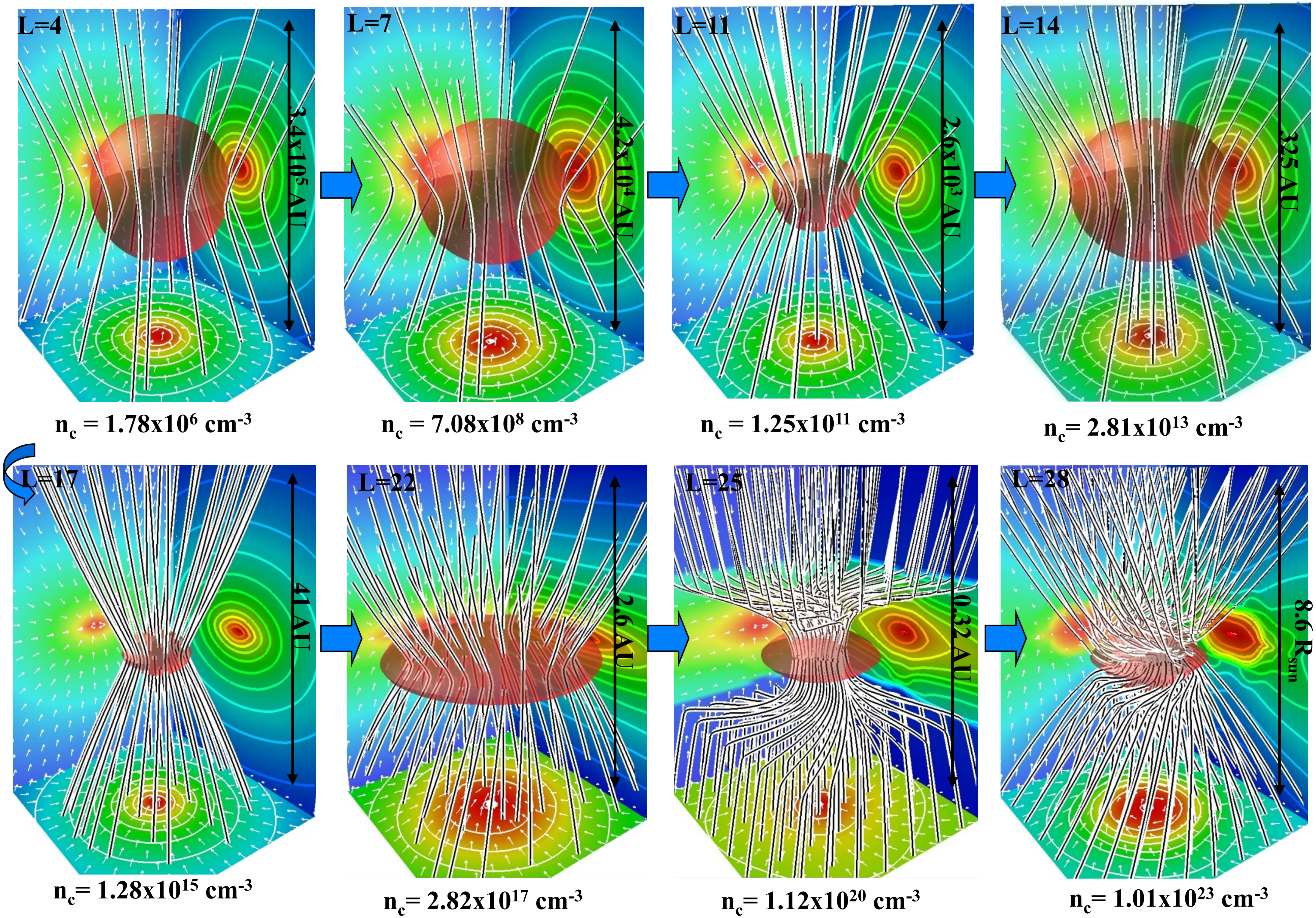

# MHD Simulations of Population III Star Formation

*Cosmological simulation by ENZO (AMR)*

**Xu et al. 2008, ApJ, 688, L57**

No initial ***B***
Biermann Battery
Induction equation

$$\frac{\partial \boldsymbol{B}}{\partial t} = \nabla \times (v \times \boldsymbol{B}) + \frac{c\nabla p_e \times \nabla n_e}{n_e^2 e}$$

$\Rightarrow$ ***B***$\approx 10^{-9}$ G  at n $\approx 10^{10}$ cm$^{-3}$
$\beta \equiv P_{th}/P_B \geq 10^{15}$

・磁場はダイナミクスに効かない
・回転エネルギーが磁場のエネルギーを超えることもない

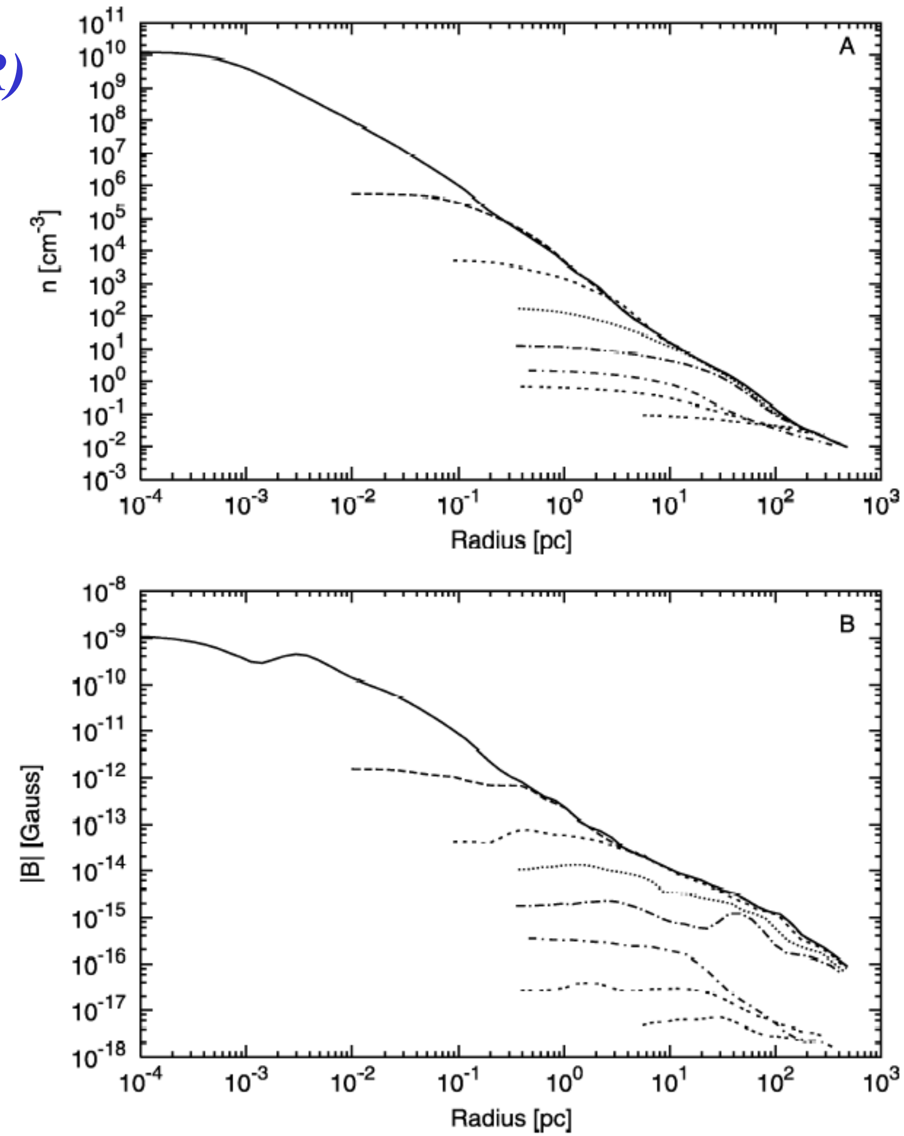


FIG. 1.—Evolution of spherically averaged radial profiles of baryon number density (*top*) and magnetic field strength (*bottom*) of the Population III star-forming halo. Lines correspond to (from bottom to top in each panel) $z$ = 40, 30, 25, 20, 19, 18, 17.61, 17.55.

# Contents

## Pop III.1 (1st generation Pop III)

- first collapse
- core fragmentation
- binary formation
- magnetic fields

## Pop III.2 (2nd generation Pop III)

- UV feedback
- Pop III star formation in pre-ionized gas (HD cooling)

## Pop II.1 (1st generation Metal Poor Star )

- metal/dust cooling

# Pre-ionization の効果

**UV ionization (e.g. Corbelli et al. 1998; Susa & Umemura 2000)**
**Shock ionization (e.g. Shapiro & Kang 1987; Ferrara 1998)**

**High $H_2$ abundance** $x_{H_2}$ ‰$10^{-3}$

⬇

**HD Molecule Formation**

$D^+ + H_2 \rightarrow H^+ + HD$ **Low density**

$D + H_2 \rightarrow H + HD$ **High density**

HD: $A_{10} \sim 5.12 \times 10^{-8}$
*c.f.* $H_2$: $A_{20} \sim 2.94 \times 10^{-11}$

**HD cooling is dominant at *T*<100~200 K**

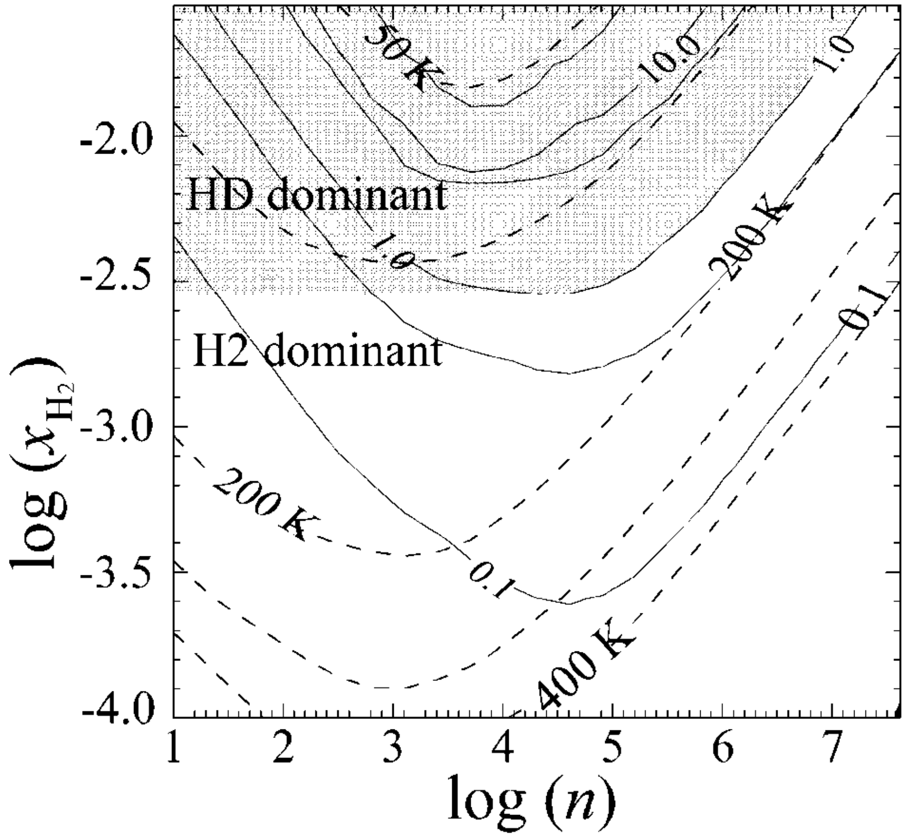


**Nakamura & Umemura 2002**

# HD冷却による初代星形成

**Nakamura & Umemura 2002, ApJ, 569, 549**

$M_* \approx 20\text{-}40 M_\odot$

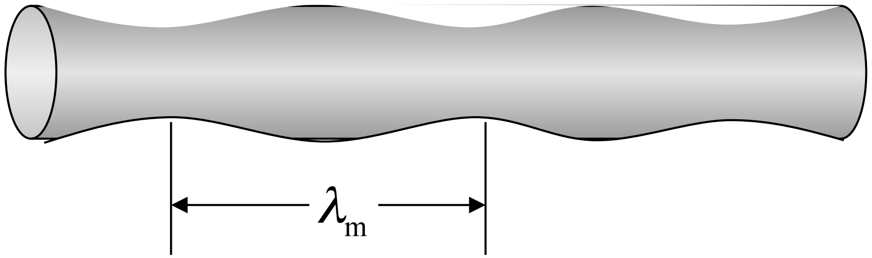


<u>**Critical density of HD**</u> $n_{crit} = 10^{6-7}\,\mathrm{cm^{-3}}$

line density: $l = \dfrac{2c_s^2}{G}$

$$M_{frag} = l\lambda_m = 54 M_\odot \left(\frac{T}{100\,\mathrm{K}}\right)^{3/2} \left(\frac{n}{10^4\,\mathrm{cm^{-3}}}\right)^{-1/2}$$

$T_i = 200\mathrm{K},\ x_{\mathrm{H_2},i} = 3\times10^{-3}$

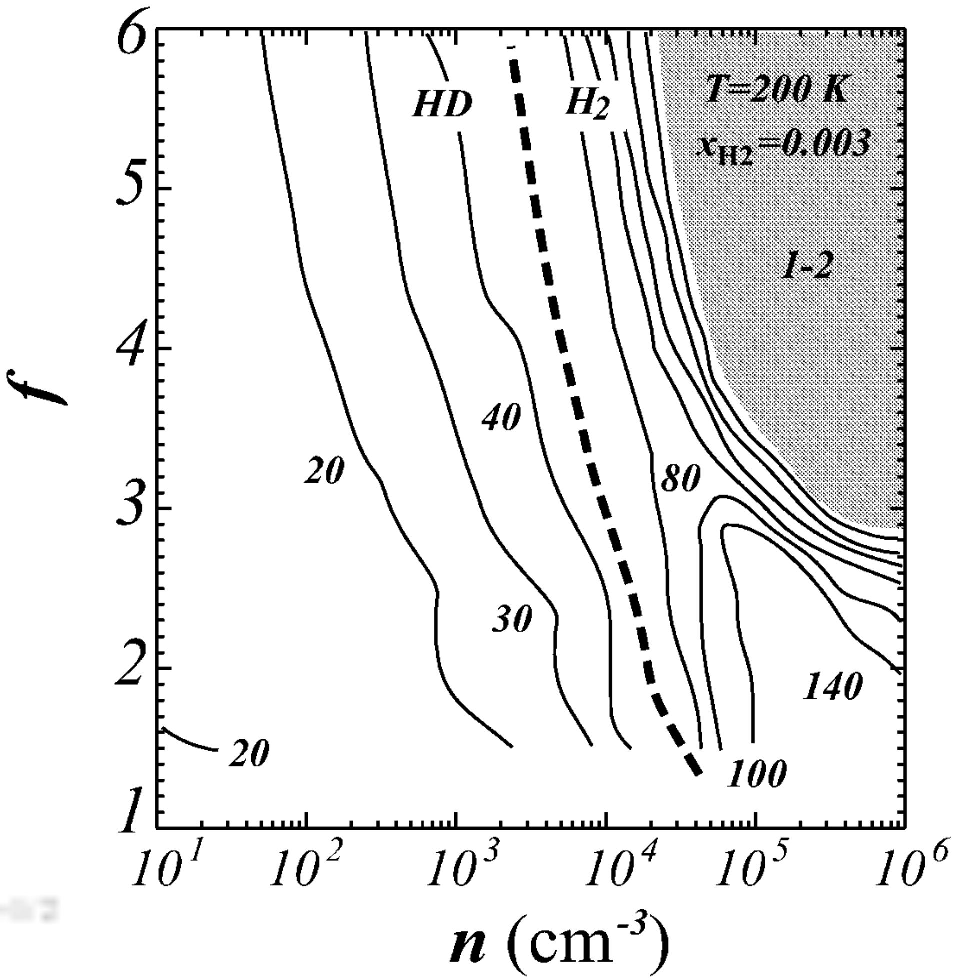

# Formation of Massive Primordial Stars in a Reionized Gas

*Cosmological Simulation*

**Yoshida et al. 2007, ApJ, 663, 687**

$M \approx 40 M_\odot$

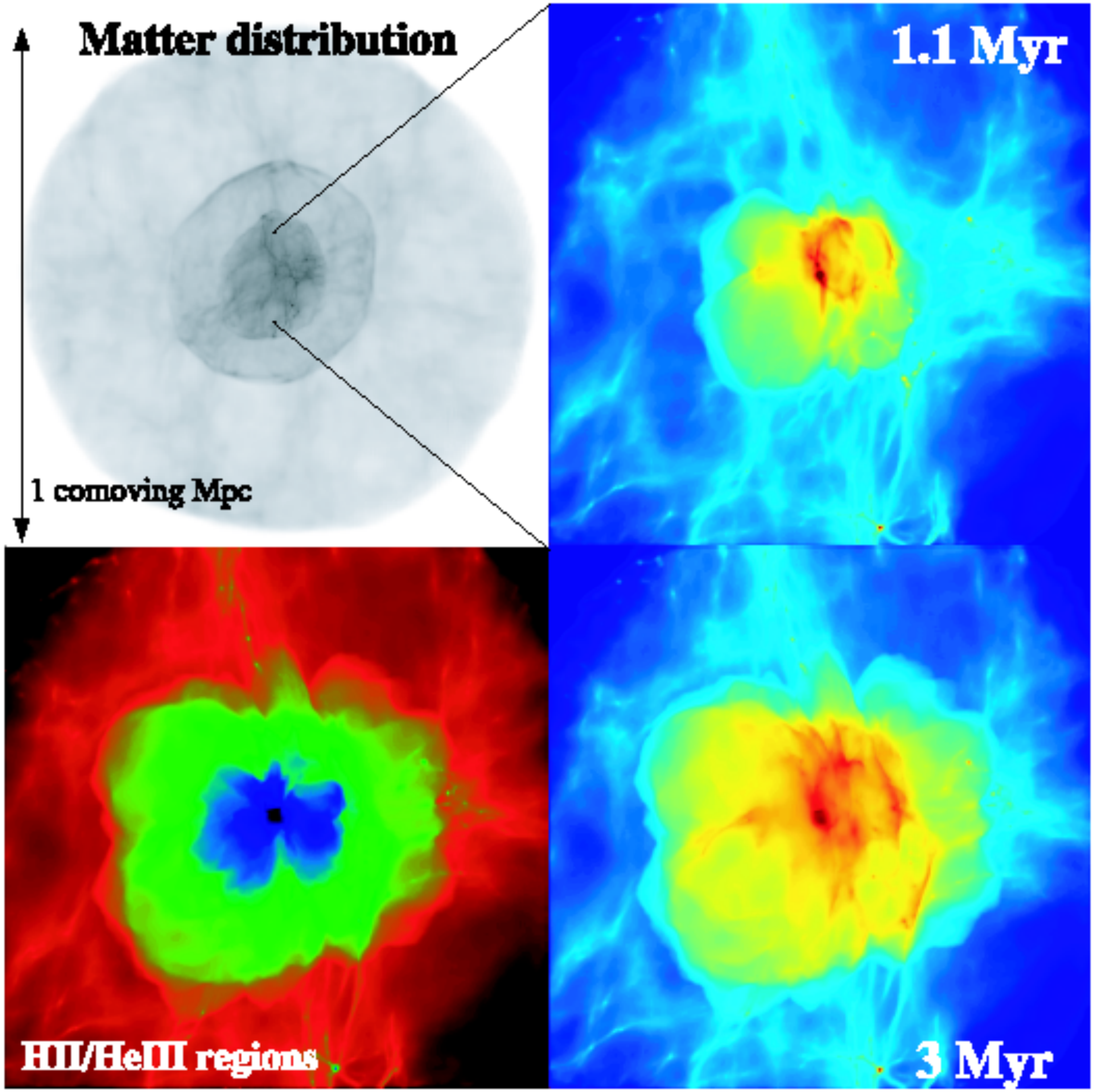

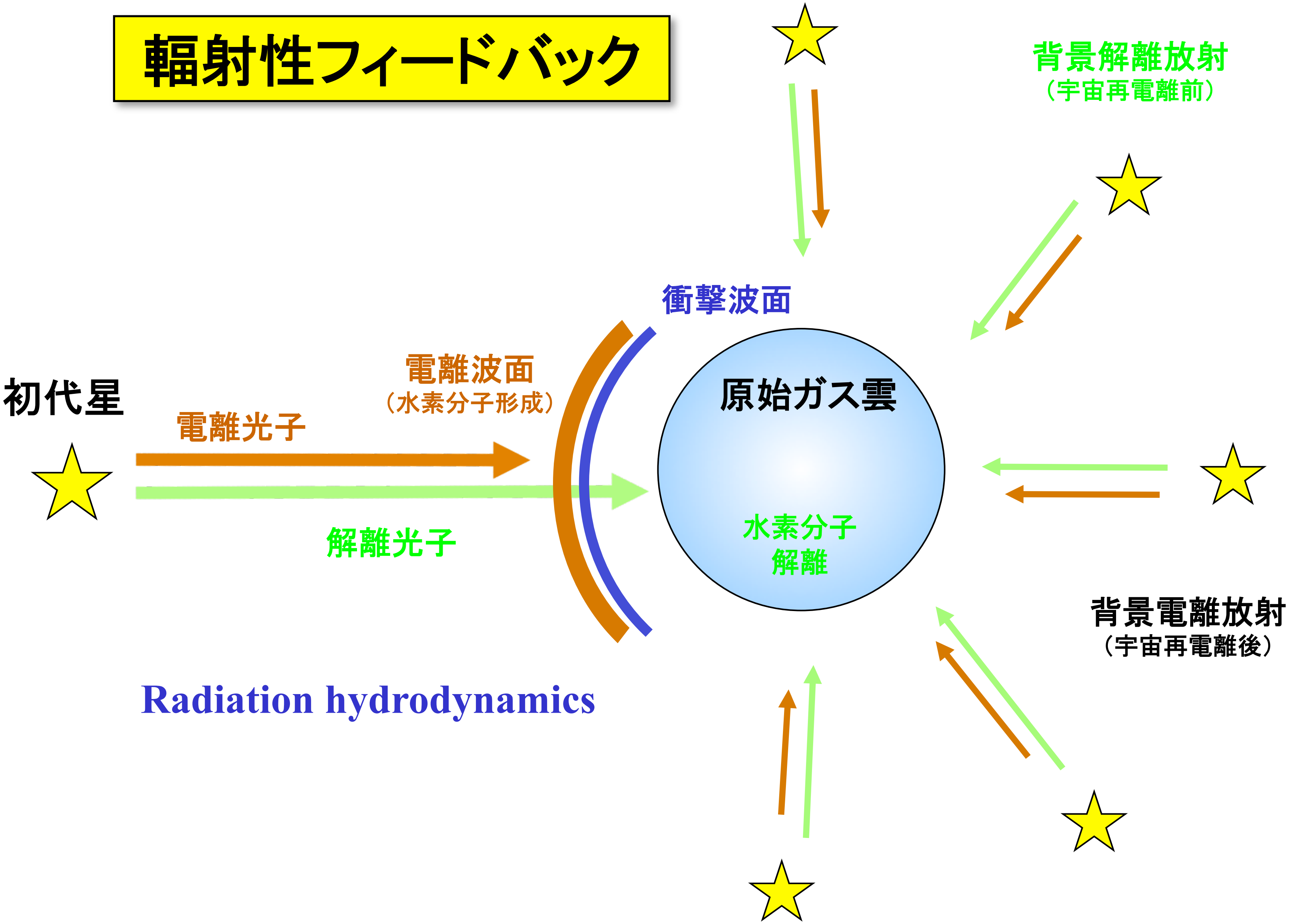
輻射性フィードバック
背景解離放射
（宇宙再電離前）
衝撃波面
電離波面
（水素分子形成）
初代星
電離光子
原始ガス雲
解離光子
水素分子
解離
背景電離放射
（宇宙再電離後）
Radiation hydrodynamics

Rate coefficient of Solomon process

$F_{LW}$ : Lyman-Werner band flux

$$k_{Solomon} = 1.13\times10^{8} F_{LW} \ \mathrm{s}^{-1}$$

Self-shielding (Draine & Bertordi 1996, ApJ, 468, 269)

$$F_{LW} = F_{LW,0} f_{shield}$$

$$f_{shield} = \min\left\{1, \left(\frac{N_{H_2}}{10^{14}\mathrm{cm}^{-2}}\right)^{-0.75}\right\}$$

# Radiation Hydrodynamics with SPH

**Susa & Umemura 2006, ApJ, 645, L93**

**TREE-GRAPE-SPH +Radiative transfer**
**+ Non-equilibrium Chemistry + Thermal processes**

## Optical depth calculations (Ray Tracing)

**Kessel-Deynet & Burkert (2000)**

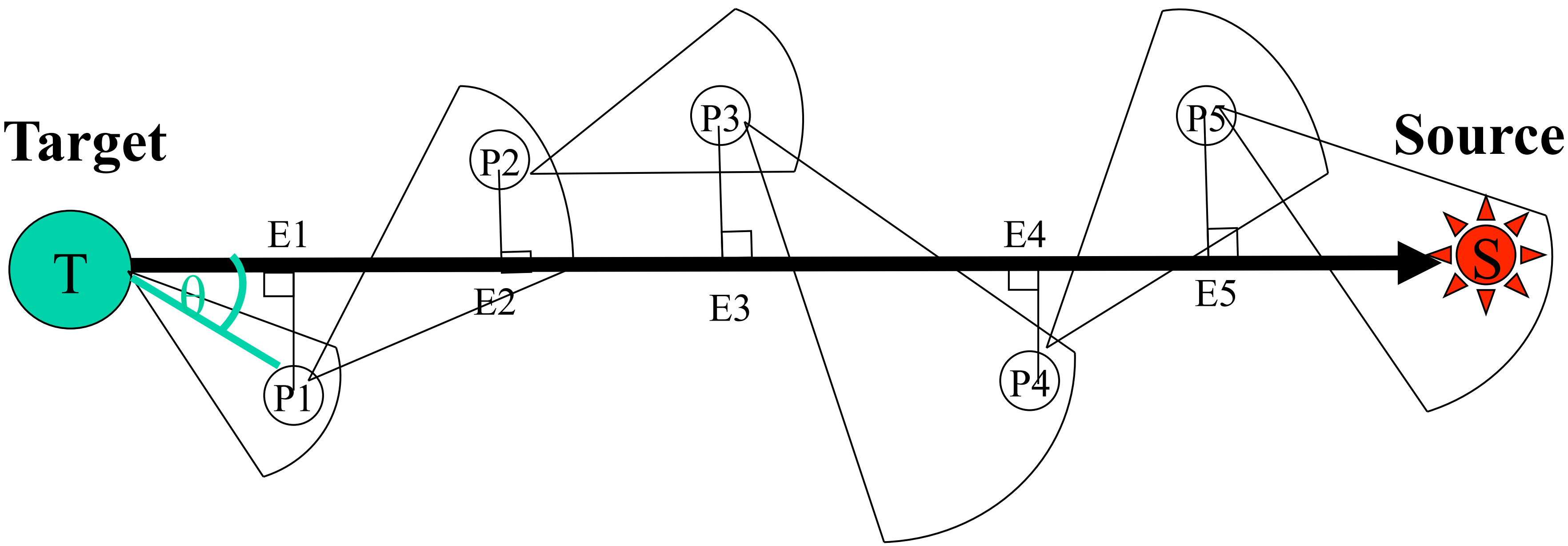


$$\tau_{TS} = \sum_i \frac{\sigma}{2}\left(n_{E_i} + n_{E_{i+1}}\right)\left(s_{E_{i+1}} - s_{E_i}\right)$$

# 輻射流体フィードバックによる星質量の減少

**$m$～$20M_\odot - 300M_\odot$**

Susa, Umemura, Hasegawa, 2009, ApJ, 702, 480

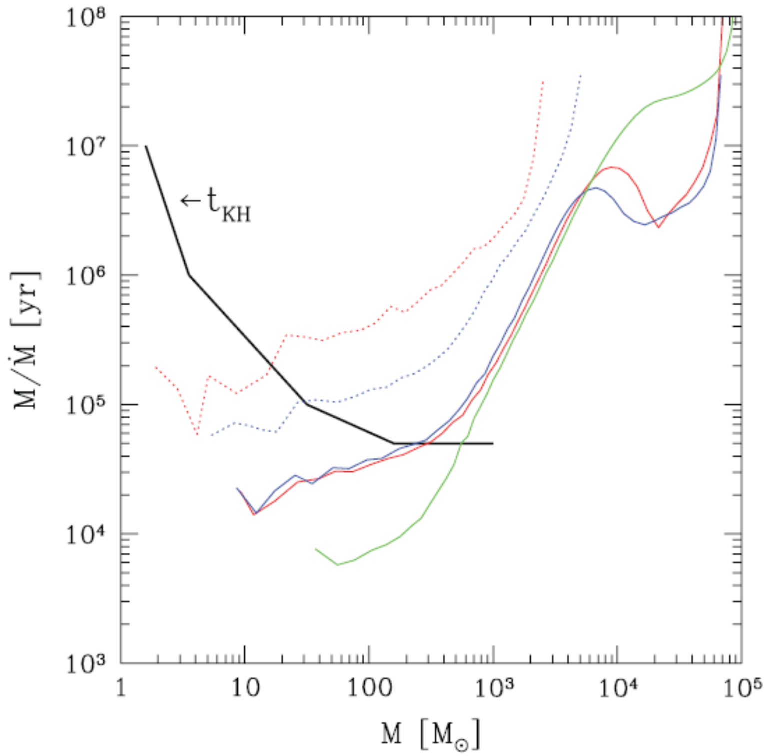


**Figure 11.** Mass accretion timescale ($M/\dot{M}$) and Kelvin–Helmholtz (KH) contraction timescale are plotted for five models in which the cores successfully collapse. All models are low temperature core models (i.e., $T_{c,min} = 150$ K). Green line: no feedback, red solid line: $n_{on} = 10^4$ cm$^{-3}$ and $D = 100$ pc, red dotted line: $n_{on} = 10^4$ cm$^{-3}$ and $D = 50$ pc, blue solid line: $n_{on} = 3 \times 10^3$ cm$^{-3}$ and $D = 150$ pc, and blue dotted: $n_{on} = 3 \times 10^3$ cm$^{-3}$ and $D = 100$ pc. The black line is the KH contraction timescale adopted from O'Shea & Norman (2007).

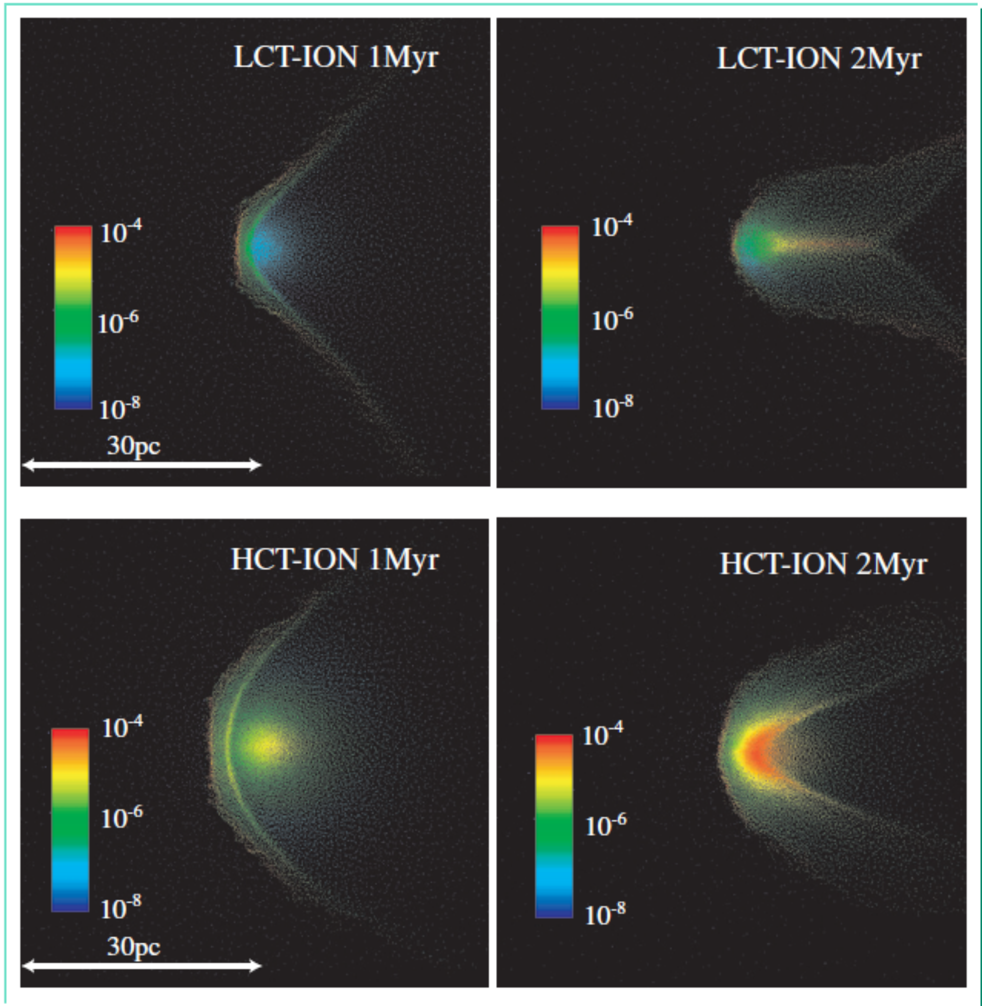


水素分子分布

# 次世代のPopIII星形成条件

Hasegawa, Umemura, Susa, 2009, MNRAS, 395,1280

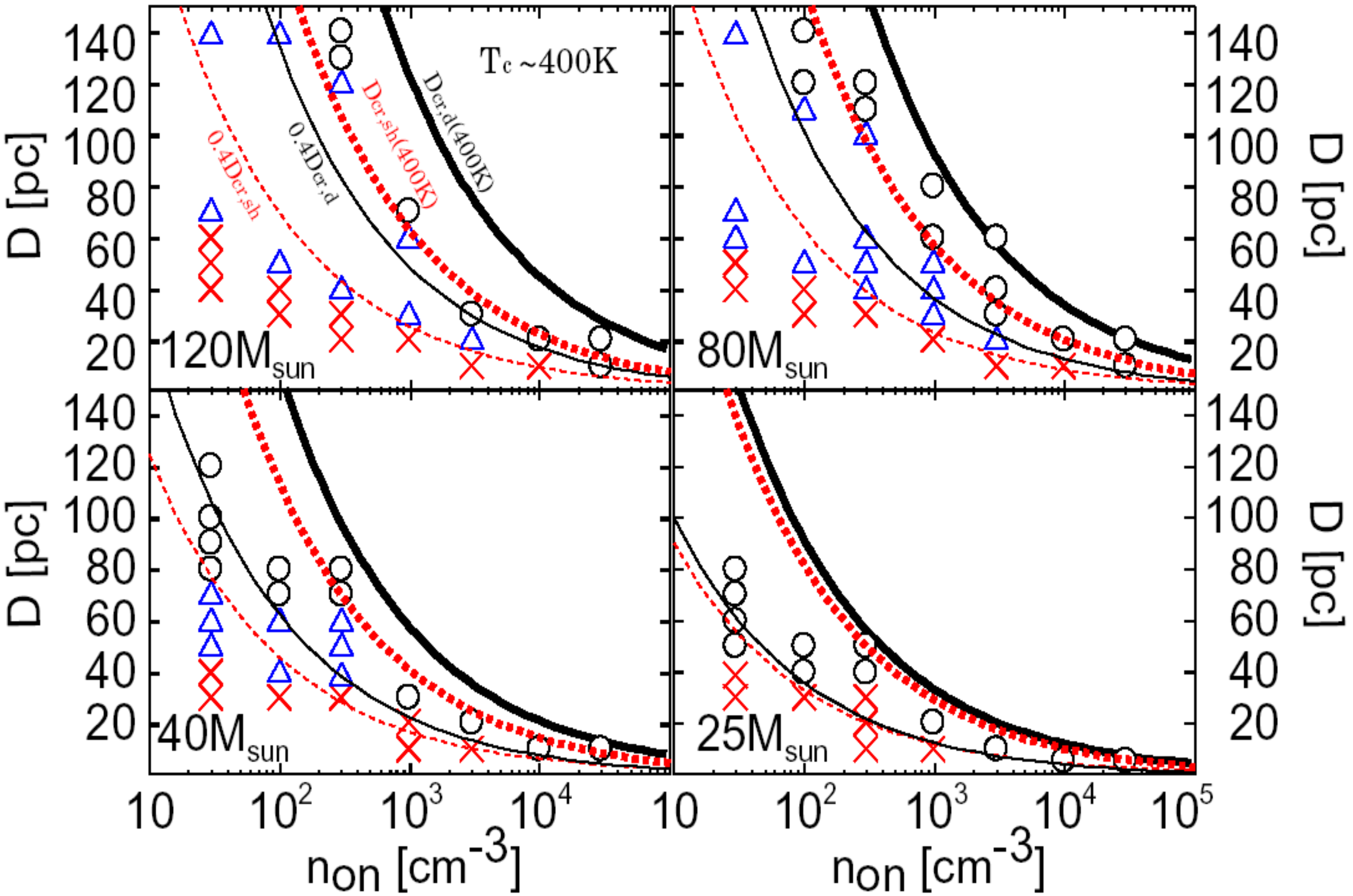


$M_*$ [illegible] $25M_\odot \Rightarrow$ 電離光子によるpositive feedback が起こる

**analytic criterion**

$$D_{\rm cr,sh} = 147{\rm pc}\left(\frac{L_{LW} f_{s,sh}}{5\times10^{23}{\rm erg\ s^{-1}}}\right)^{\frac{1}{2}}\left(\frac{n_c}{10^3{\rm cm^{-3}}}\right)^{-\frac{7}{16}}\left(\frac{T_c}{300{\rm K}}\right)^{-\frac{3}{4}}$$

# PopIII Star Formation

| *Fundamental* | *Cosmological* |
|---|---|
| 熱的不安定 | ダークマターによる温度上昇 |
| ガス降着率 | 球対称計算と整合 |
| 重力不安定による分裂 | 見えている？ |
| 隣接星のフィードバックによる質量減少 | これから（cosmological RHD） |
| 背景紫外線の効果（含HD分子冷却） | 整合 |
| PopIII連星形成 | 可能性が示された |
| 磁場の効果 | 要検討 |

# Contents

## Pop III.1 (1st generation Pop III)

- first collapse
- core fragmentation
- binary formation
- magnetic fields

## Pop III.2 (2nd generation Pop III)

- UV feedback
- Pop III star formation in pre-ionized gas (HD cooling)

## Pop II.1 (1st generation Metal Poor Star )

- metal/dust cooling

# Fate of Pop III Stars

Heger & Woosley
2002, ApJ, 567, 532

**$8M_\odot < m$ ☒ $25M_\odot$:**
**type II supernova**

**$25M_\odot$ ☒ $m$ ☒ $140M_\odot$:**
**supernova (hypernova)**
**→ black hole (core collapse)**

**$140M_\odot$ ☒ $m$ ☒ $260M_\odot$:**
**pair instability supernova**
**(no evidence from abundance pattern)**

**$m$ ☒ $260M_\odot$:**
**black hole (implosion)**

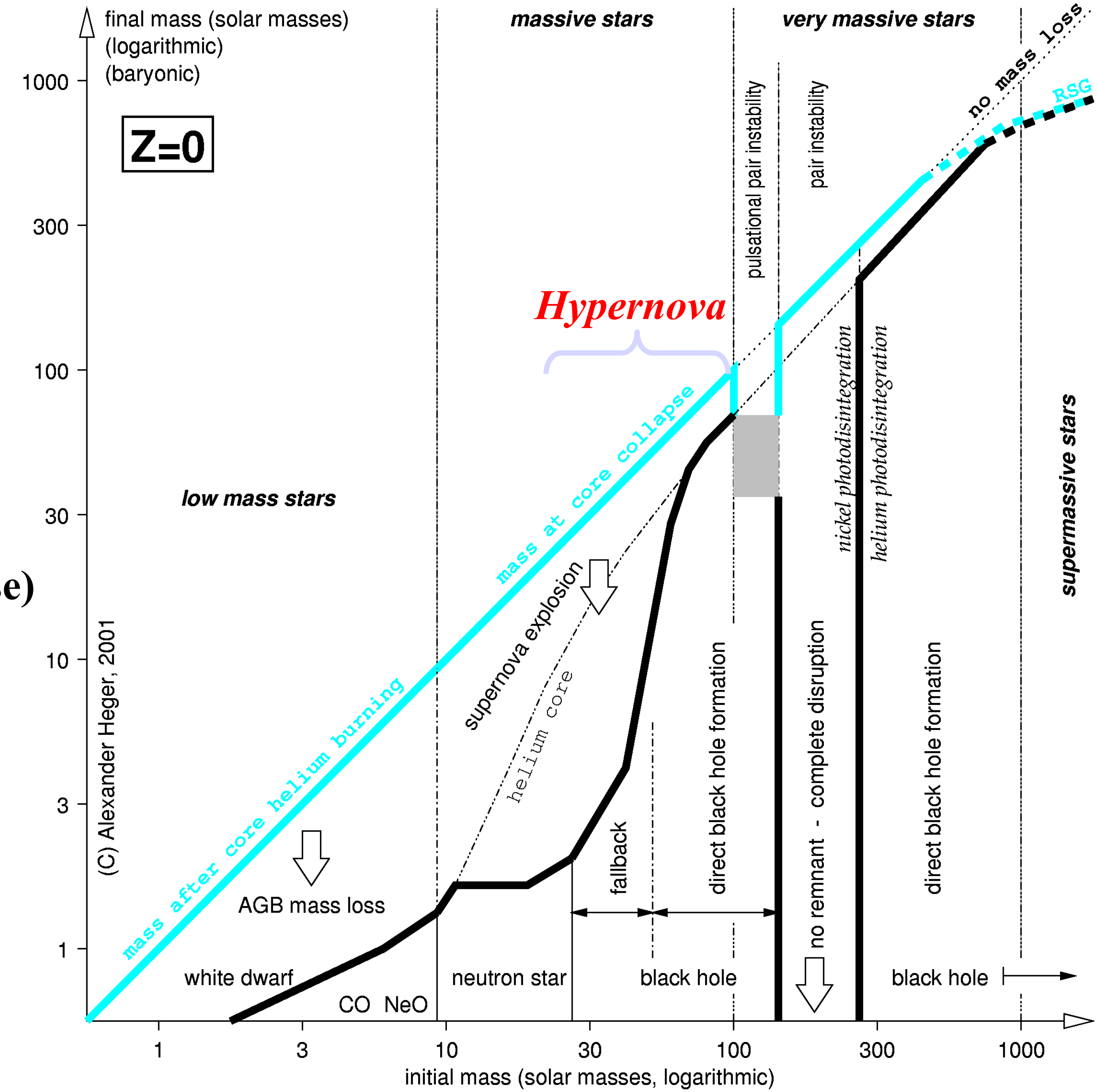

# Stellar Evolution with Various Metallicity

Omukai, Tsuribe, Schneider & Ferrara (2005)

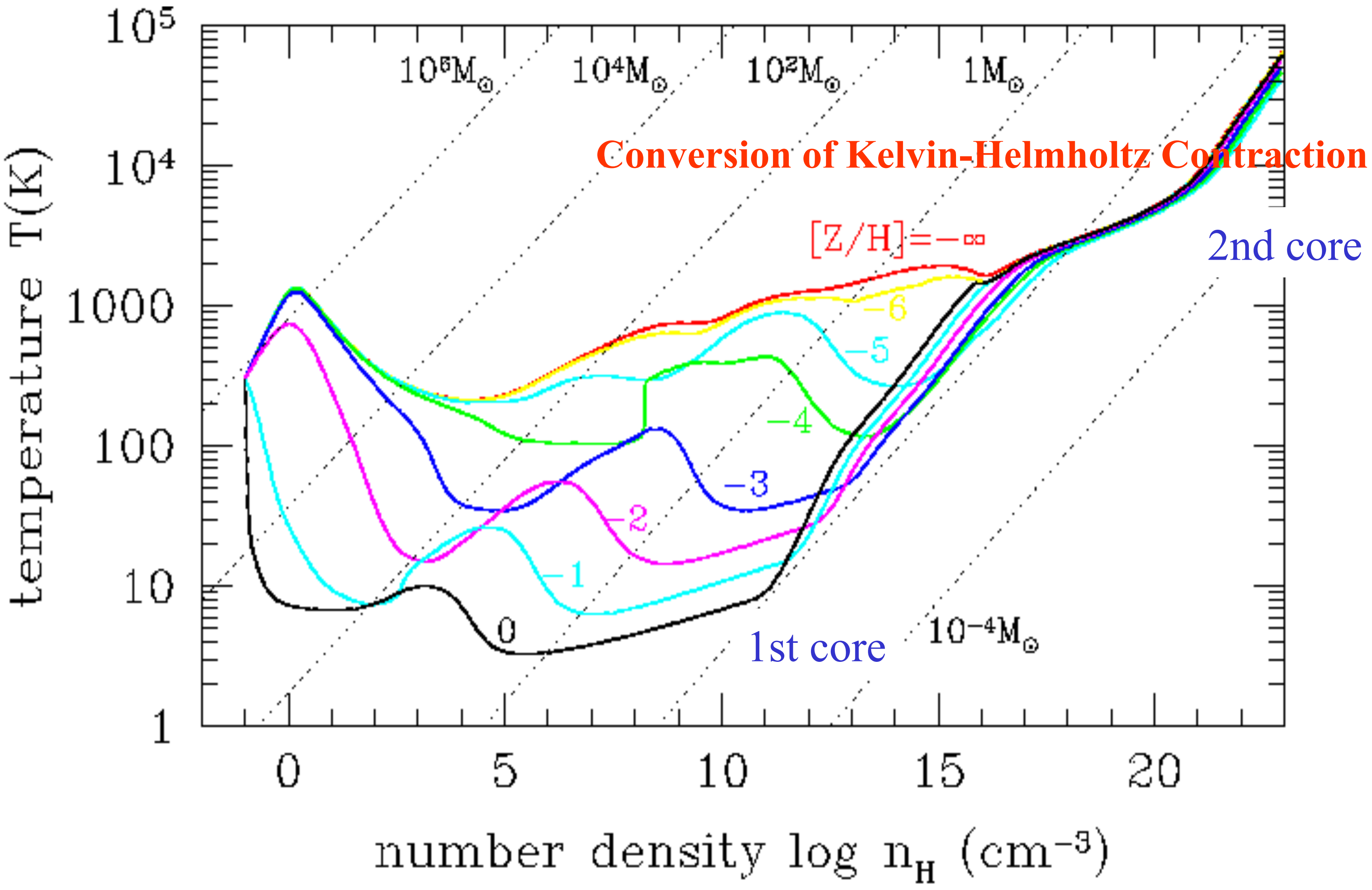

# Population II.1

Bromm et al 2001; Schneider et al 2002; Bromm & Loeb 2003; Omukai et al 2005;
Santoro & Shull 2006; Schneider et al 2006; Tsuribe & Omukai 2006; Clark, Glover & Klessen 2007;
Smith & Sigurdsson 2007

ZとIMFの関係は？

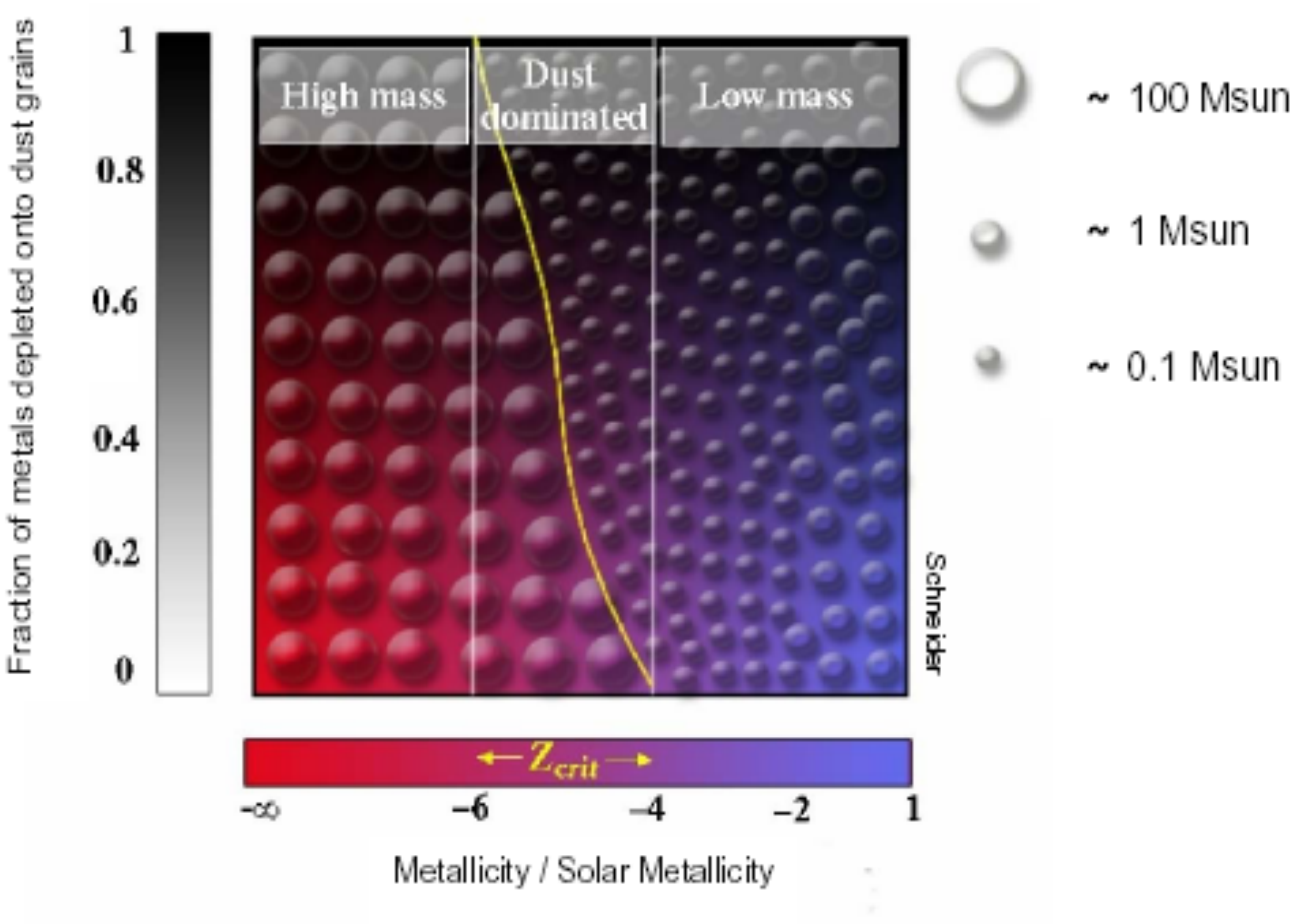

# Fragmentation in Very Low Metallicity

*Fundamental*

**Bromm, Ferrara, Coppi & Larson 2001**

The fragmentation of the $Z \approx 10^{-3} Z_{\odot}$ gas leads to relatively numerous low-mass clumps.

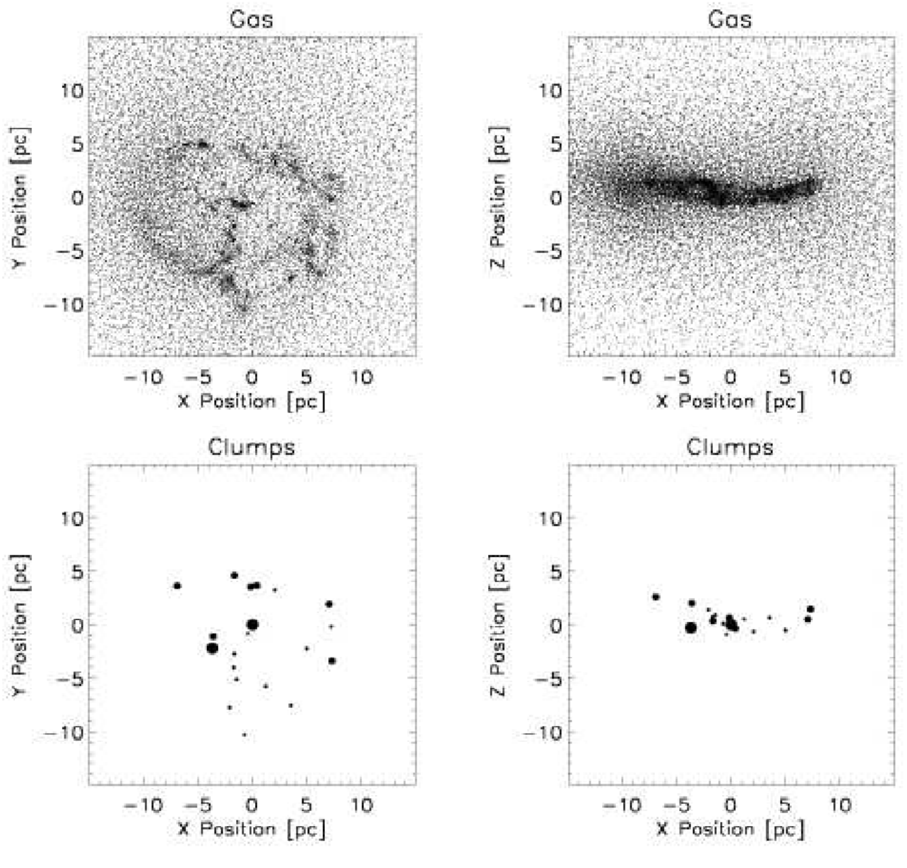


**Tsuribe & Omukai 2006**

$Z \approx 10^{-6}$-$10^{-5} Z_{\odot}$

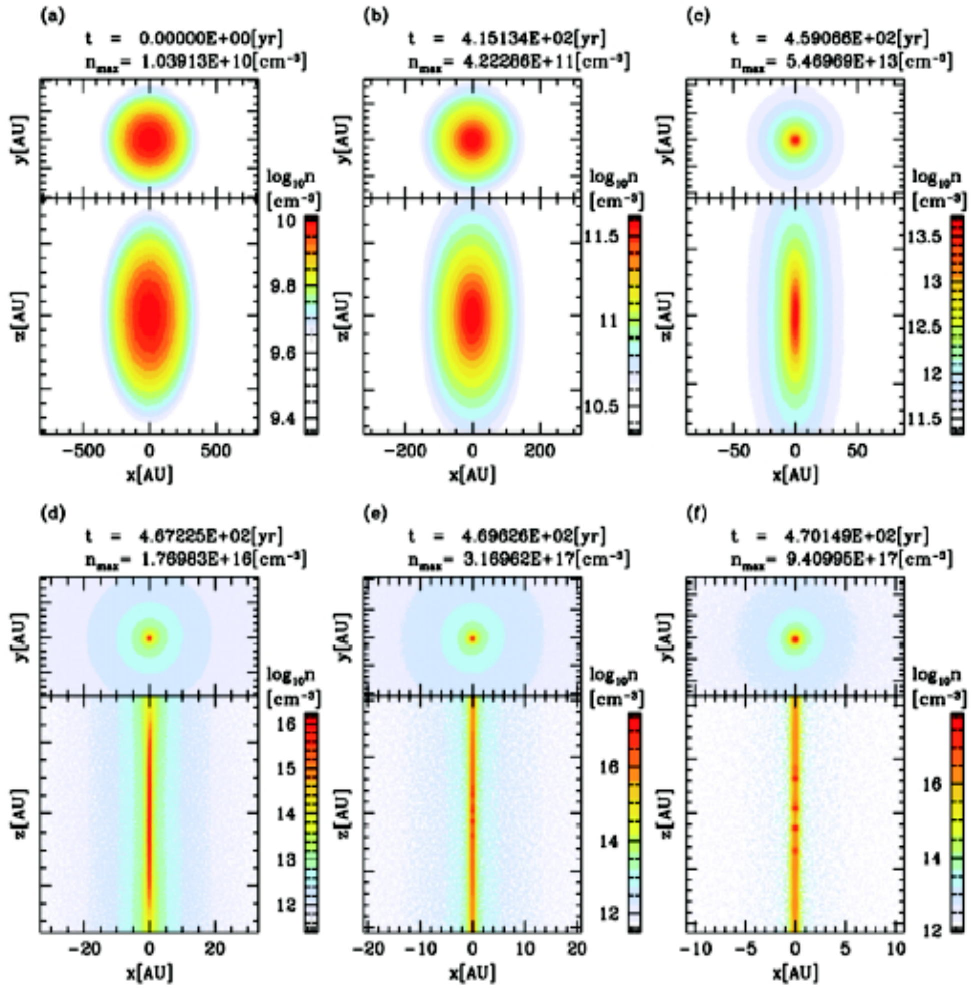

# 低金属量ガス雲中での星形成

町田正博 (京大), 大向一行(NAOJ), 松本倫明(法政大), 犬塚修一郎(京大)

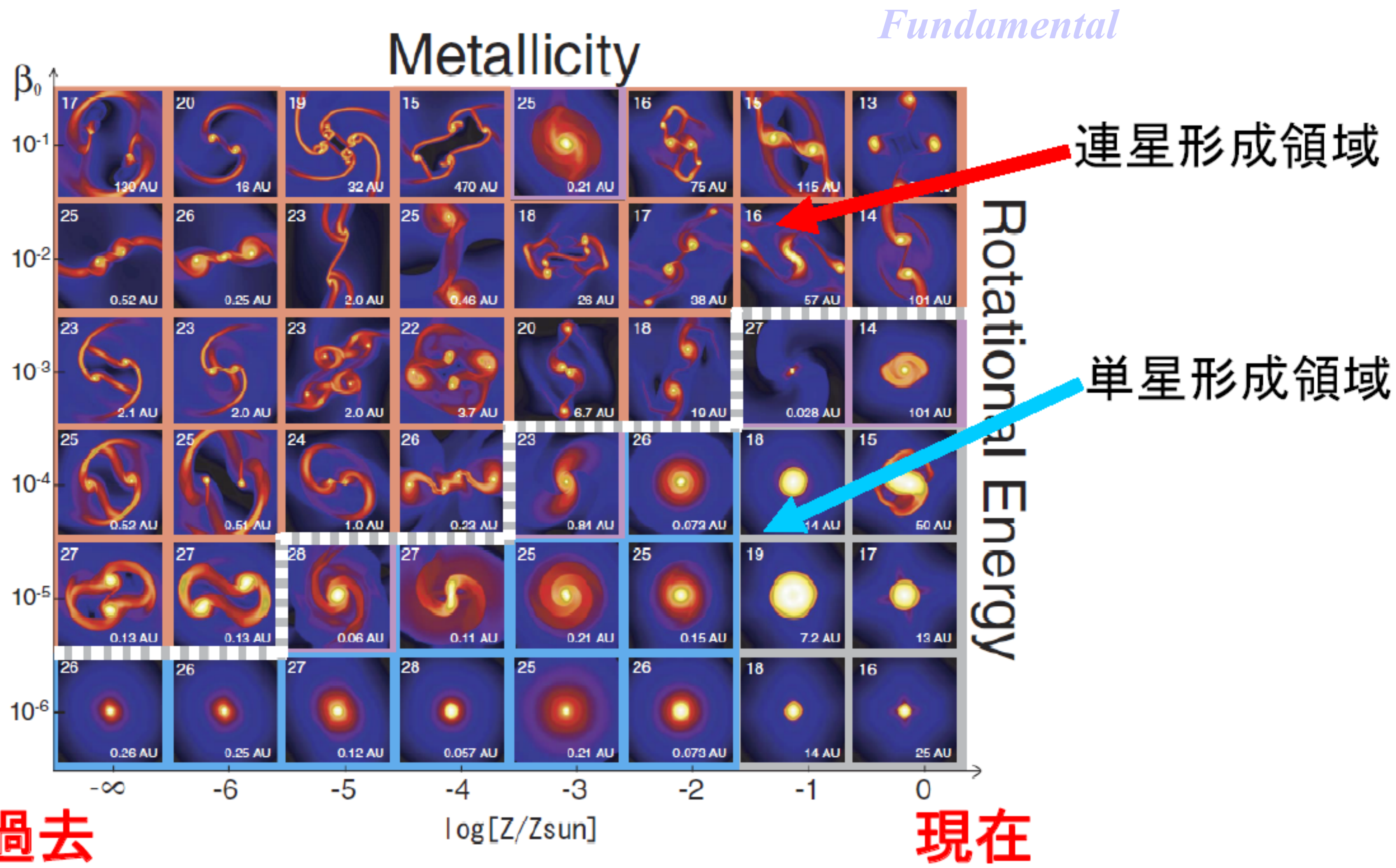

# 宇宙再電離

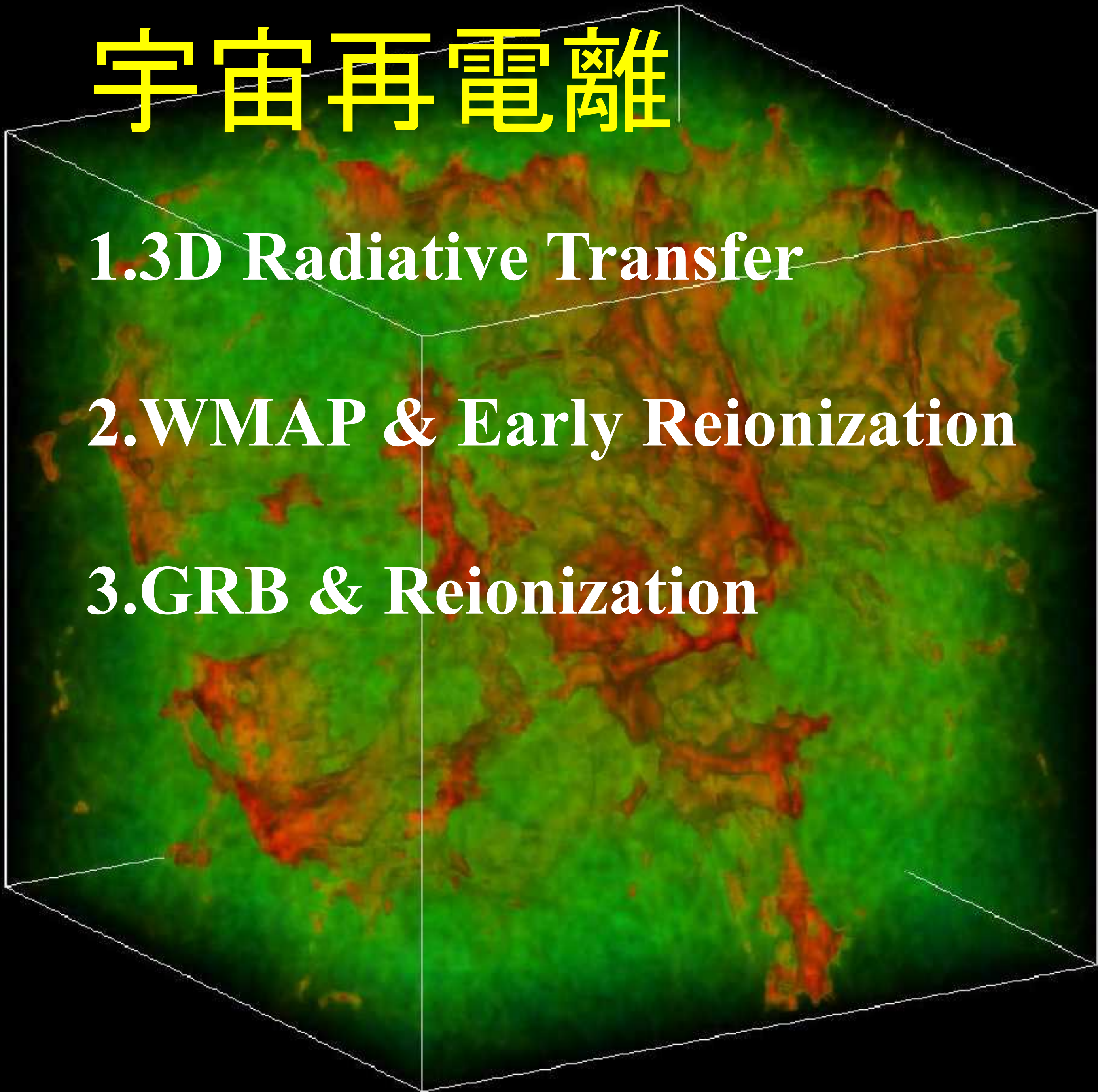

1. 3D Radiative Transfer
2. WMAP & Early Reionization
3. GRB & Reionization

# Continuum Depression $D_A \equiv \int_{\nu_{Ly\alpha}}^{\nu_{Ly\beta}} \frac{f_{cont} - f_{obs}}{f_{cont}} d\nu \Big/ (\nu_{Ly\beta} - \nu_{Ly\alpha})$

## SDSSp J103027.10+052455.0 (z=6.28)

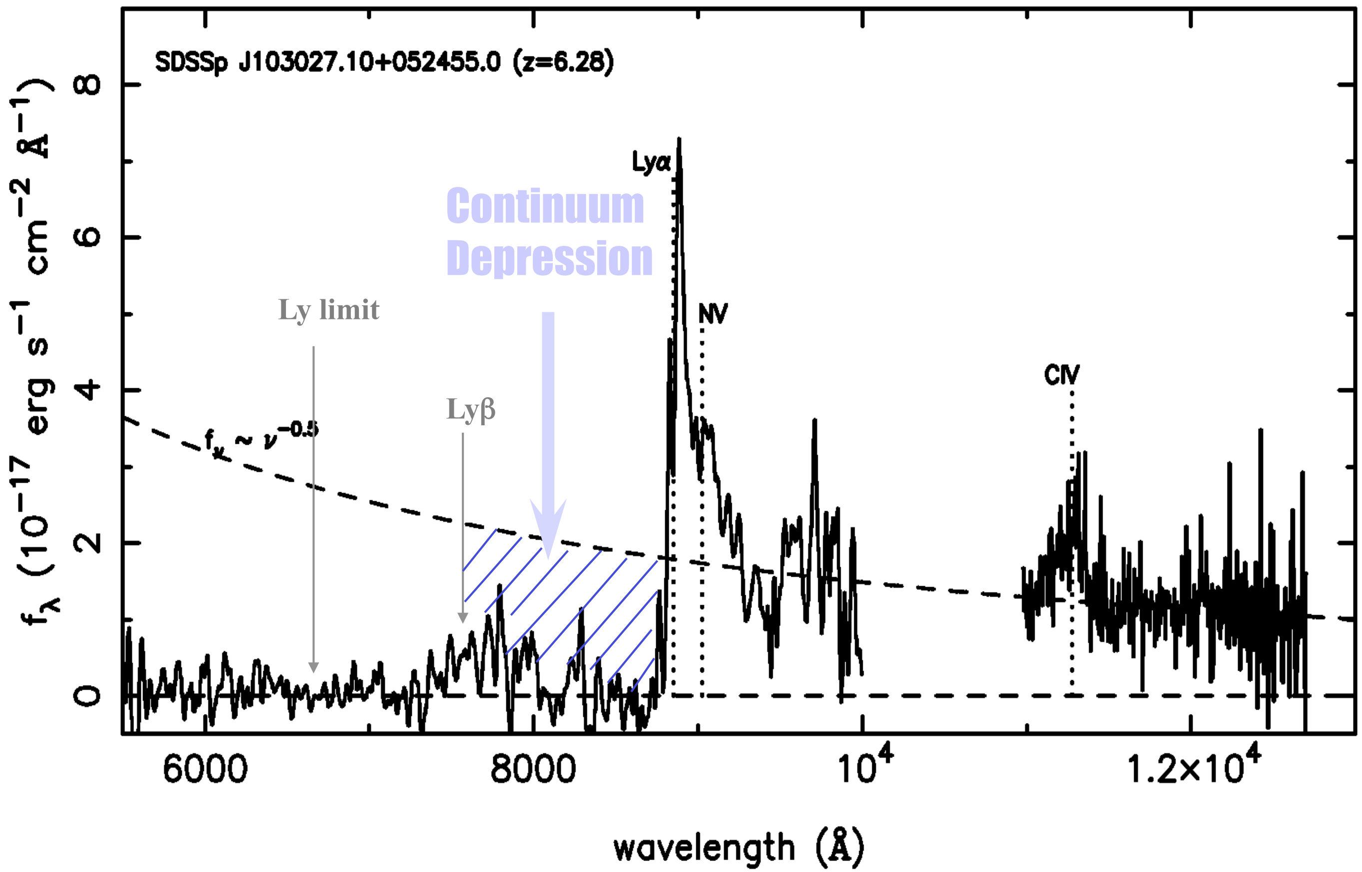


Figure 6. Combined optical + near IR spectrum of SDSS 1030+0524. The optical spectrum is a 3600 second exposure taken with ARC 3.5m telescope (same as in Figure 5). The near IR spectrum is a 3000 second exposure taken with Keck/NIRSPEC. The resolution of the near IR spectrum is $R \sim 1500$.

## Lyα Continuum Depression

$$D_A \equiv \int_{\nu_{\mathrm{Ly}\alpha}}^{\nu_{\mathrm{Ly}\beta}} \frac{f_{\mathrm{cont}} - f_{\mathrm{obs}}}{f_{\mathrm{cont}}} d\nu \Big/ (\nu_{\mathrm{Ly}\beta} - \nu_{\mathrm{Ly}\alpha})$$

① **Evolution of $I_{UV}$:**

**$I_{21} \approx 1$ at z=3**

**$I_{21} \approx 0.1$ at z=4**

**$I_{21} \approx 0.01$ at z=5**

② **$z_{reion} \approx$ 7-10**

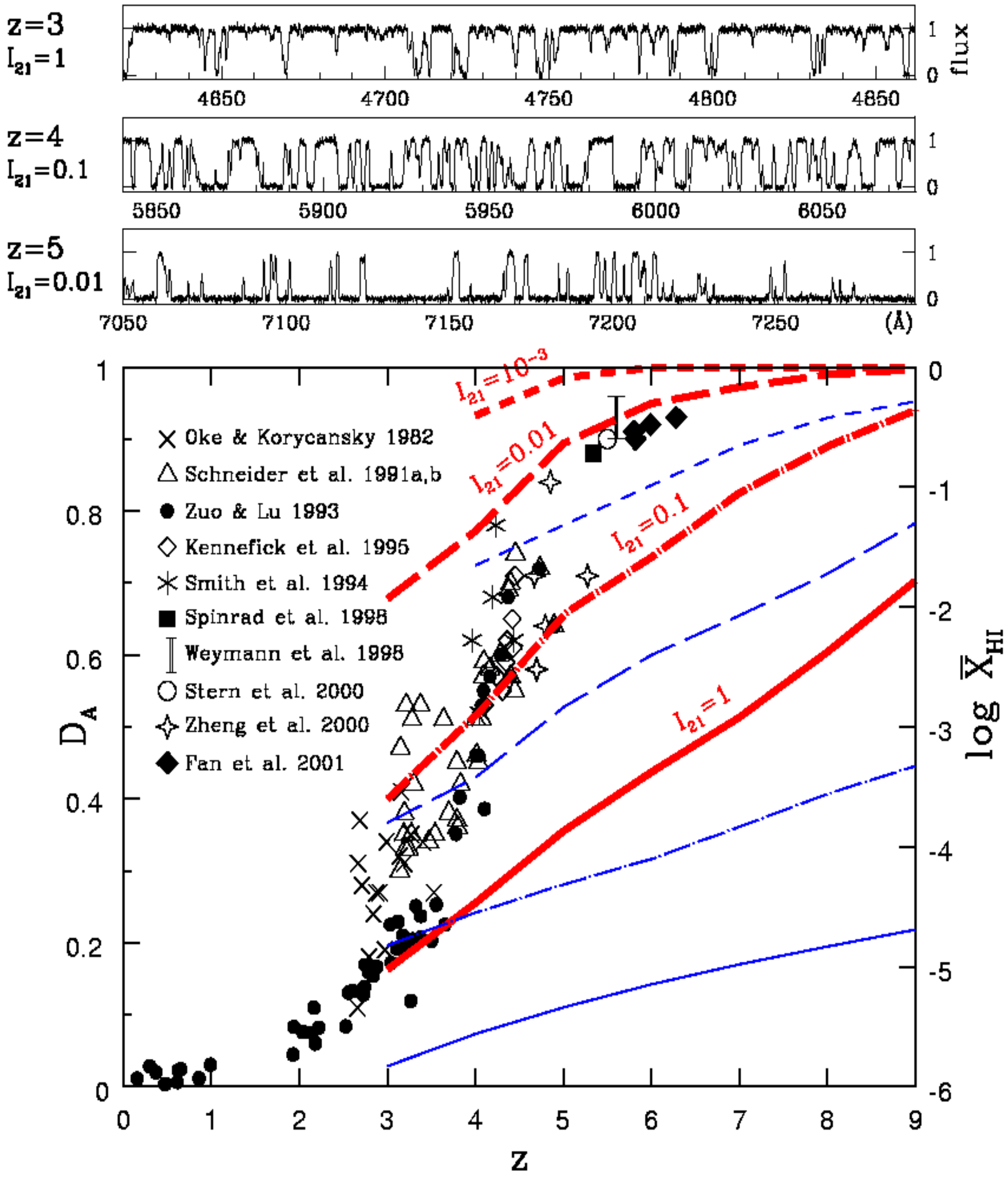

# Radiative Transfer Equation

$$\frac{1}{c}\frac{\partial I_\nu}{\partial t} + \mathbf{n}\cdot\nabla I_\nu = \chi_\nu (S_\nu - I_\nu)$$

**Lorentz-Transformed Boltzmann Equation for Photon Distribution Function**

**6 Degrees of Freedom = 3D (space) + 2D (directions) + 1D (frequency)**

***Space:*** $N^3 = 128^3$ **in (8Mpc)$^3$** $\left(\Rightarrow \frac{1}{c}\frac{\partial I_\nu}{\partial t} = 0\right)$

***Directions:*** $N_\theta \times N_\varphi = 128^2$

***Frequency:*** $N_\nu = 6$ **lines for H & He, analytic integration for continuum**

- **Total operations:** $f N_{iter} N^3 N_\theta N_\varphi N_\nu = 11.4$ **Tflops·hr** ($f \approx 2000$, $N_{iter} = 100$)
- **Performed with the CP-PACS (614GFLOPS)**

# Reionization History in an Inhomogeneous Universe

**The reionization of an inhomogeneous universe is not a prompt event, but a fairly slow process !**

$I_{21}$=0.1

0.3Gyr

0.5Gyr

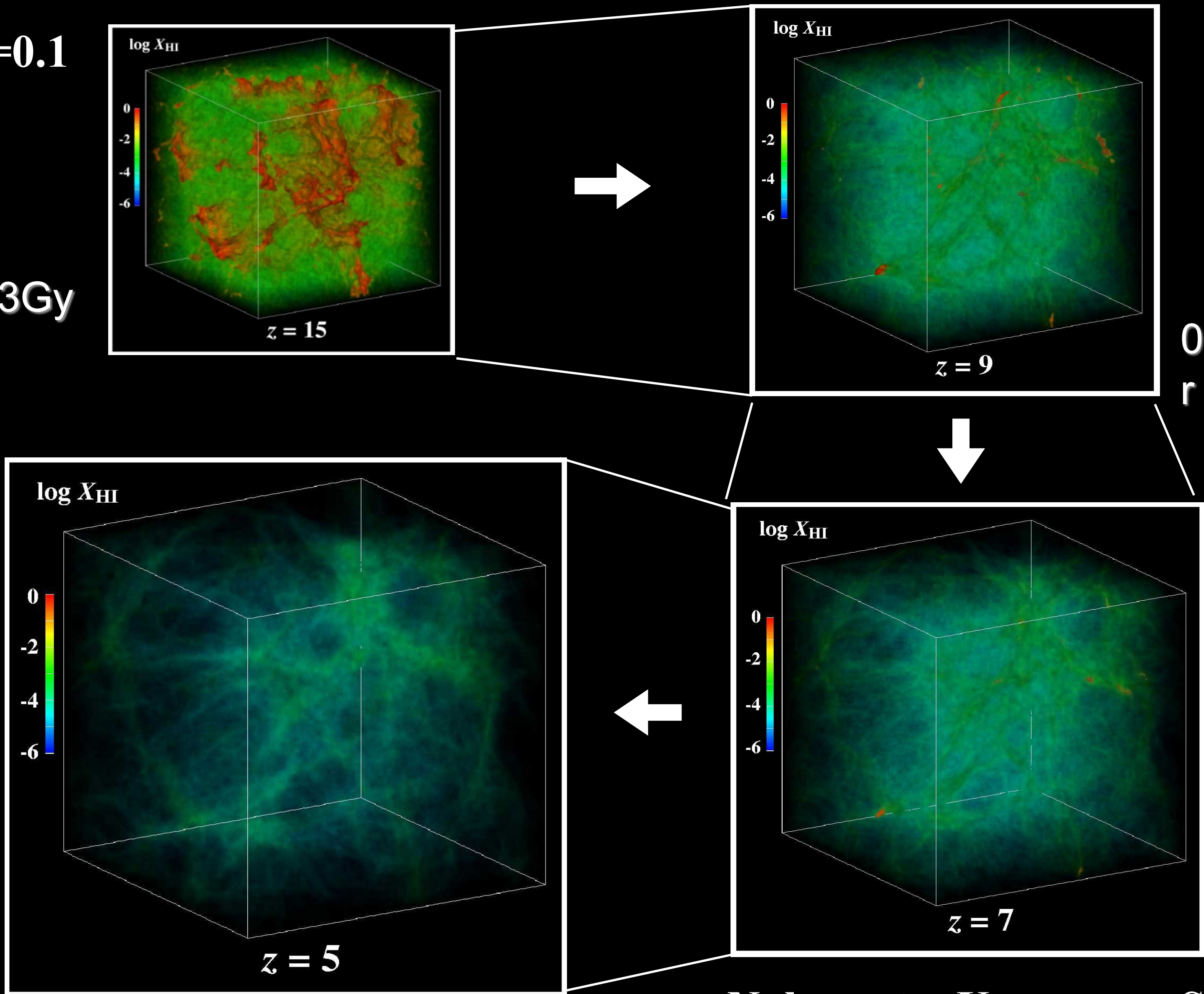


0.7Gyr

1Gyr

Nakamoto, Umemura, Susa, 2001

# Propagation of Ionizing Front

**Yoshida et al. 2003**

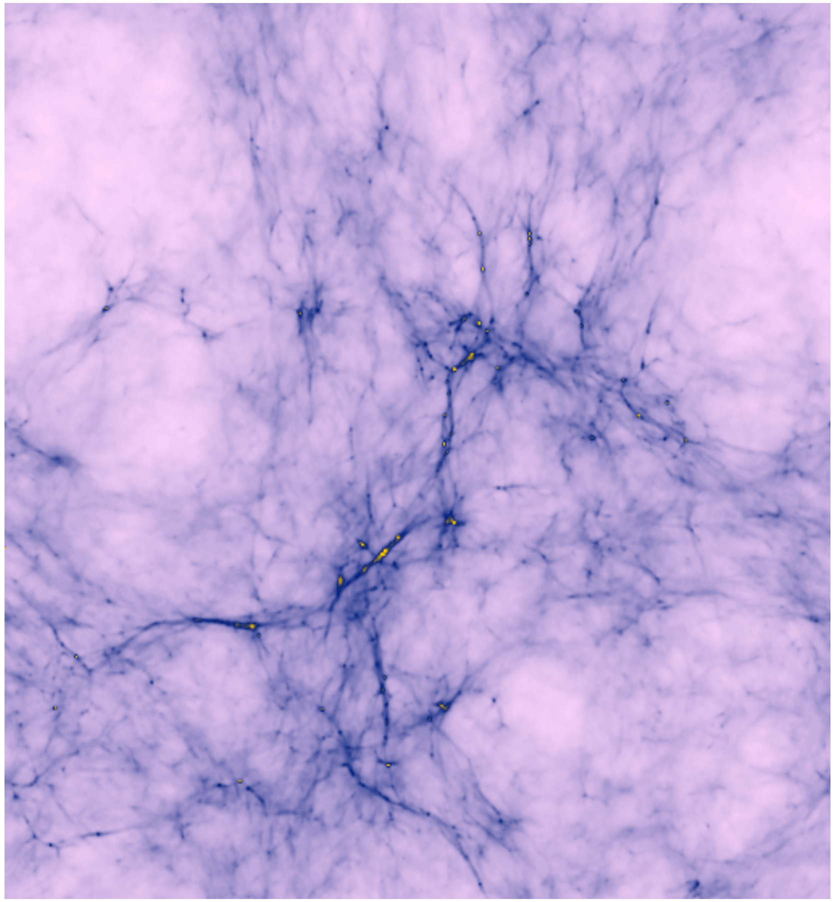

**Stars in molecular gas clouds**

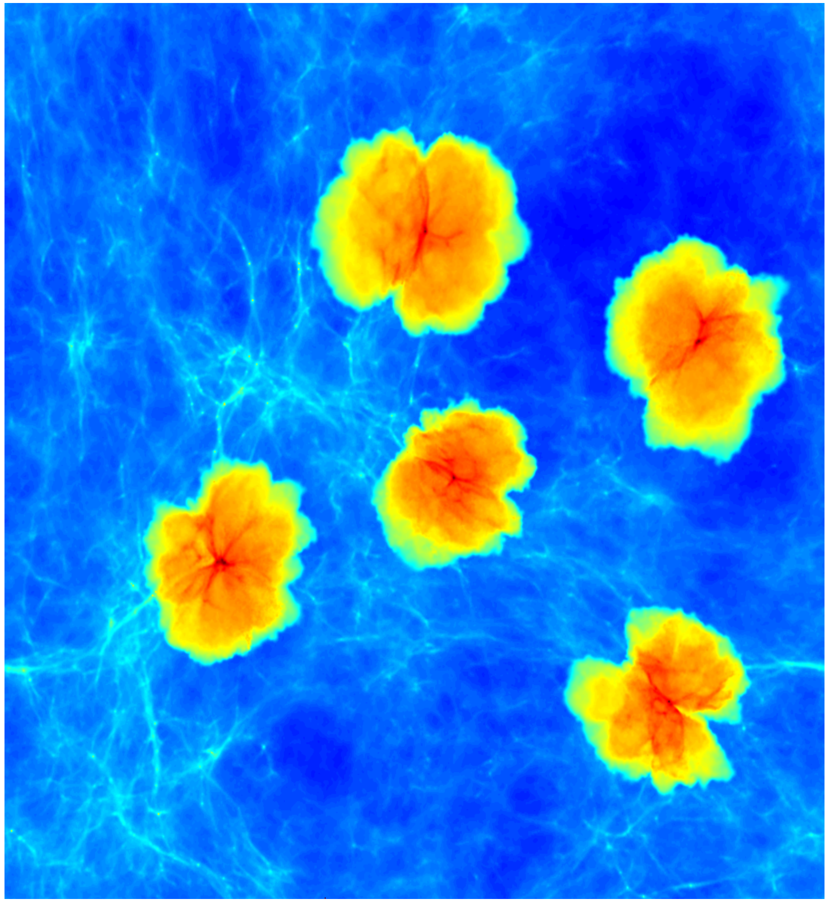

**HII regions + soft UV**

# Cosmological Radiative Transfer Codes Comparison Project I: The Static Density Field Tests

**2006, MNRAS, 371, 1057**

**Ilian T. Iliev, Benedetta Ciardi, Marcelo A. Alvarez, Antonella Maselli, Andrea Ferrara, Nickolay Y. Gnedin, Garrelt Mellema, Taishi Nakamoto, Michael L. Norman, Alexei O. Razoumov, Erik-Jan Rijkhorst, Jelle Ritzerveld, Paul R. Shapiro, Hajime Susa, Masayuki Umemura, Daniel J. Whalen**

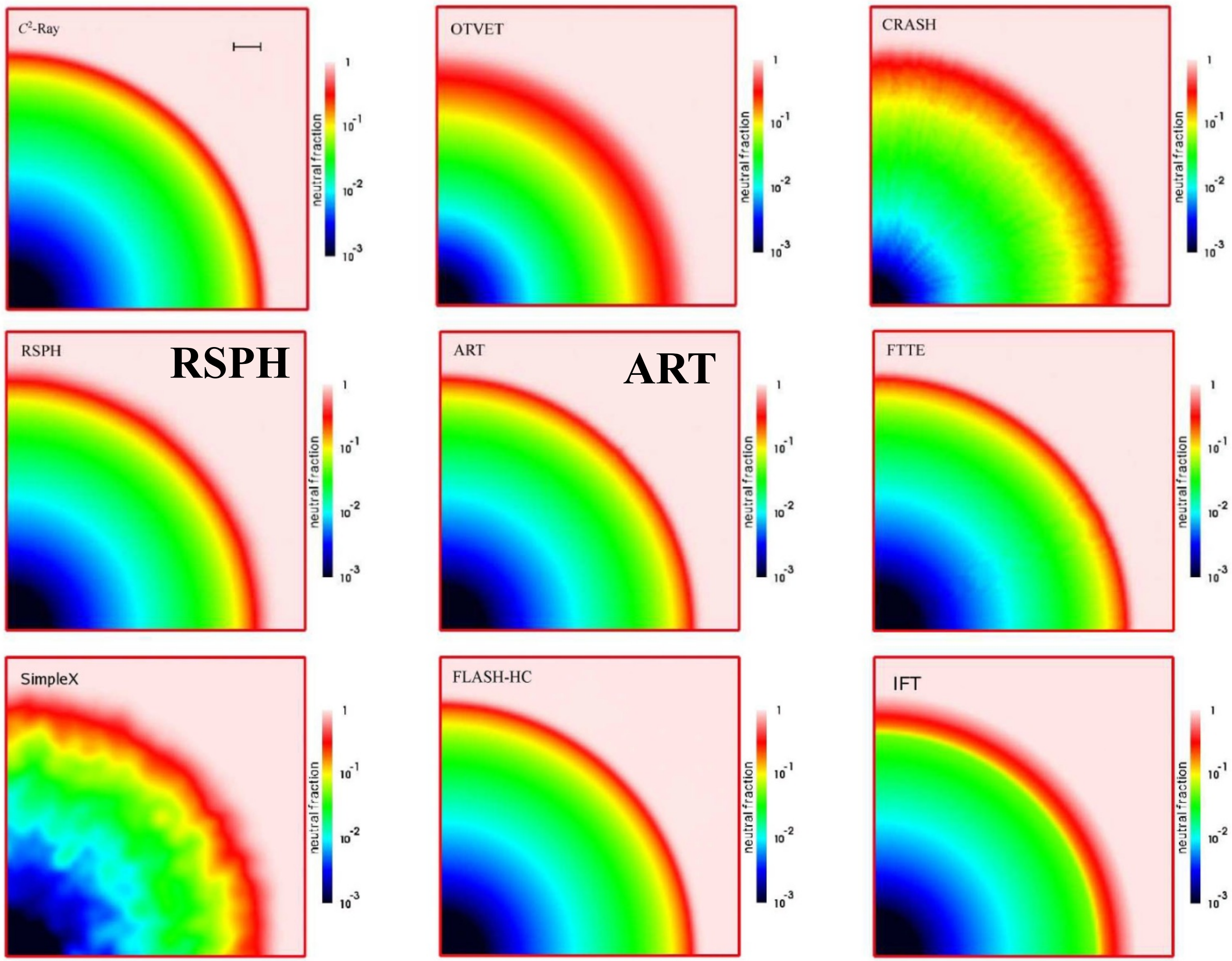


**Figure 6.** Test 1 (H II region expansion in an uniform gas at fixed temperature): Images of the H I fraction, cut through the simulation volume at coordinate $z = 0$ at time $t = 500$ Myr (final Strömgren sphere) for (left to right and top to bottom) $C^2$-Ray, OTVET, CRASH, RSPH, ART, FTTE, SimpleX, FLASH-HC

WMAP polarization pattern
&
宇宙再電離

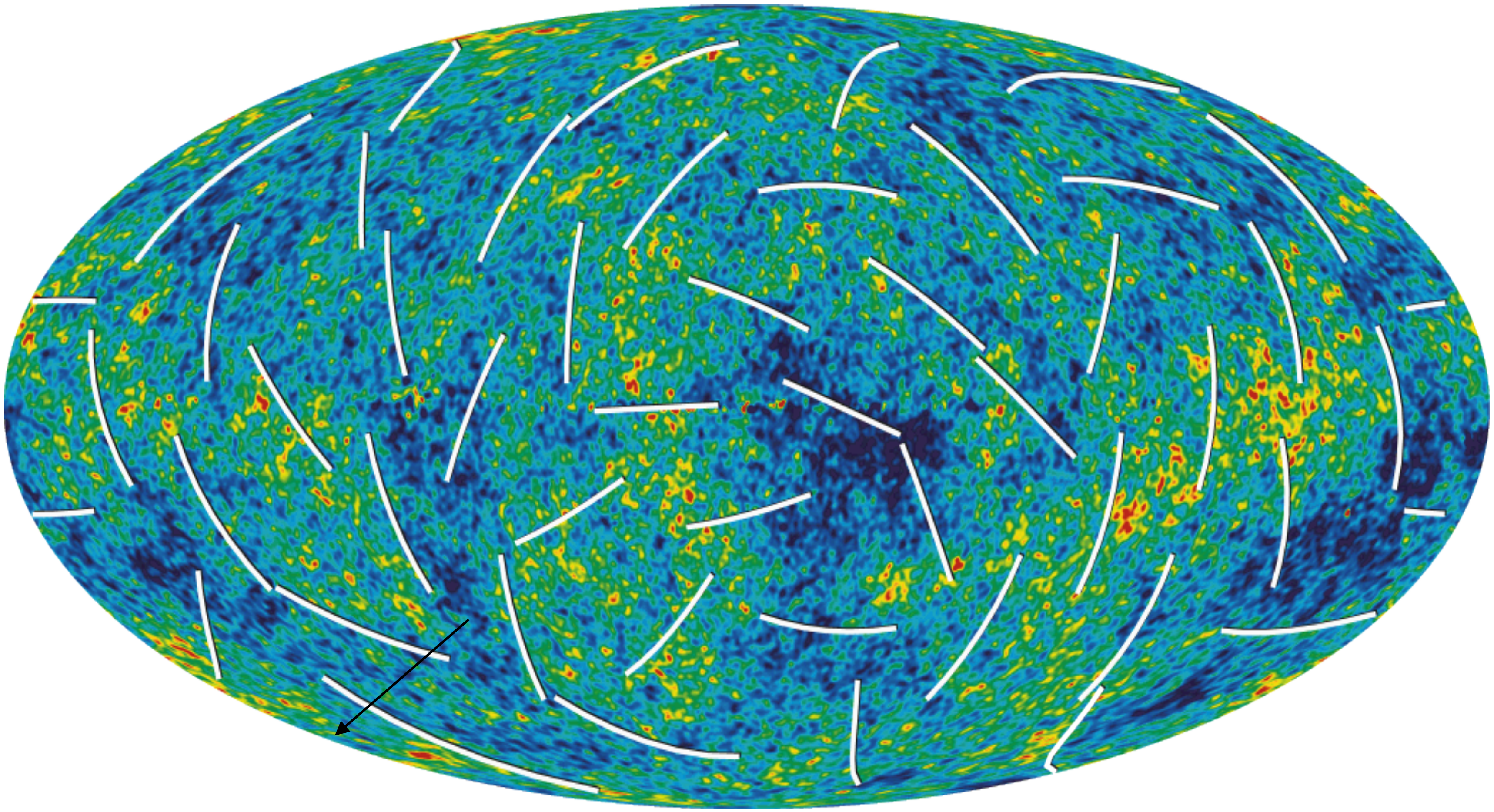

$$\tau_e = 0.084 \pm 0.016$$

$$z_{\text{reion}} = 10.9 \pm 1.4$$

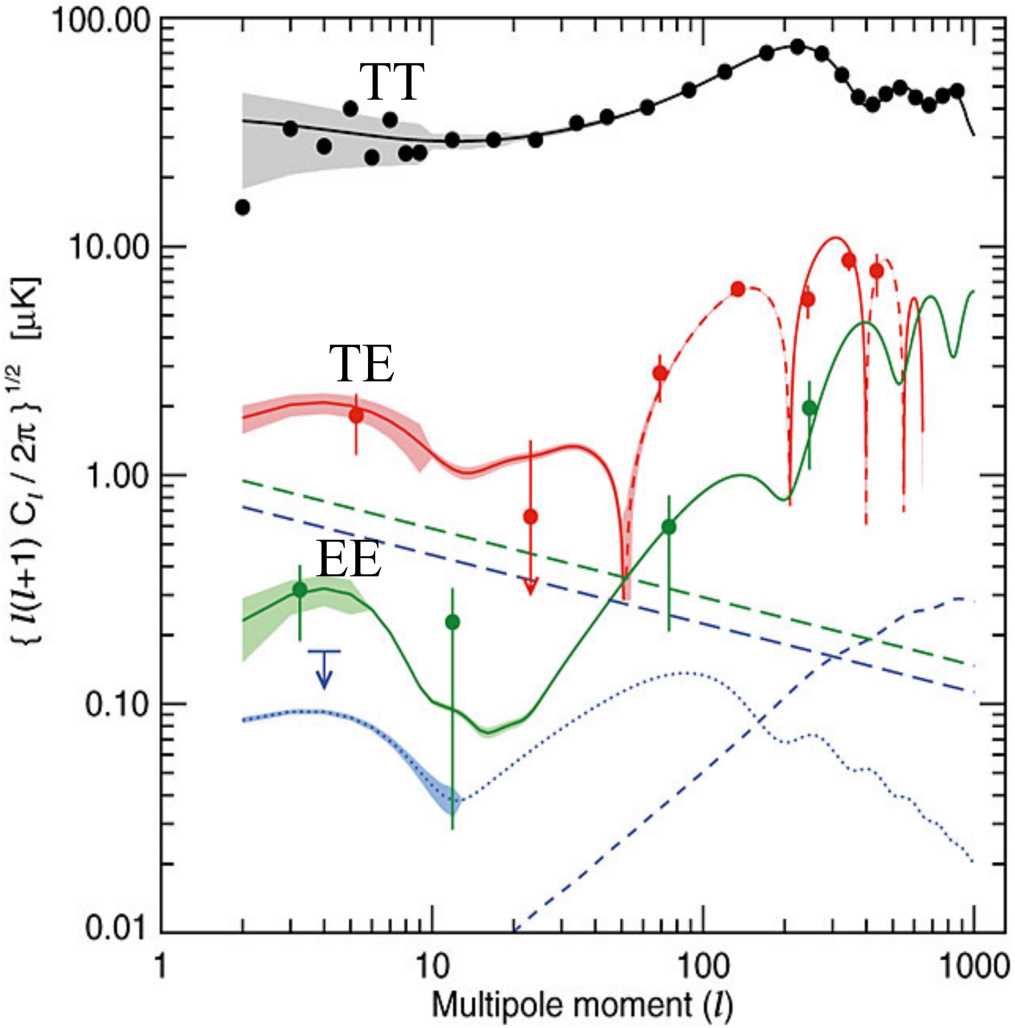


FIG. 25.— Plots of signal for TT (black), TE (red), EE (green) for the best fit model. The dashed line for TE indicates areas of anticorrelation. The cosmic variance is shown as a light swath around each model. It is binned in $\ell$ in the same way as the data. Thus, its variations reflect transitions between $\ell$ bin sizes. All error bars include the signal times noise term. The $\ell$ at which each point is plotted is found from the weighted mean of the data comprising the bin. This is most conspicuous for EE where the data are divided into bins of $2 \leq \ell \leq 5$, $6 \leq \ell \leq 49$, $50 \leq \ell \leq 199$, and $200 \leq \ell \leq 799$. The lowest $\ell$ point shows the cleaned QV data, the next shows the cleaned QVW data, and the last two show the pre-cleaned QVW data. There is possibly residual foreground contamination in the second point because our model is not so effective in this range as discussed in the text. For BB (blue dots), we show a model with $r = 0.3$. It is dotted to indicate that at this time *WMAP* only limits the signal. We show the $1\sigma$ limit of 0.17 $\mu$K for the weighted average of $\ell = 2-10$. The BB lensing signal is shown as a blue dashed line. The foreground model (Equation 25) for synchrotron plus dust emission is shown as straight dashed lines with green for EE and blue for BB. Both are evaluated at $\nu = 65$ GHz. Recall that this is an average level and does not emphasize the $\ell$s where the emission is low.

# Early Reionization Process

**Ciardi, Ferrara & White 2003, MNRAS, 334, L17**

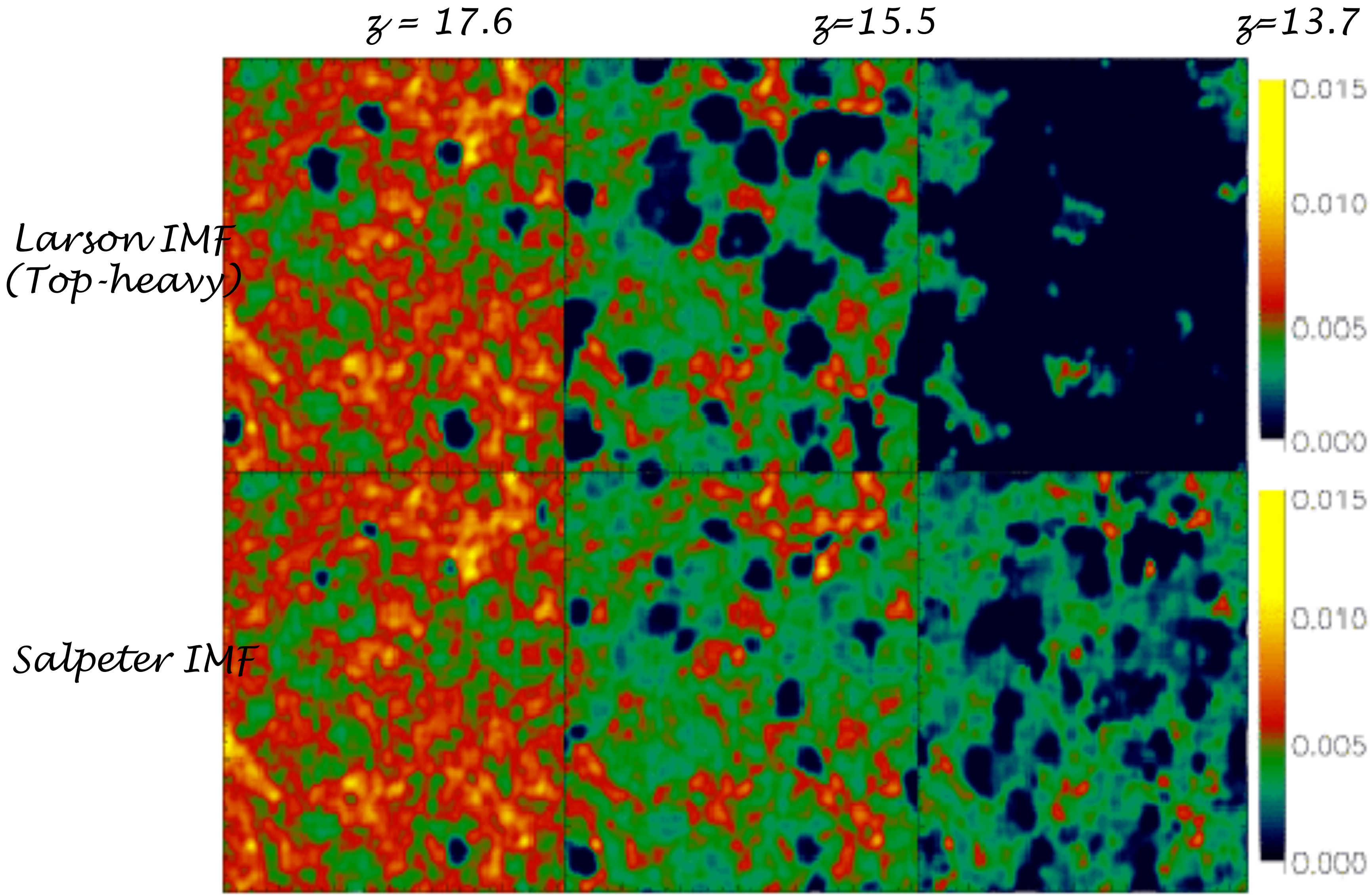

# Simulations of Reionization by Pop III Stars

Cen 2003; Ciardi, Ferrara & White 2003; Somerville & Livio 2003; Fukugita & Kawasaki 2003; Wyithe & Loeb 2003; Sokasian et al. 2004; Ricotti & Ostriker 2004

Sokasian et al. 2004, MNRAS, 350, 47

1 Pop III star per halo of $10^6 M_\odot$, $f_{esc}$=1
WMAP 1st year $\tau_e$=0.17±0.04 (Spergel+03)
WMAP Five year $\tau_e$=0.084±0.016 (Komatsu+09)

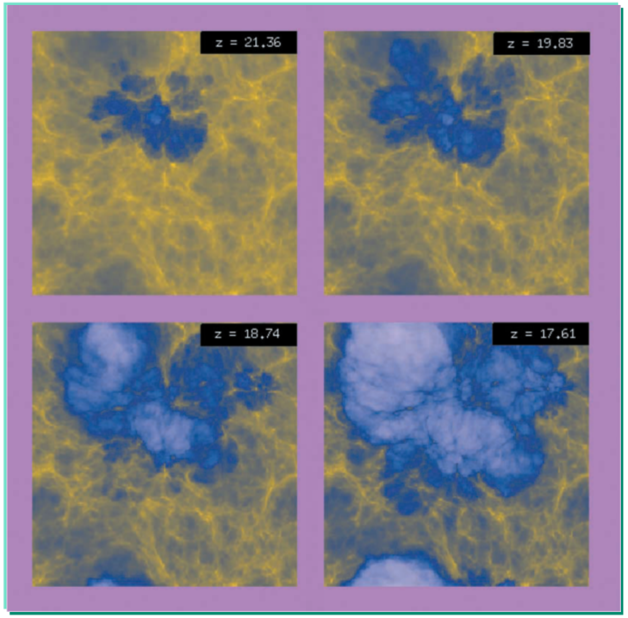


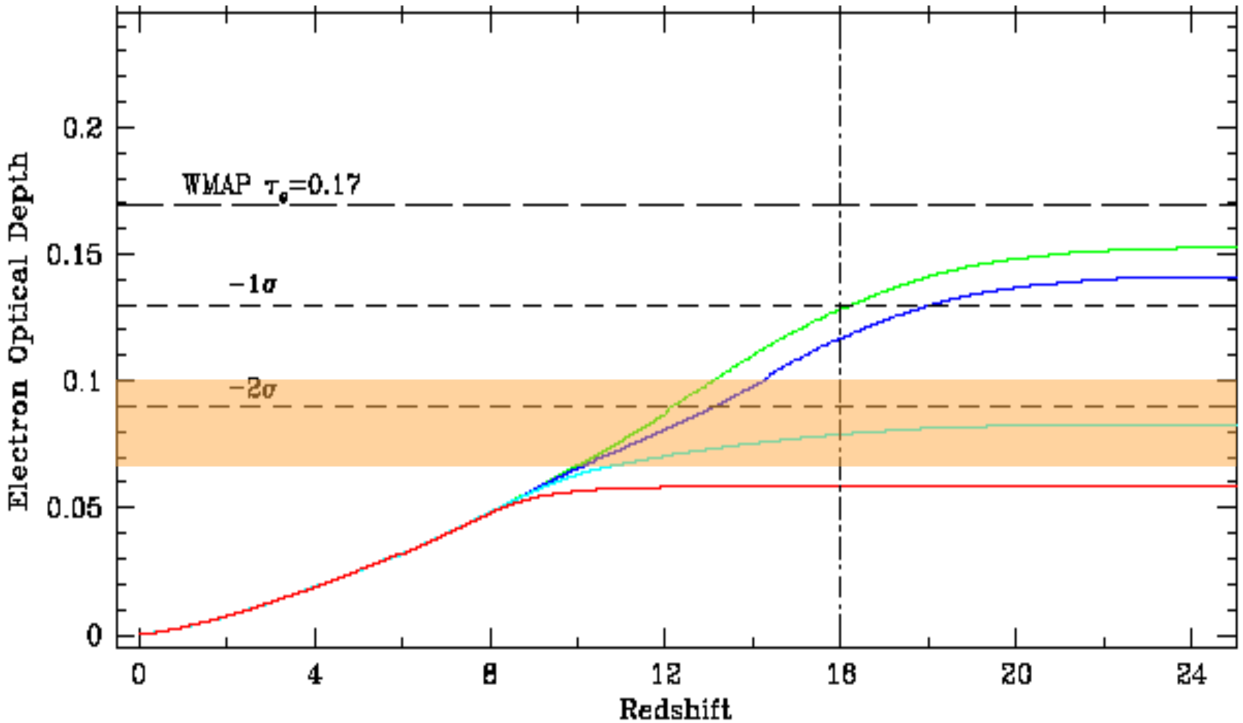

# GRBの赤方偏移

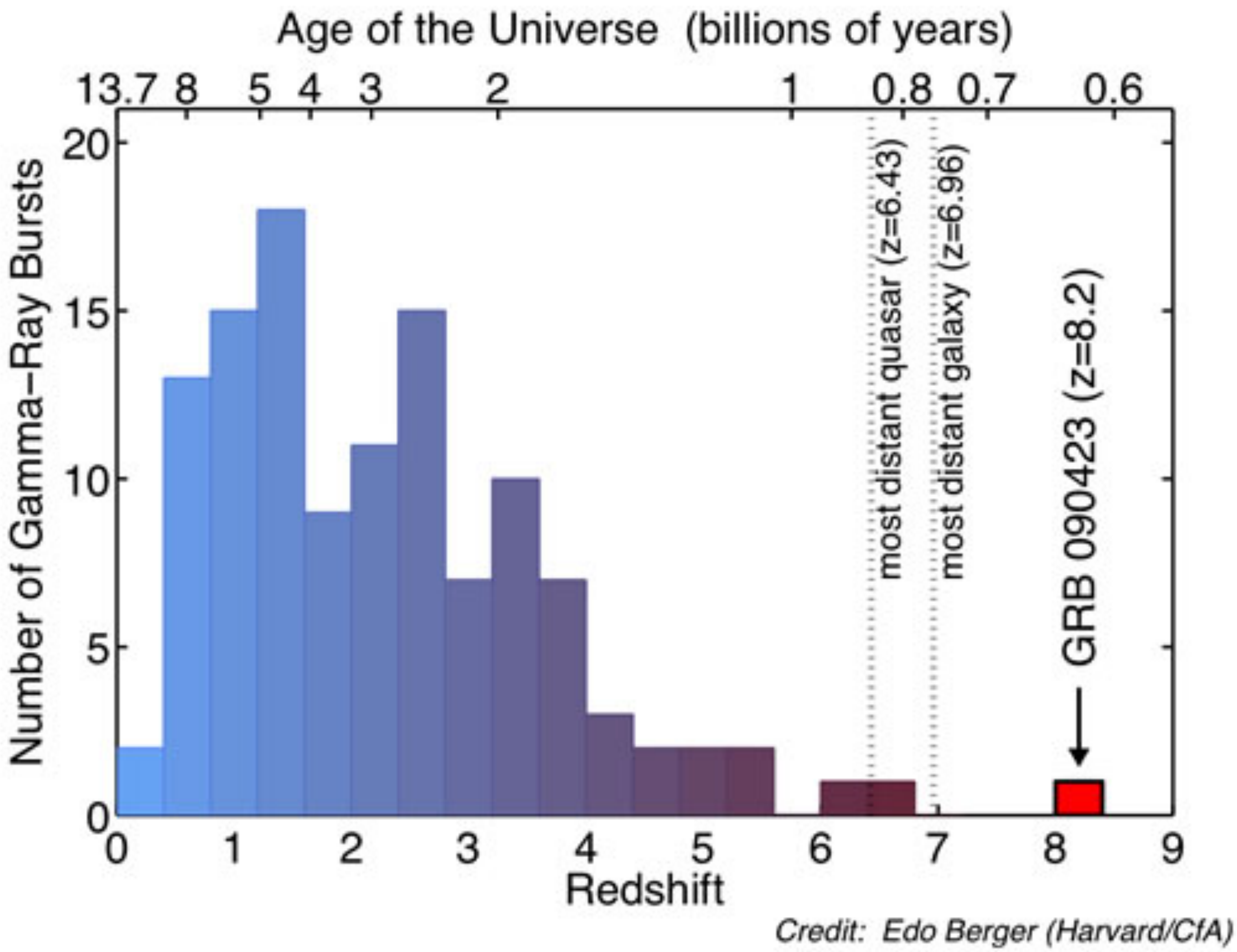

Age of the Universe (billions of years)
13.7 8 5 4 3 2 1 0.8 0.7 0.6
Number of Gamma-Ray Bursts
0
5
10
15
20
most distant quasar (z=6.43)
most distant galaxy (z=6.96)
GRB 090423 (z=8.2)
0 1 2 3 4 5 6 7 8 9
Redshift
Credit: Edo Berger (Harvard/CfA)

# Yonetoku Relation
# ($E_p$ - $L_p$)

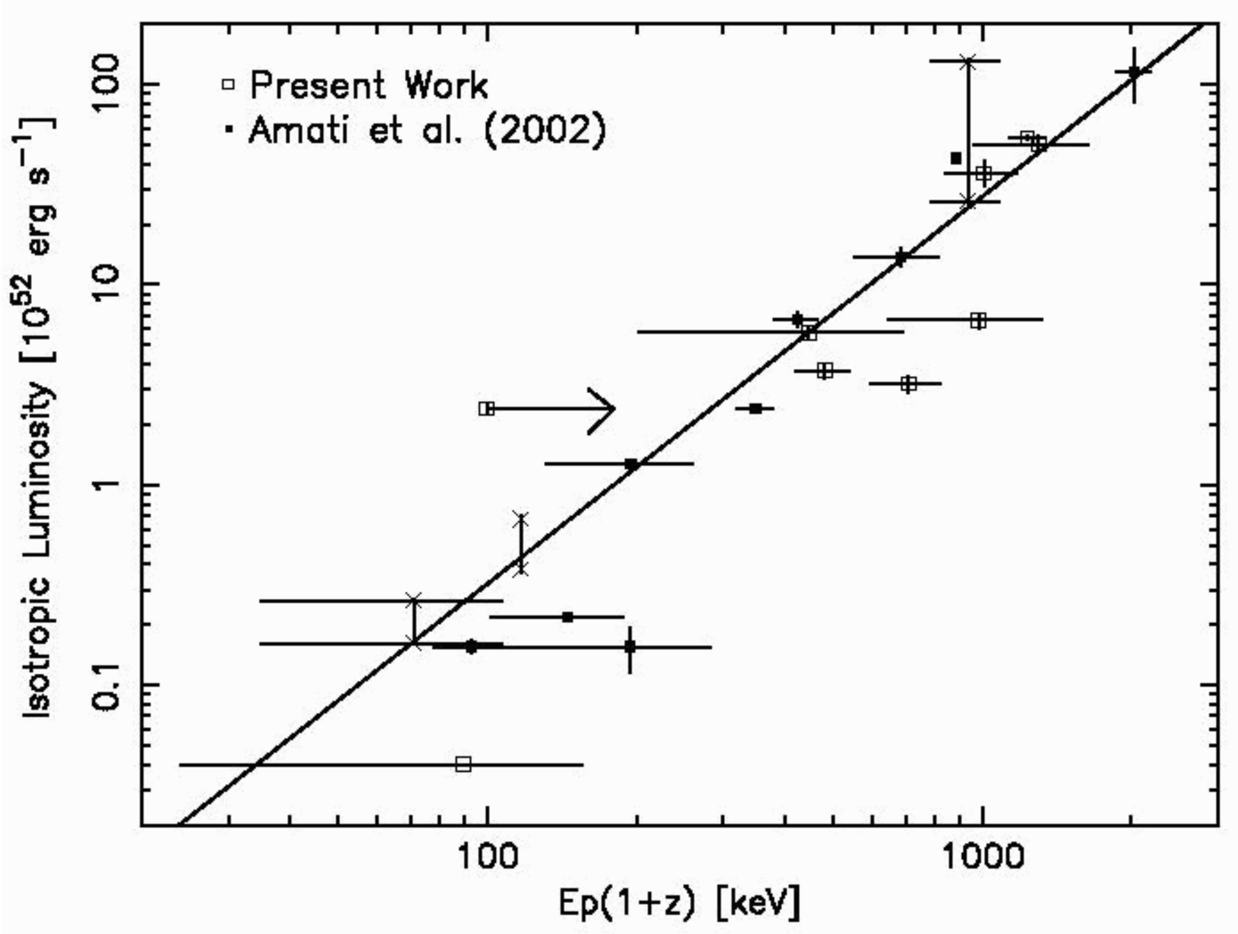


**Yonetoku et al. 2004, ApJ, 609, 935**

$$L_{52} = 4.29\times10^{-5} \, [\, Ep\,(1+z)\,]^{1.94}$$

# Pop III SFR derived from GRB Events

Murakami, Yonetoku, MU, Matsubayashi, Yamazaki 2005, ApJ, 625, L13

689 GRBs
$E_p$-Luminosity relation

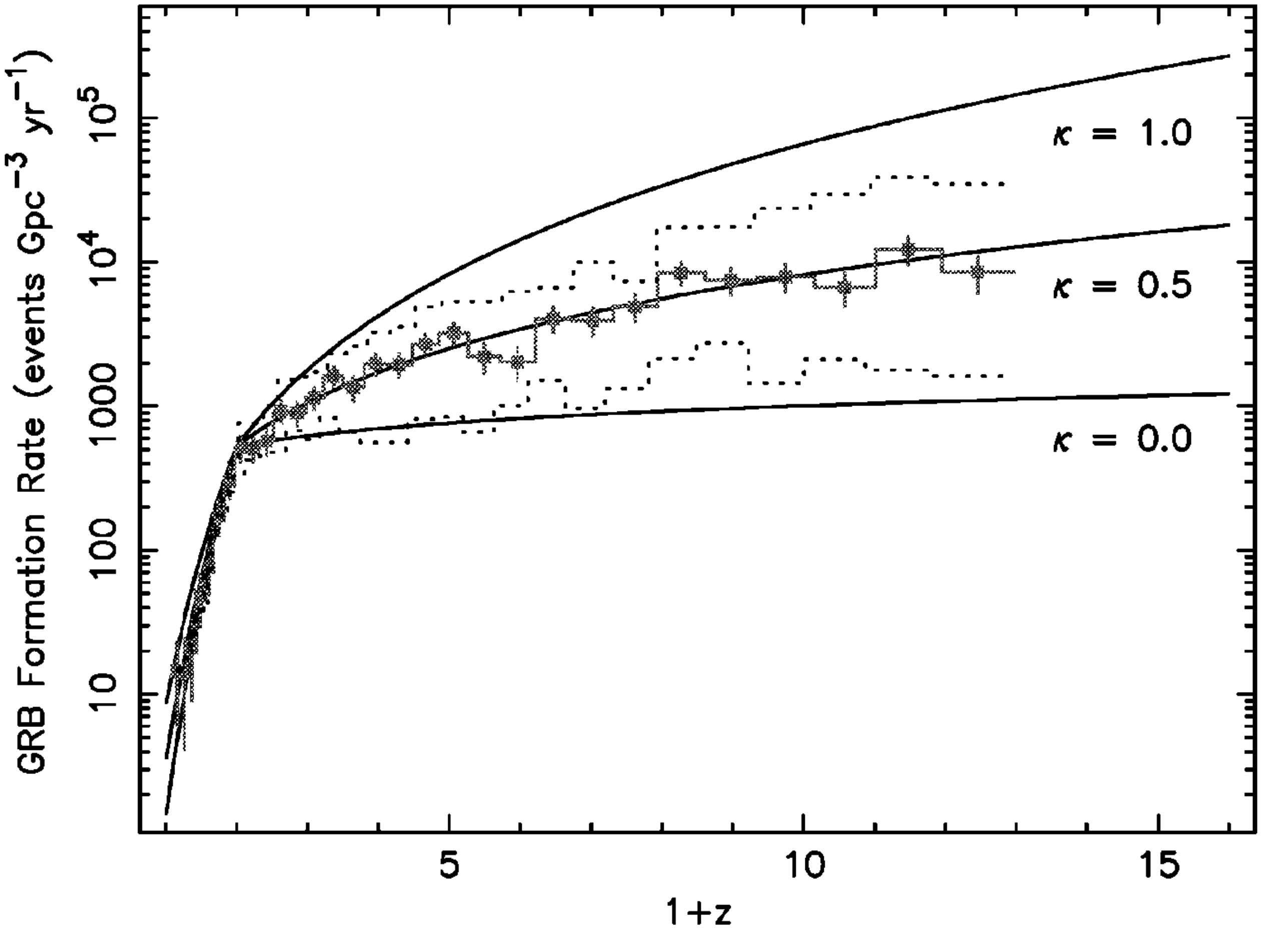


$$\dot{\rho}_*^{\rm III} \simeq 3 \times 10^2 f_{\rm GRB}^{\rm III} \dot{\rho}_{\rm GRB}\ M_\odot\ {\rm Gpc}^{-3}\ {\rm yr}^{-1}$$

$$f_{\rm GRB}^{\rm III} \simeq 0.5 f_*^{\rm III}/(1 - 0.5 f_*^{\rm III}).$$

# Reionization criterion

## $f_{esc}$>3-10% at z=10

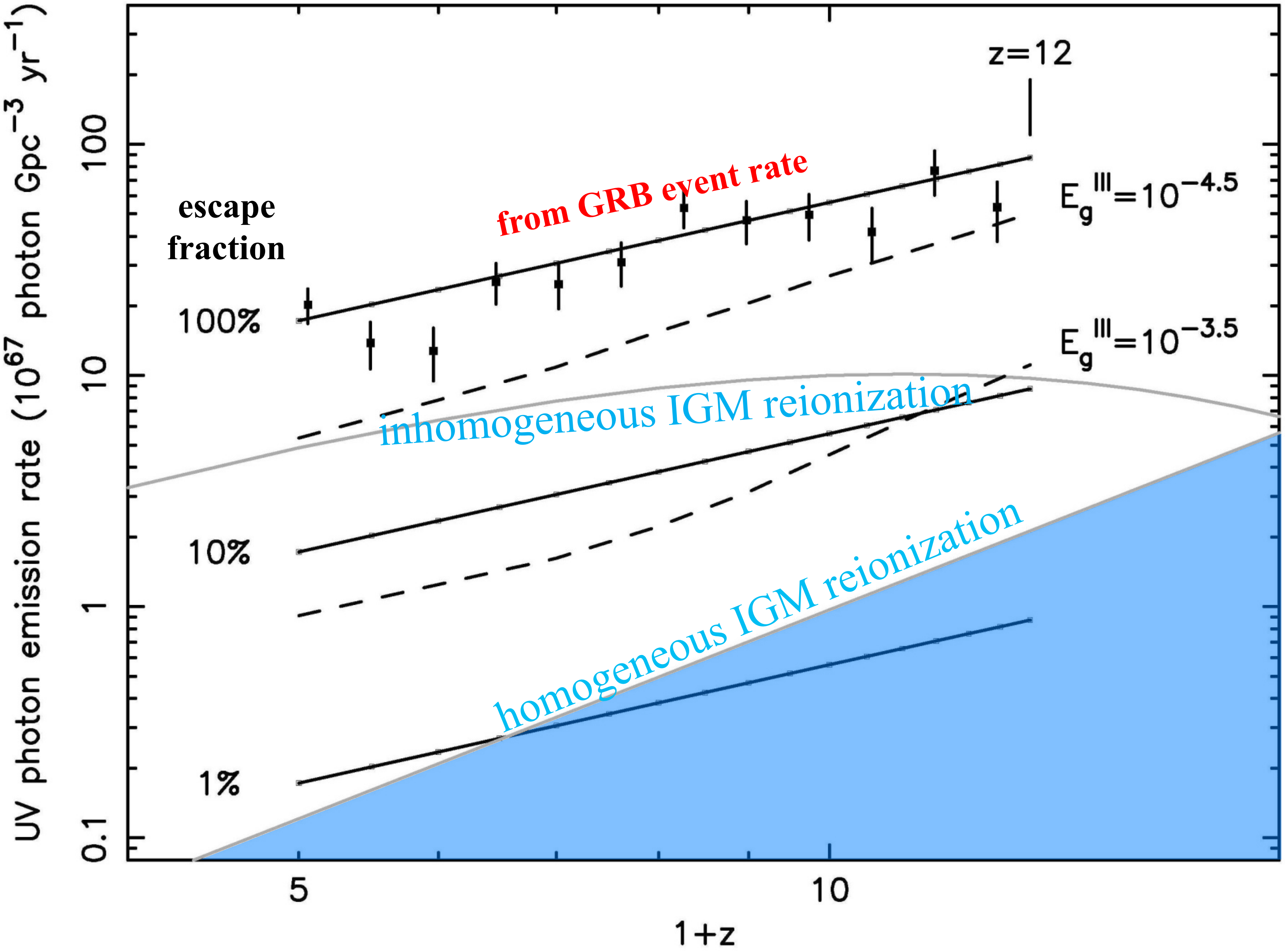

# Reionization with GRB-derived SFR

Wyithe et al, 2010, MNRAS, 401, 2561

**Semi-analytic model + Lyα forest + WMAP 5 year**

**$f_{esc}$=3-6% (68% confidence)**

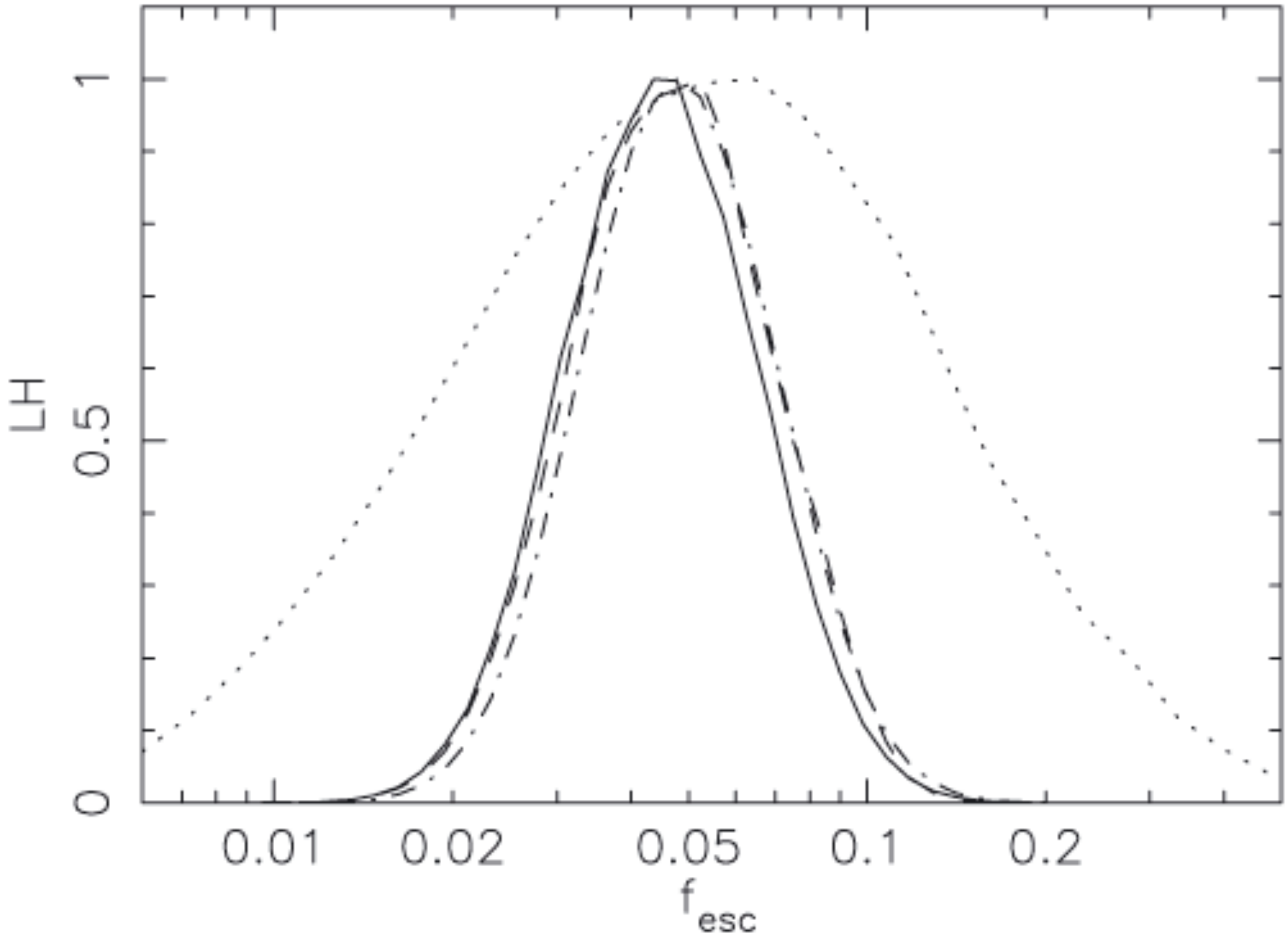

Ouchi et al. 2009, ApJ, 706, 11136

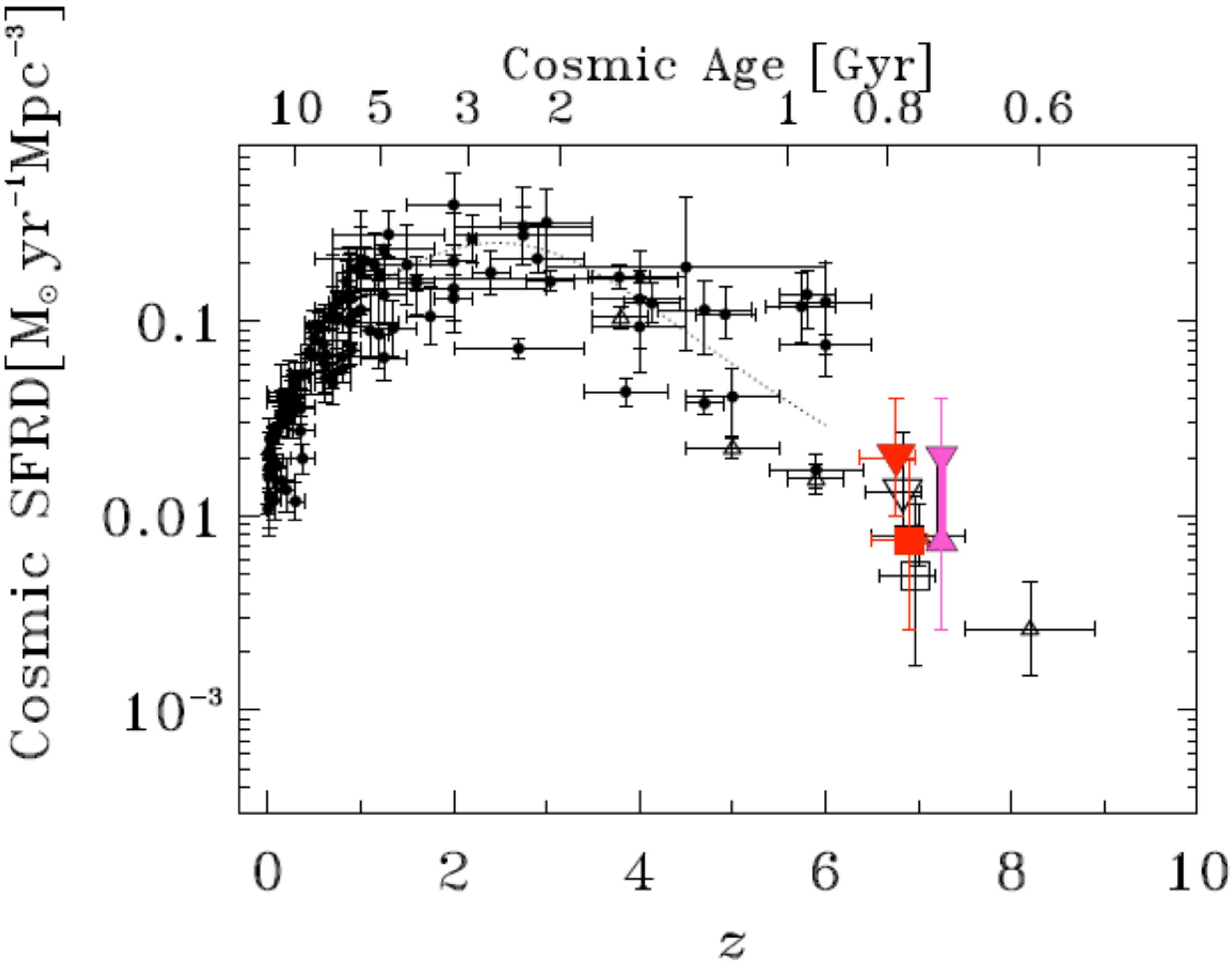

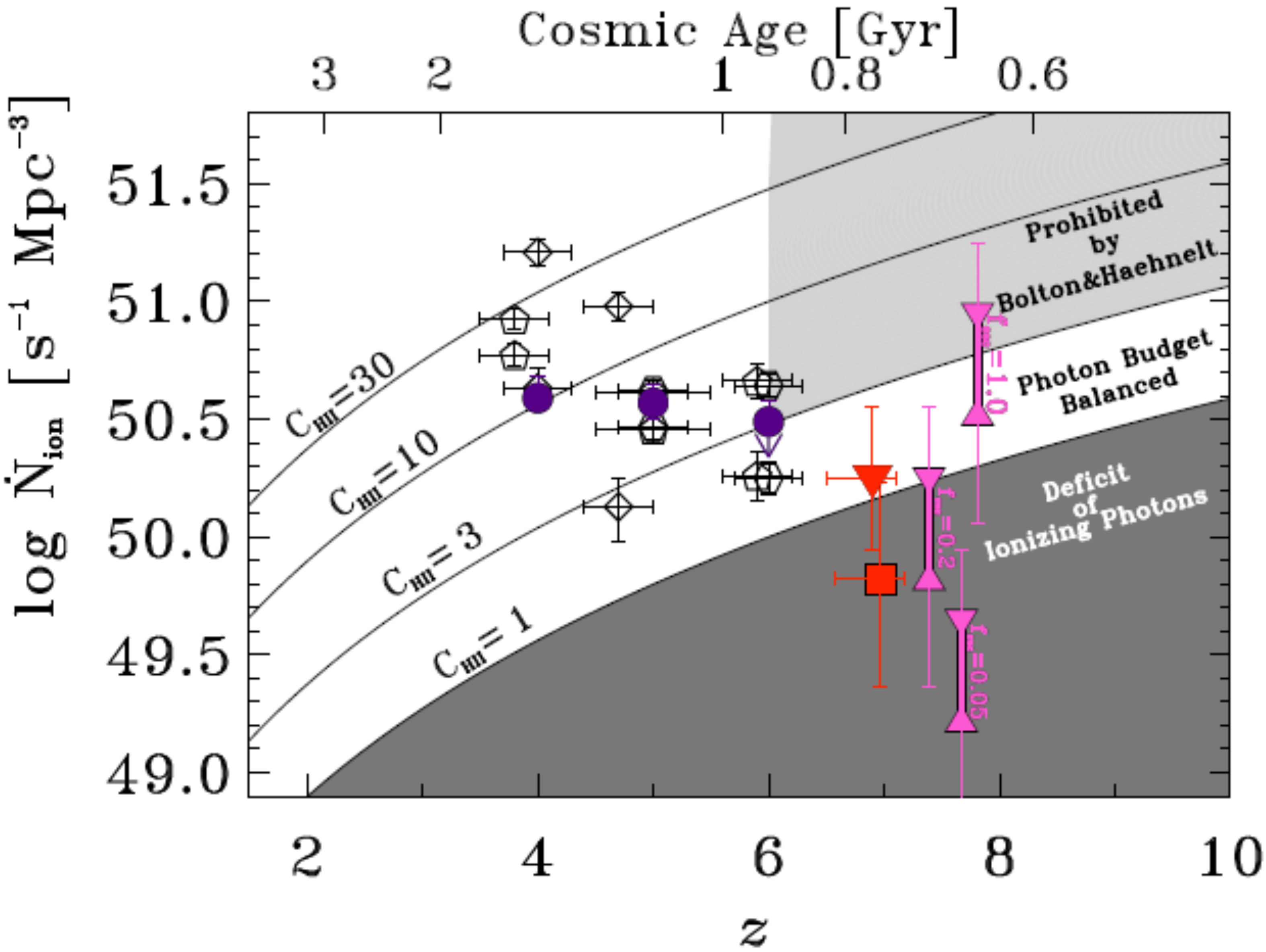

Cosmic Age [Gyr]
3
2
1
0.8
0.6
log $\dot{N}_{ion}$ [s$^{-1}$ Mpc$^{-3}$]
51.5
51.0
50.5
50.0
49.5
49.0
2
4
6
8
10
z
$C_{HII}$=30
$C_{HII}$=10
$C_{HII}$= 3
$C_{HII}$= 1
Prohibited by Bolton&Haehnelt
Photon Budget Balanced
Deficit of Ionizing Photons

# 銀河形成

**1.Missing Satellites Problem**

**2.Origin of Galactic Morphology**

**3.Downsizing of Galaxy Formation**

# Missing Satellites Problem

J, 524, L19 $2\times 10^{12} M_\odot$

**Galac**

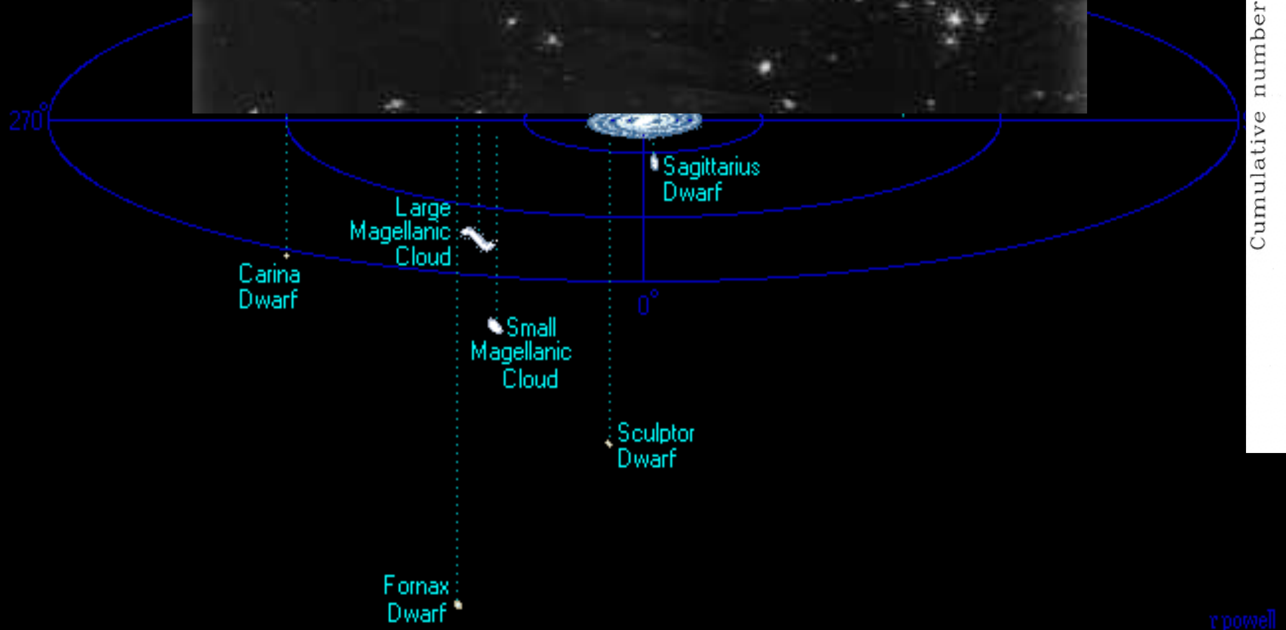


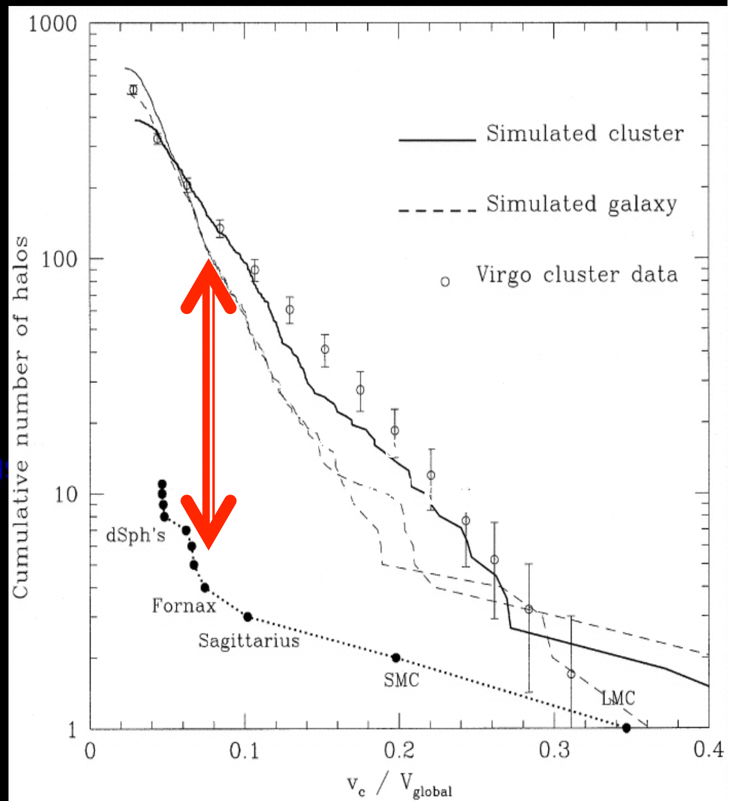

# Feedbacks on Dwarf Formation

*UV Feedback before & after SF*

- **Optically-thin Approx.**

  **MU & Ikeuchi 1984, 1985; Ikeuchi 1986; Rees 1986; Bond et al. 1988; Efstathiou 1992; Babul & Rees 1992; Chiba & Nath 1994; Thoul & Weinberg 1996**

- **Radiative Transfer by Pure Absorption Approx.**

  **Kepner et al. 1997; Kitayama & Ikeuchi 1999**

- **Full Radiative Transfer**

  **Tajiri & MU 1998; Barkana & Loeb 1999; Kitayama et al. 1999, 2000; Shapiro et al. 2003; Shaviv & Dekel 2003; Ricotti 2003; Susa & MU 2004a, b**

*SN Feedback after SF*

**Dekel & Silk 1986; Yepes et al. 1997; Efstathiou 2000; Kay et al. 2002; Marri & White 2003; Wada & Venkatesan 2003; Ricotti & Ostriker 2004**

## Three Elements for Galaxy Formation

**CDM Fluctuations**

**Random Gaussian Density Fields**

**Cooling Diagram (Rees & Ostriker 1977)**

+

**Self-Shielding**

***No stars form unless baryonic matter is self-shielded from UVB !***

# 自己遮蔽(Self-Shielding)

**Spherical top-hat cloud**

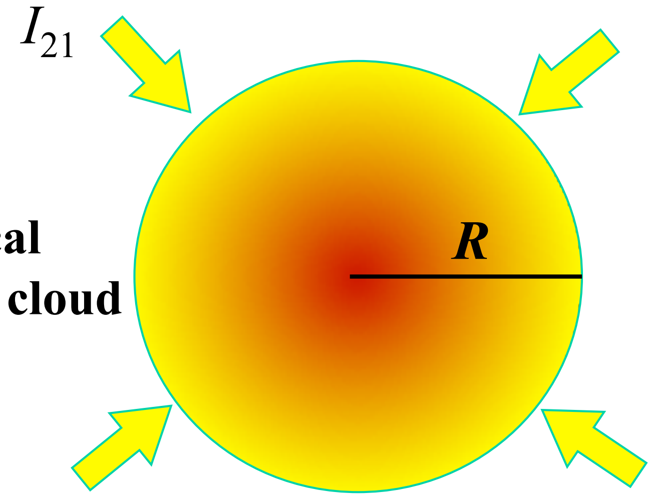


Tajiri & Umemura 1998

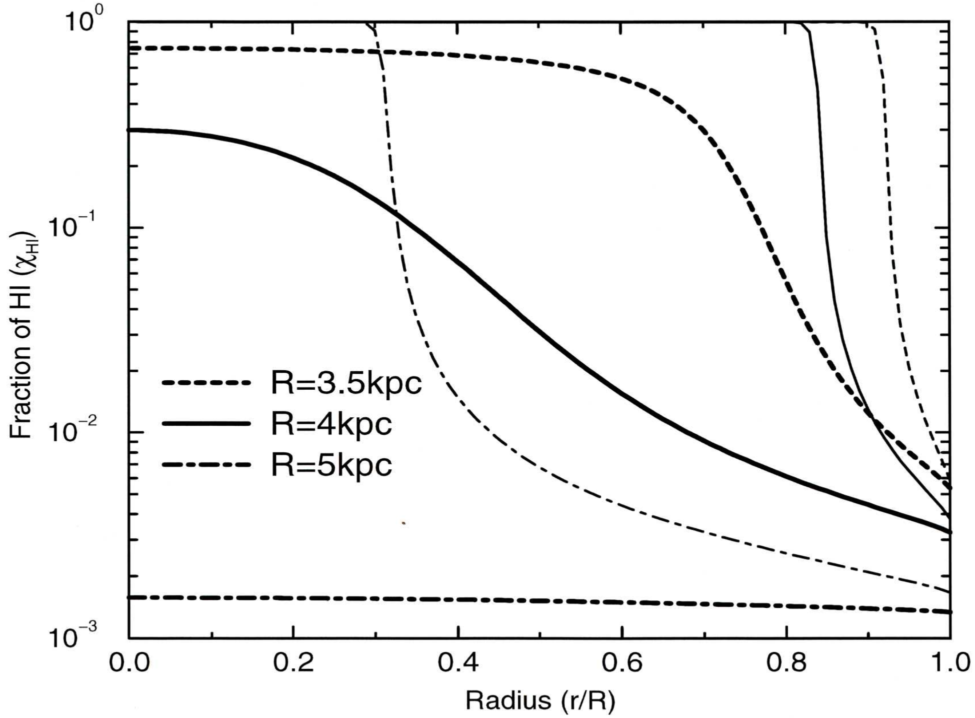


$$n_{crit} = 1.5 \times 10^{-2} M_8^{-1/5} (I_{21}/\alpha)^{3/5} \ \ \mathrm{cm}^{-3}$$

$$(M_8 = M/10^8 M_\odot, \ \ T = 10^4 \mathrm{K})$$

$$\tau_{\rm crit} \equiv n_{\rm HI} a_{\nu_L} R_{\rm crit} = 0.6 \frac{\alpha + 3}{\alpha}$$

# UV Effects

**Kitayama et al. 2001, MNRAS, 326, 1353**

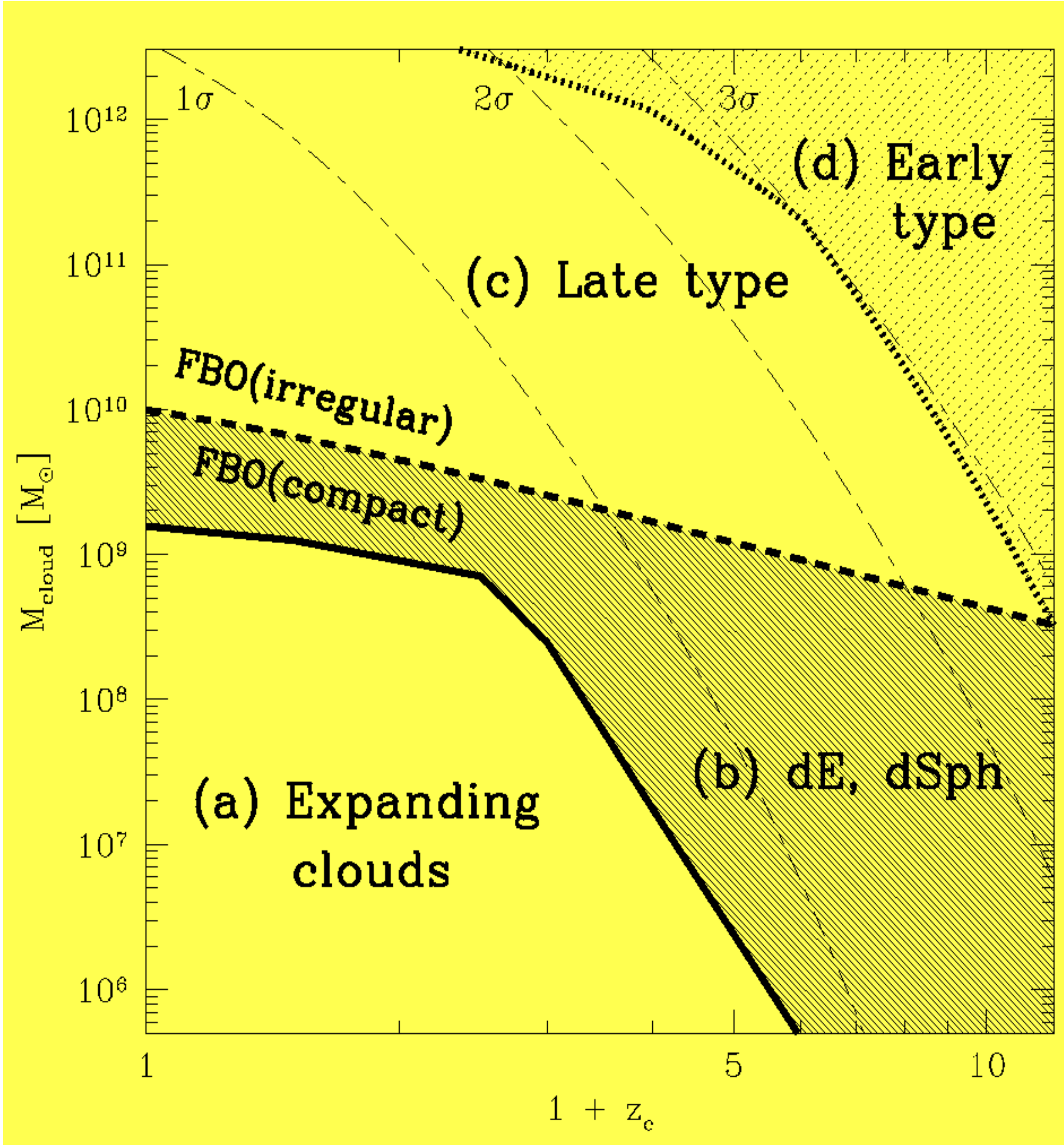


**Dynamics:**
Spherical hydrodynamics

**UV:**
Radiative transfer

**$H_2$ :**
Non-equilubrium chemistry

# RSPH
(Radiation Smoothed Particle Hydrodynamics)

## Hydrodynamics + Self-Gravity + Radiation transfer

(Susa & Umemura 2003)

1. 流体：SPH（コアルーチン：Umemura 1993）

2. 自己重力
並列版：GRAPE-6

3. 化学反応, 放射冷却ルーチン：Susa & Kitayama (2000)

4. 輻射輸送:
Kessel-Deynet &Burkert 法(2000)
on-the-spot近似（散乱光子はその場で吸収）

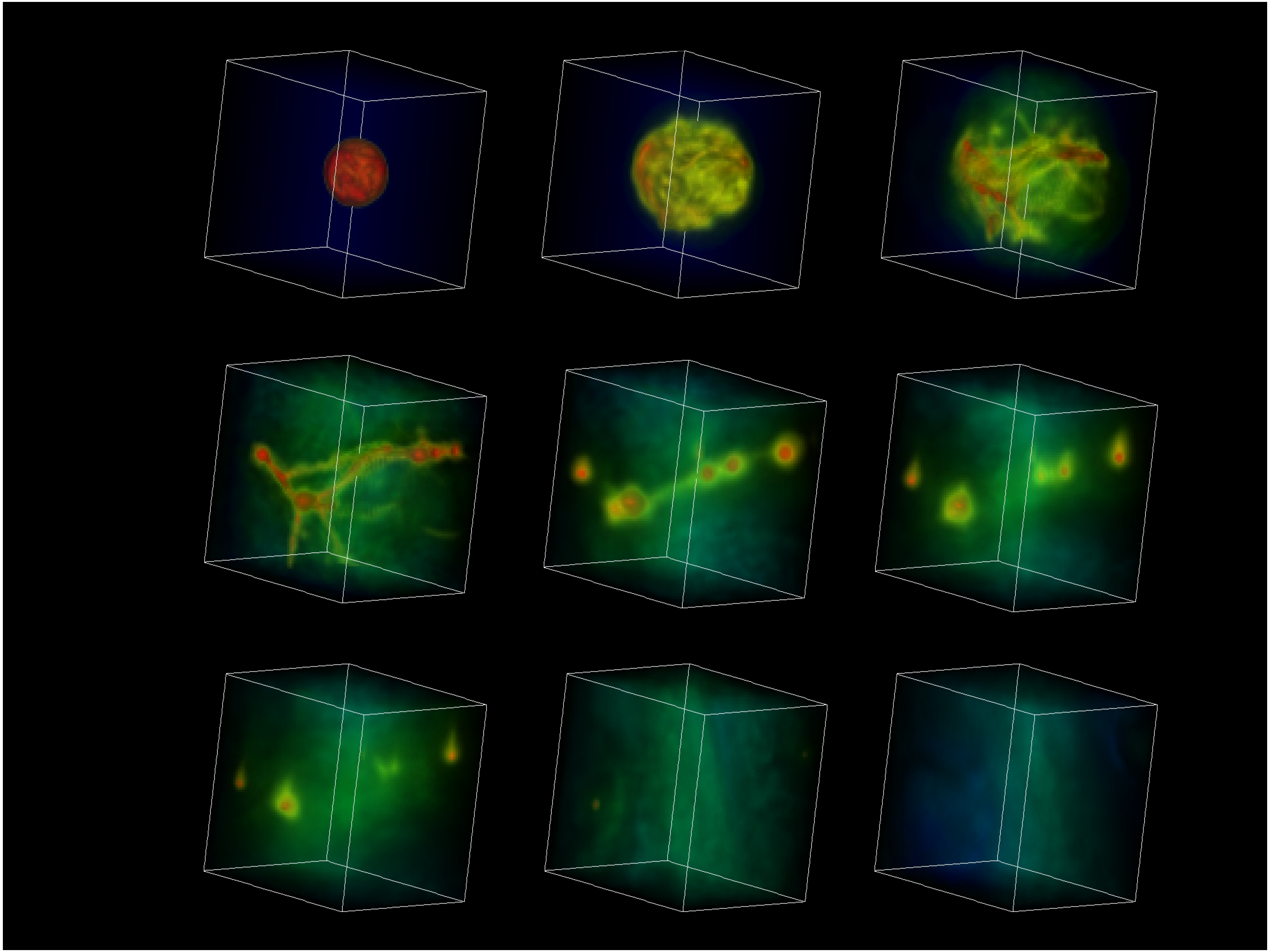

# Effects of Early Reionization on the Substructure Problem

**Susa & Umemura 2004, ApJL, 610, L5**

$$M_{vir} = 10^{6-8} M_\odot$$

$$V_{circ} \sim 20 \text{ km s}^{-1}$$

**Fluctuations >2.5σ are photo-evaporated.**

**Early reionization is so devastating for small systems.**

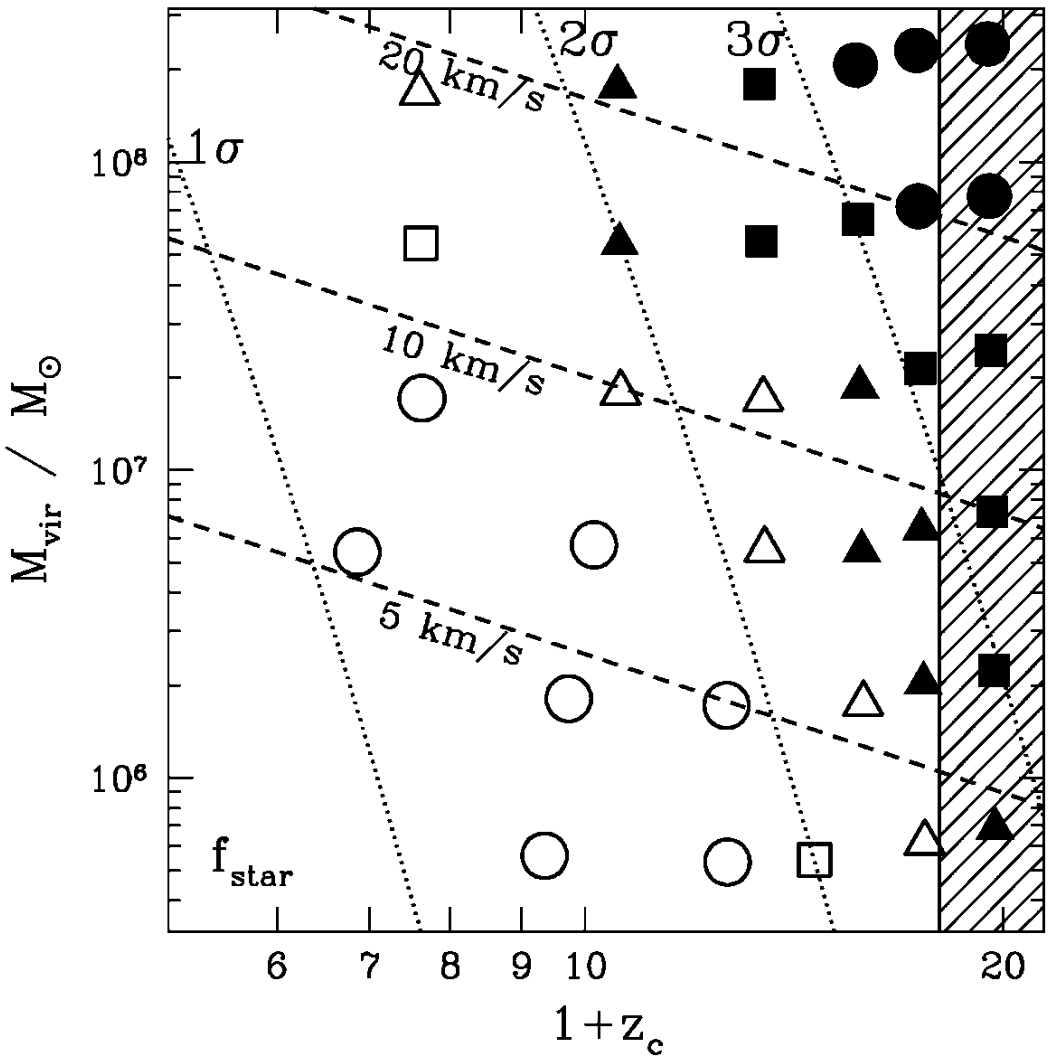

# Galaxy Formation in a UV Background

**Susa & Umemura 2000, MNRAS, 316, L17**

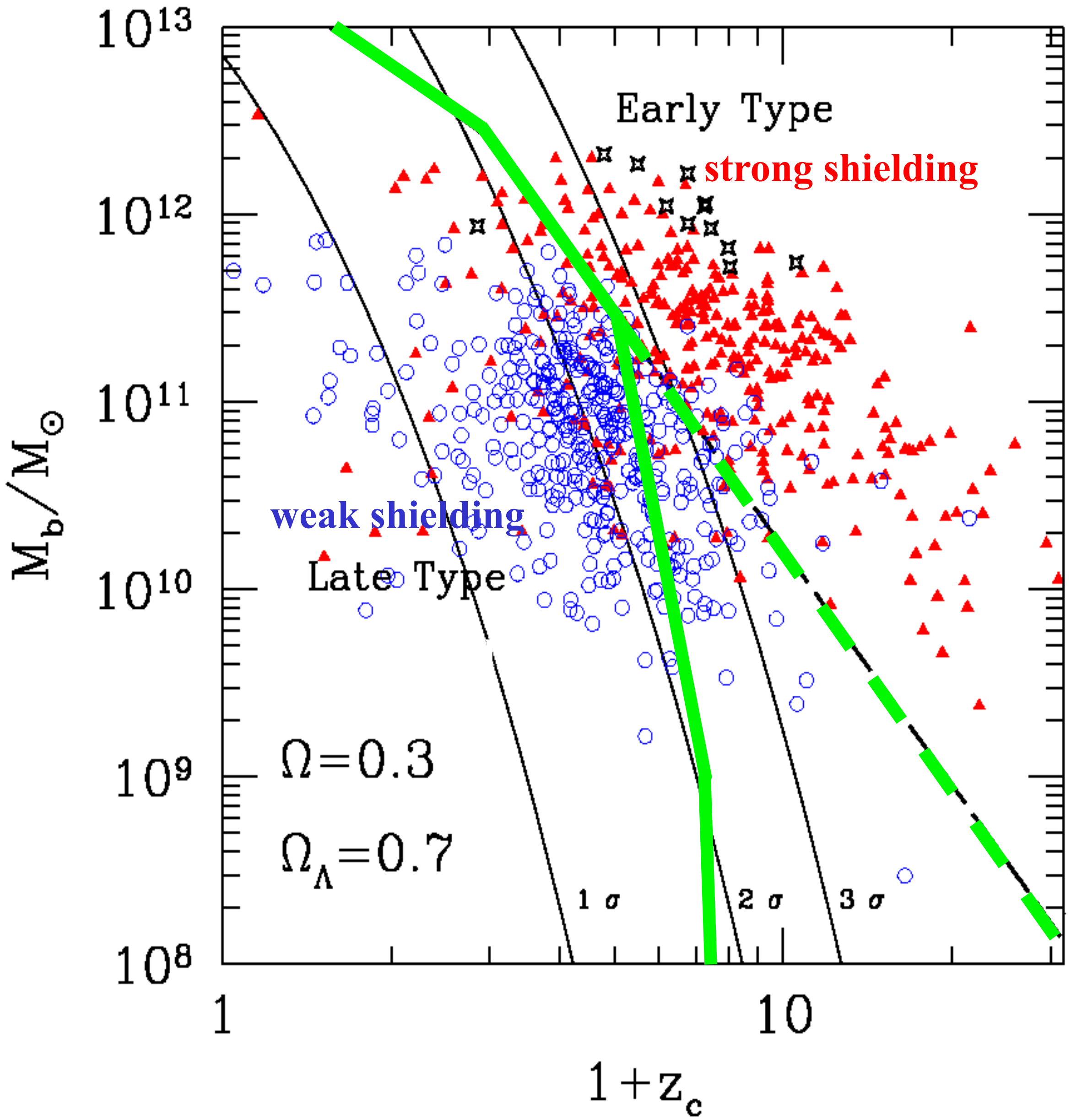

# Cosmological Radiative Transfer Codes Comparison Project II: Radiation Hydrodynamic Tests

**2009, MNRAS, 371, 1057**

**Iliev, Ilian T.; Whalen, Daniel; Mellema, Garrelt; Ahn, Kyungjin; Baek, Sunghye; Gnedin, Nickolay Y.; Kravtsov, Andrey V.; Norman, Michael; Raicevic, Milan; Reynolds, Daniel R.; Sato, Daisuke; Shapiro, Paul R.; Semelin, Benoit; Smidt, Joseph; Susa, Hajime; Theuns, Tom; Umemura, Masayuki**

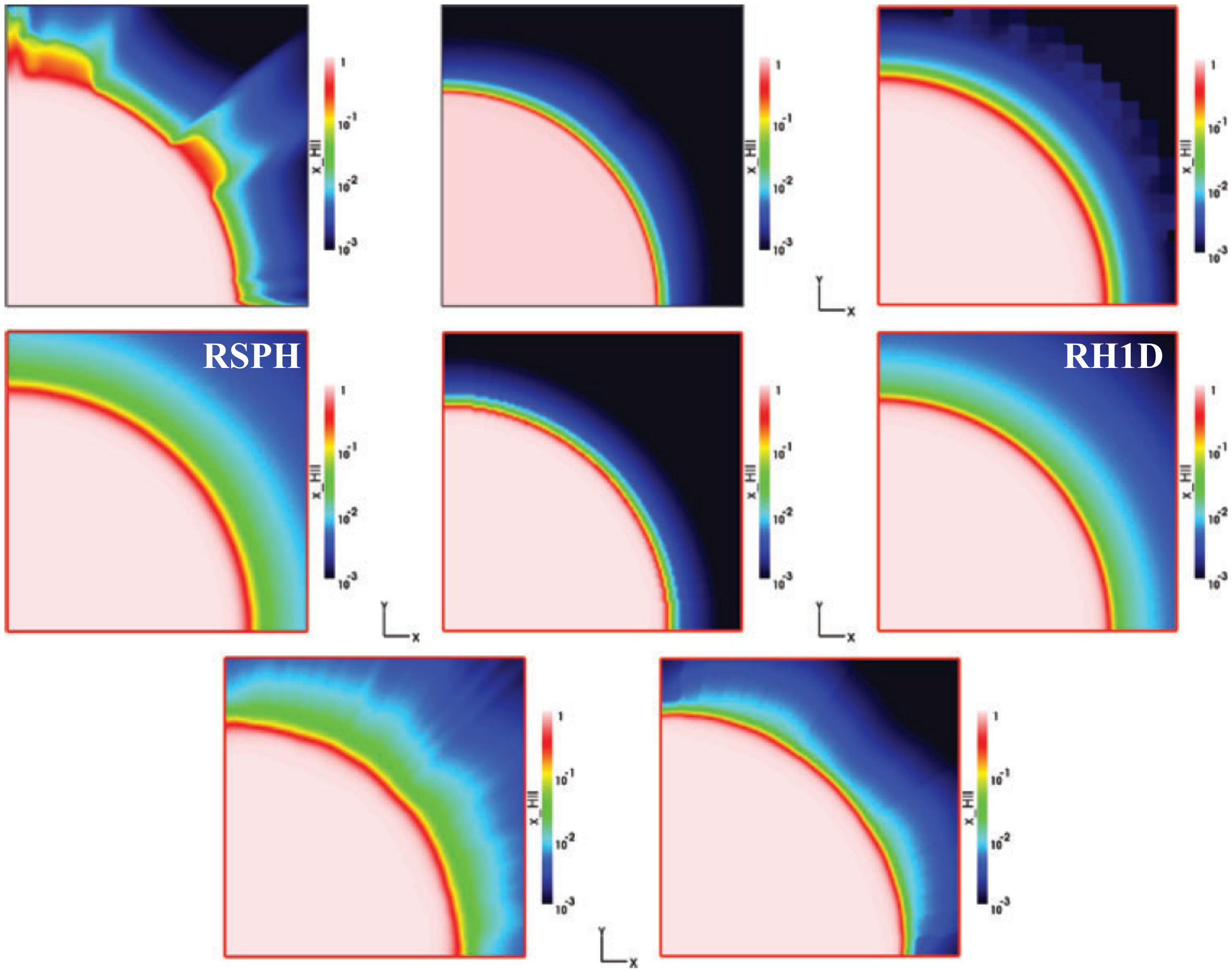


**Figure 21.** Test 6 (H II region gas-dynamic expansion down a power-law initial density profile): images of the H II fraction, cut through the simulation volume at coordinate $z = 0$ at time $t = 25$ Myr for (left to right and top to bottom) CAPREOLE+C$^2$-RAY, TVD+C$^2$-RAY, HART, RSPH, ZEUS-MP, RH1D, LICORICE and FLASH-HC.

# *START*

## *SPH with Tree-based Accelerated Radiative Transfer*

Hasegawa & Umemura (2010, MNRAS, 407, 2632)

w/o diffuse photons

on-the-spot approximation (Case B)

with diffuse photons

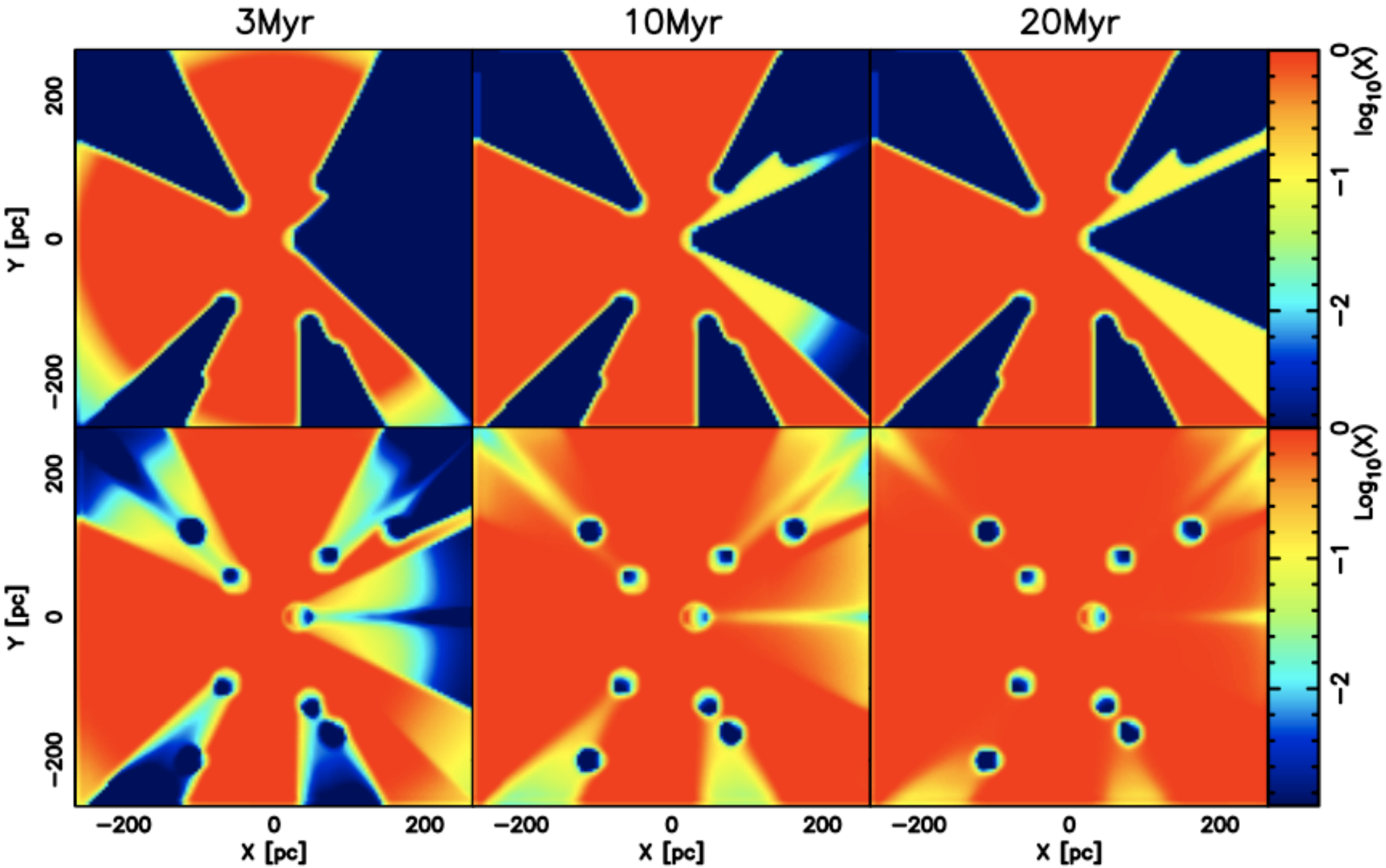


**Photo-ionization of Inhomogeneous Media**

# Spectroscopic confirmation of a galaxy at redshift z=8.6

Lehnert et al. 2010, nature, 467, 940

Hubble Ultra Deep Field (WFC3) : red $Y_{105}$–$J_{125}$ color
SINFONI spectrograph at the ESO Very Large Telescope

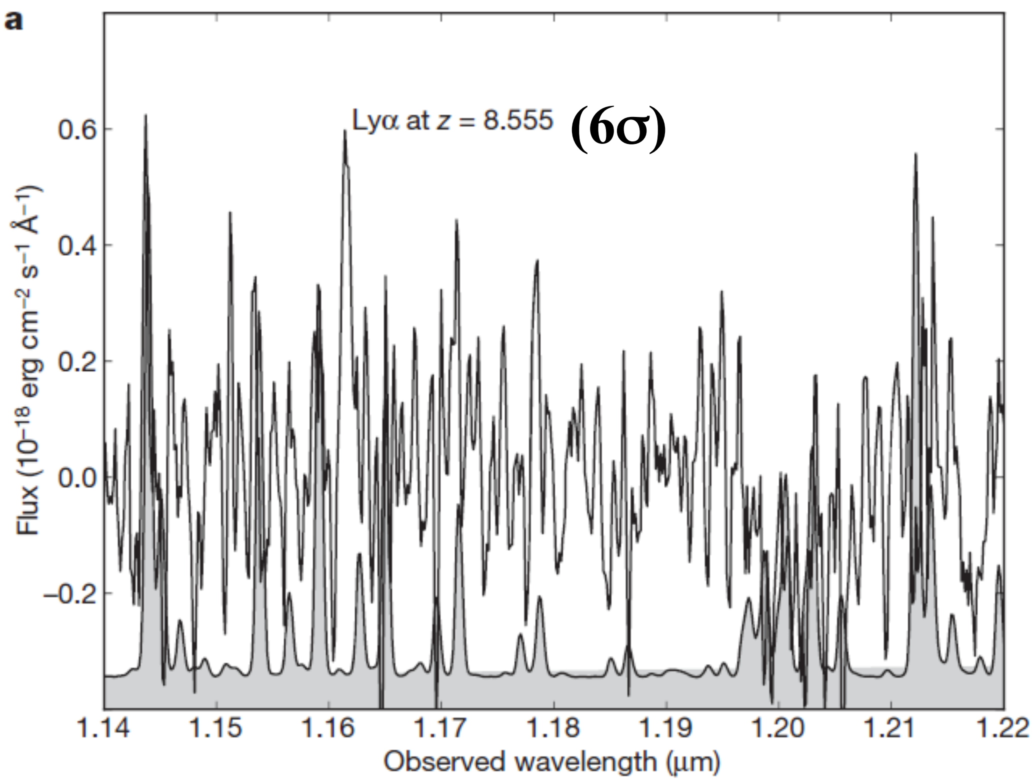


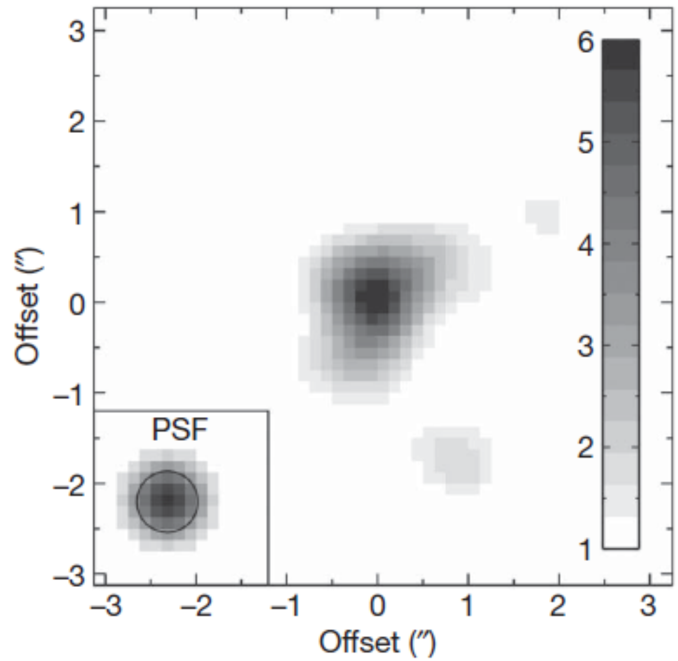


grey=night sky pattern

⇒ LAE at z=8.5549±0.0002

# From Primeval Irregulars to Present-day Ellipticals

Mori and Umemura, 2006,
Nature, 440, 644

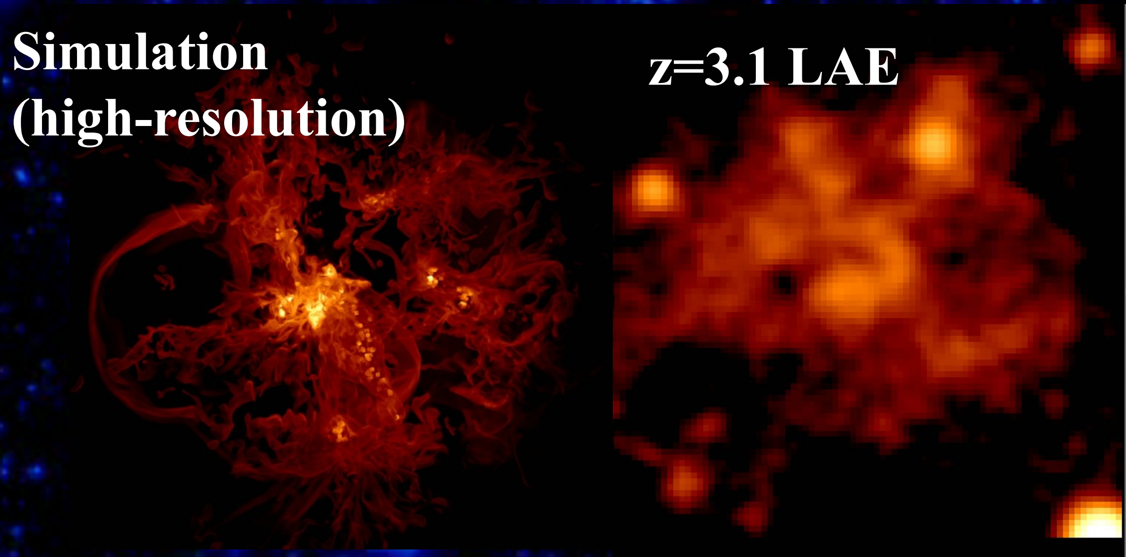


Total Mass: $10^{11}\ M_{\odot}$
Gas Mass: $1.3\times10^{10}\ M_{\odot}$
# of Subunits: 20
Box Size: 134 kpc
Grid Points: $1024^3$

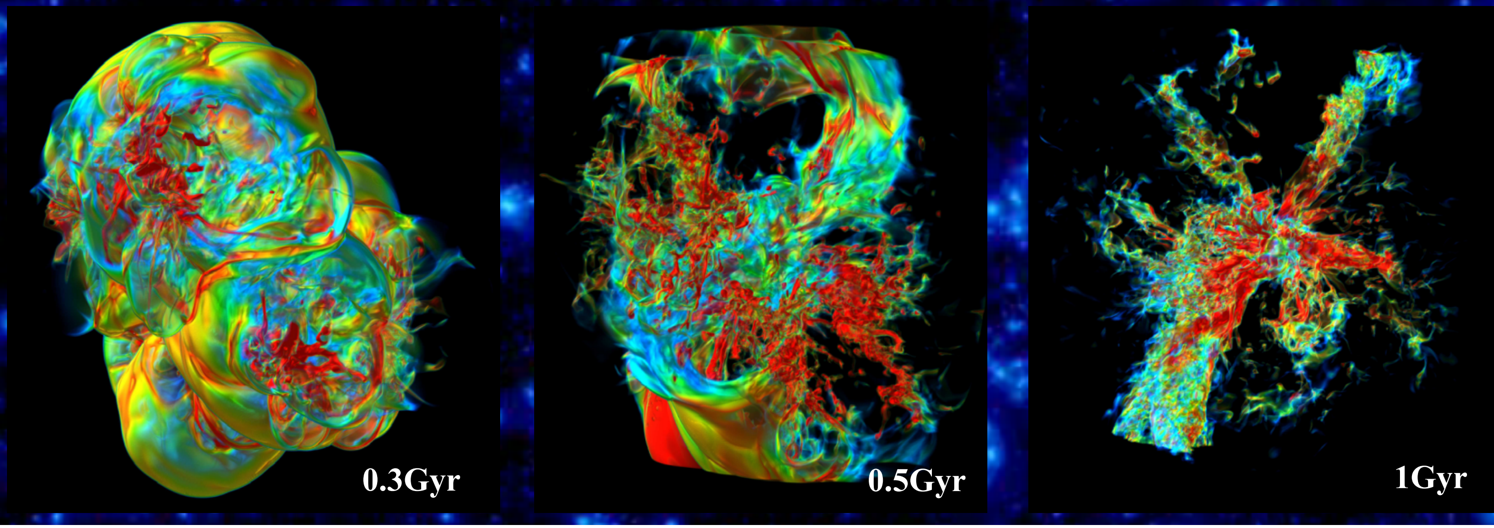

# Lyman α Emitters (LAE) Evolves into Elliptical Galaxies

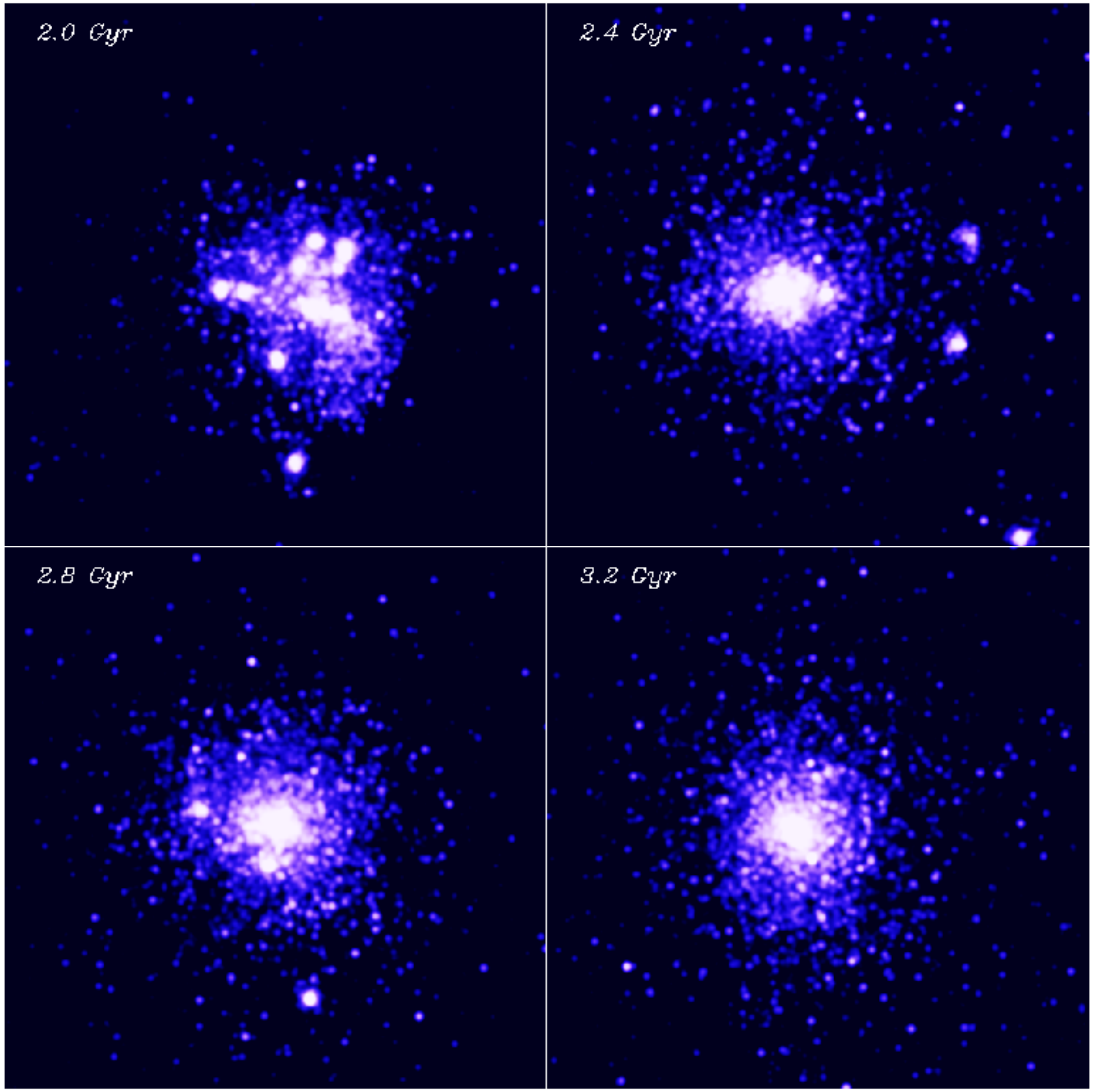


The virializaion of the total system is almost completed 3 Gyrs.

The resultant system at
13 Gyrs (redshift $z$=0) :

Stellar mass:
$M_{*}=1.1\times10^{10}\ M_{\odot}$

Central velocity dispersion:
$V_0=133$ km s$^{-1}$

Effective radius: $R_e=3.97$ kpc

$B$-band mag.: $M_B= -17.2$

$V$-band mag.: $M_V= -18.0$

Color: $U$-$V$=1.15
$V$-$K$=2.85

**These values are consistent with the properties of the present-day less-massive elliptical galaxies.**

# 天の川創生プロジェクト(国立天文台)

・Baba, J., Asaki, Y., Makino, J., Miyoshi, M., Saitoh, T.R., & Wada, K. 2009, ApJ, 706, 471
・Saitoh, T.R., Daisaka, H., Kokubo, E., Makino, J., Okamoto, T., Tomisaka, K., Wada, K., & Yoshida, N. 2009, PASJ, 61, 481
・Saitoh, T.R., Daisaka, H., Kokubo, E., Makino, J., Okamoto, T., Tomisaka, K., Wada, K., & Yoshida, N. 2008, PASJ, 60, 667

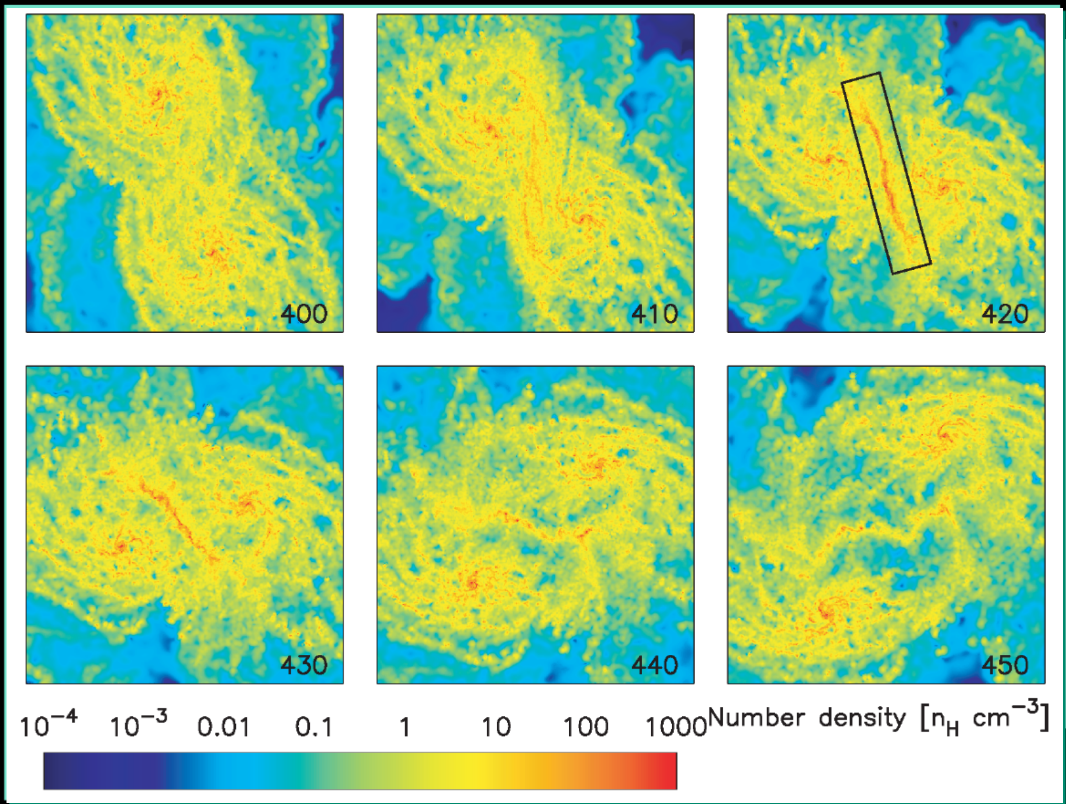


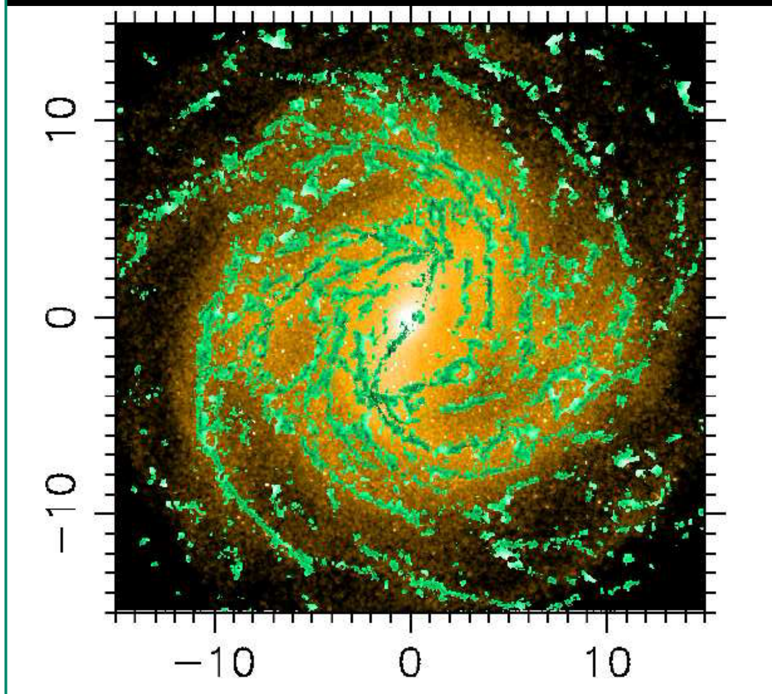

# 巨大ブラックホール形成

1.SMBH-Bulge Relation

2.Growth of SMBH

3.Downsizing of SMBH

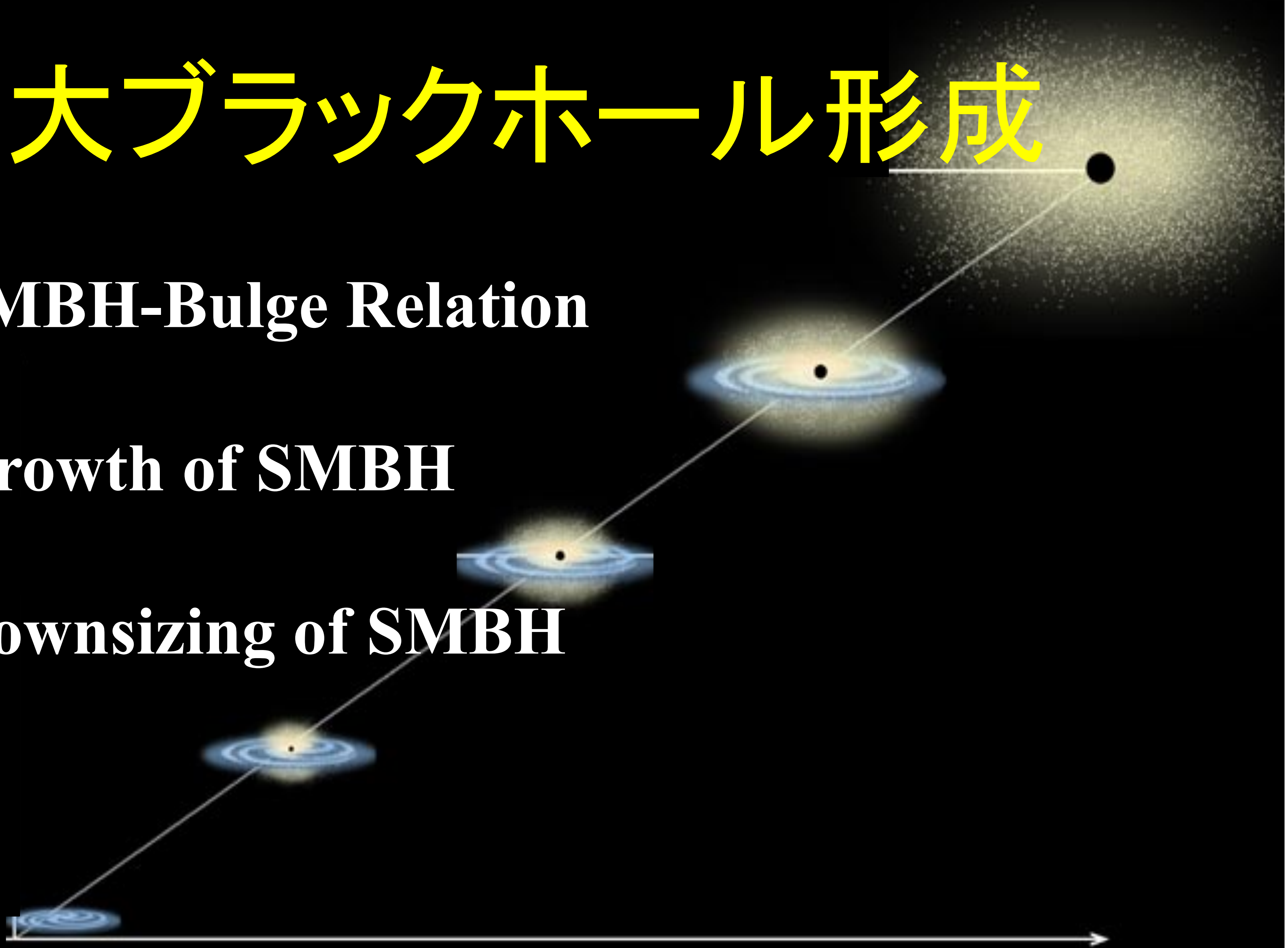

# 超巨大BHー銀河バルジ関係
## (マゴリアン関係)

$M_{BH}/M_{bulge} \approx 0.001$

Marconi & Hunt 2003, ApJ, 589, 21

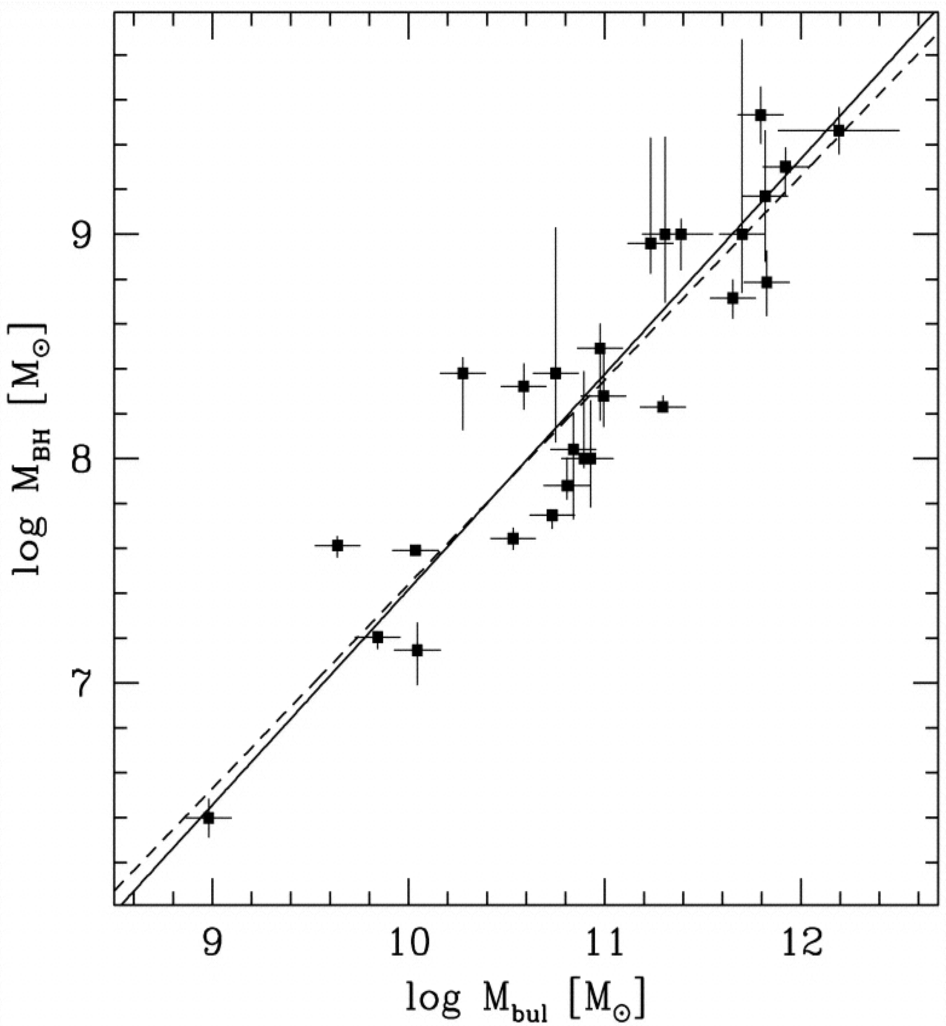


$M_{BH} \propto \sigma^{3.96\pm0.42}$

Gultekin et al. 2009, ApJ, 698, 198

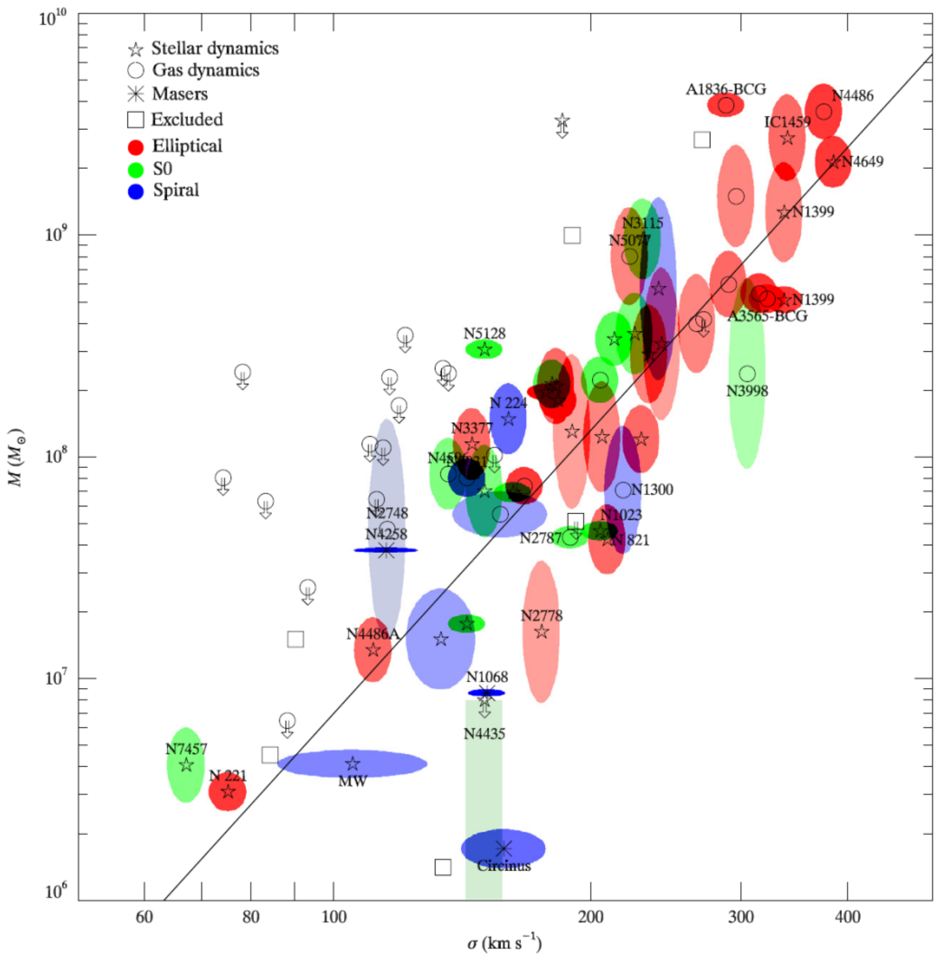

# “Downsizing” in SMBH Formation

***More massive BHs formed at higher redshifts.***

Ueda et al. 2003, ApJ, 598, 886

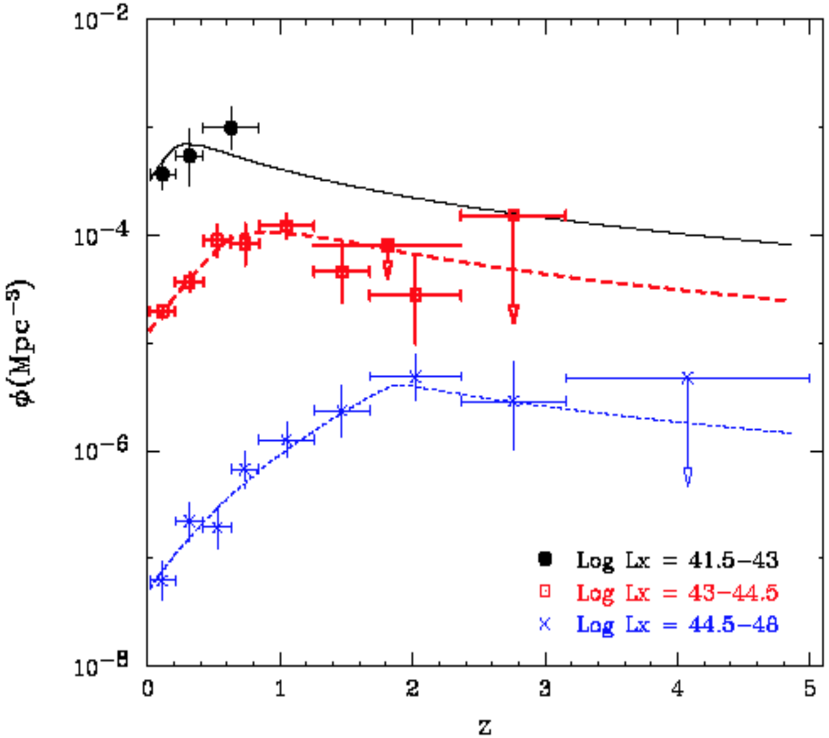


Marconi et al. 2004, MNRAS, 351, 169

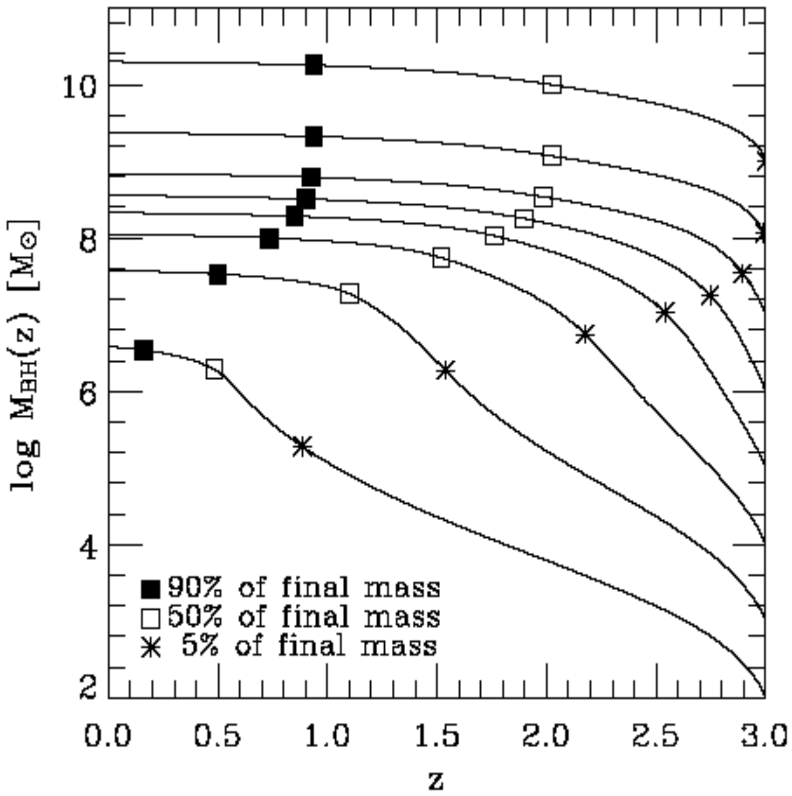

# “Downsizing” in Galaxy Formation

***More massive galaxies formed at higher redshifts.***

Cowie et al. 1996, AJ, 112, 839

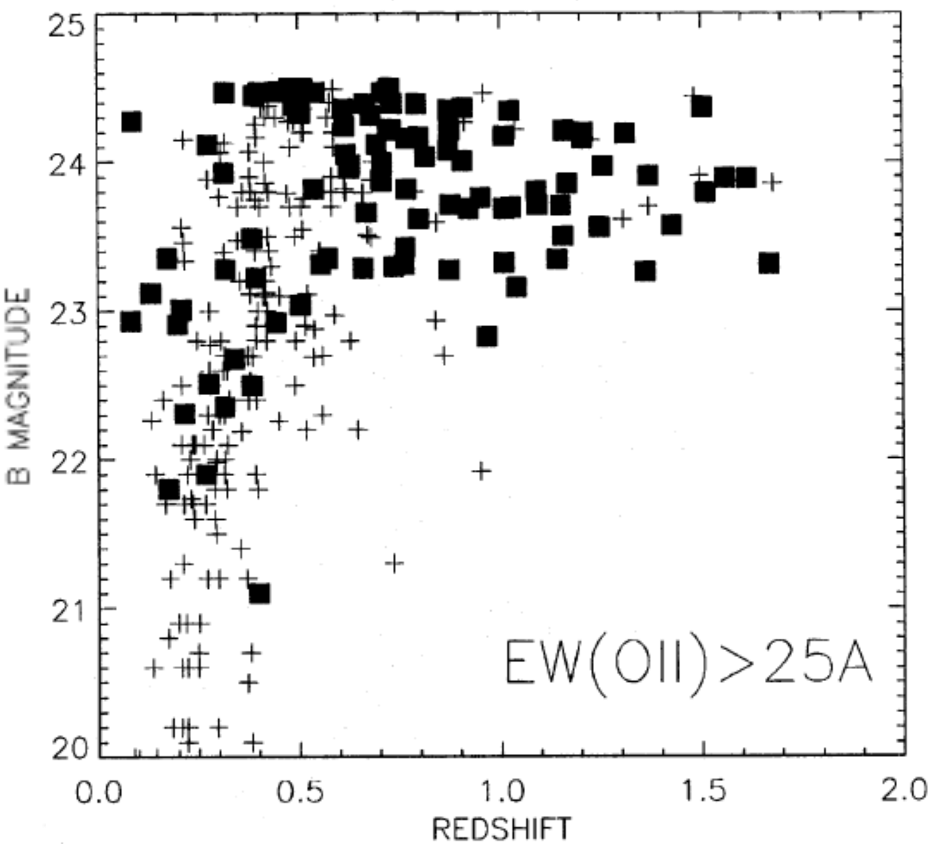


Kodama et al. 2004, MNRAS, 350, 1005
SXDS(Subaru/*XMM–Newton* Deep Survey)

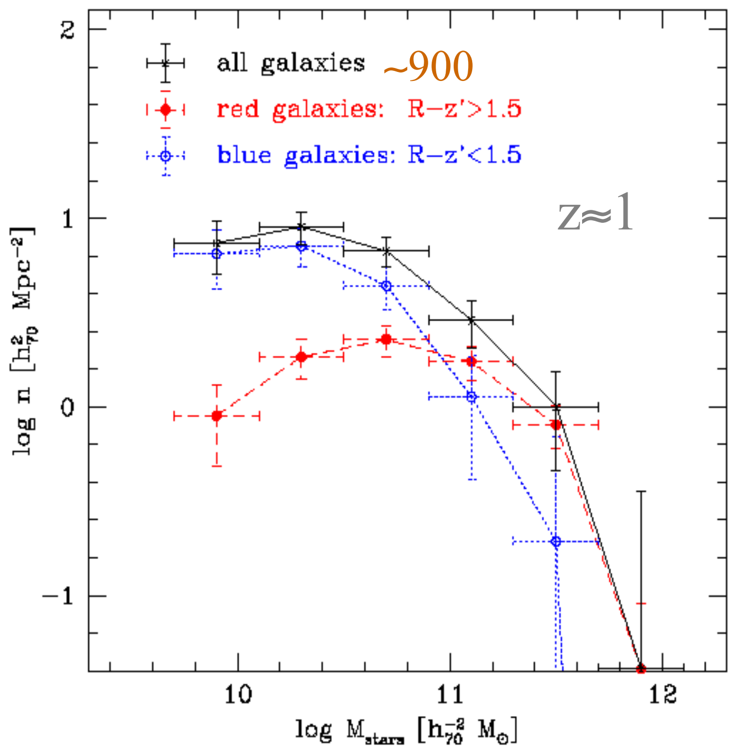


**Figure 10.** Field-corrected stellar mass functions for the $z \sim 1$ galaxies. The solid curve shows the total mass function, while dashed and dotted curves show the mass functions for red and blue galaxies, respectively, separated at $R - z' = 1.5$. The error bars shown here are purely Poissonian, and the errors due to field-to-field variation are shown later in Fig. 11.

超巨大ブラックホールのダウンサイジング

+

銀河のダウンサイジング

+

SMBH-bulge 関係

||

*重いバルジほど昔星形成を終了した*

ハッブル銀河分類は物理的だった！？

# Soltan's Argument (1982)

Integration of QSO LF

$$\Omega_{BH}(QSO) \approx 1.8 \times 10^{-6}$$

Yu & Tremaine 2002, MNRAS, 335, 965

$$\Omega_{BH}(QSO) \approx (2.4 - 4.8) \times 10^{-6}$$

Marconi et al. 2004, MNRAS, 351, 169

SMBH-bulge mass relation at z=0

$$\Omega_{BH}(bulge) \approx 2.1 \times 10^{-6}$$

$\Downarrow$

QSO BHの最終フェーズはガスアクリーションで太った

# SMBH Formation by Radiation Drag in Bulge

Umemura, 2001, ApJ, 560, L29
Kawakatsu & Umemura, 2002, MNRAS, 329, 572

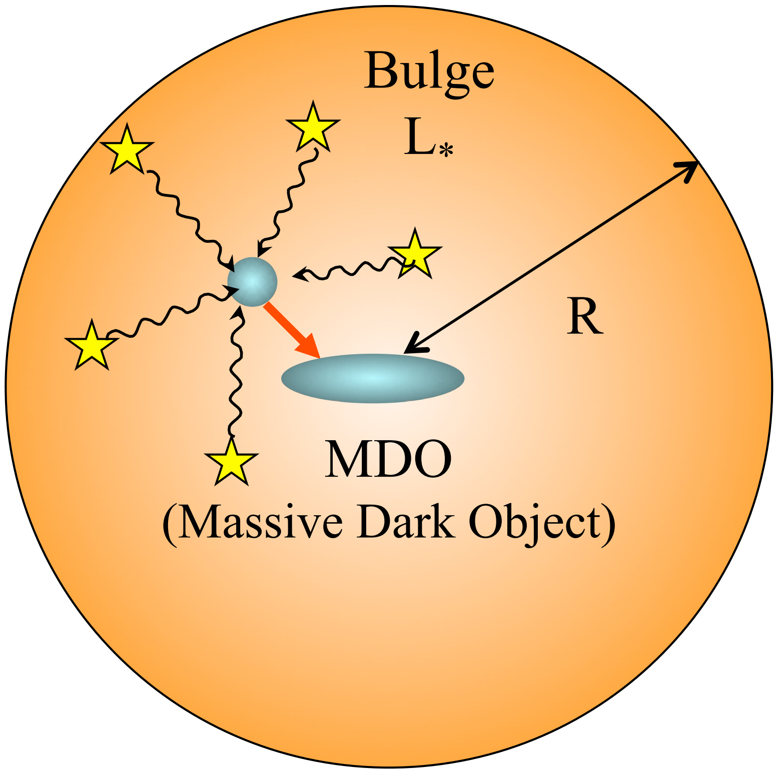


Angular Momentum Extraction

*Poynting-Robertson Effect*

$$\frac{d\ln J}{dt} \simeq -\frac{\chi E}{c} \simeq -\frac{\chi L_*}{c^2 R^2} = -\frac{L_*}{c^2 M_g}(1-e^{-\tau})$$

Mass Accretion Rate

$$\dot{M} \equiv -M_g \frac{d\ln J}{dt} \simeq \frac{L_*}{c^2}(1-e^{-\tau})$$

$$\frac{M_{\rm BH}}{M_{\rm bulge}} \simeq 0.14\varepsilon = 0.001$$

$\varepsilon = 0.007$ : Hydrogen burning energy conversion efficiency

by 岡本

# $M_{BH}$-$M_{bulge}$ relation w/o quasar mode feedback

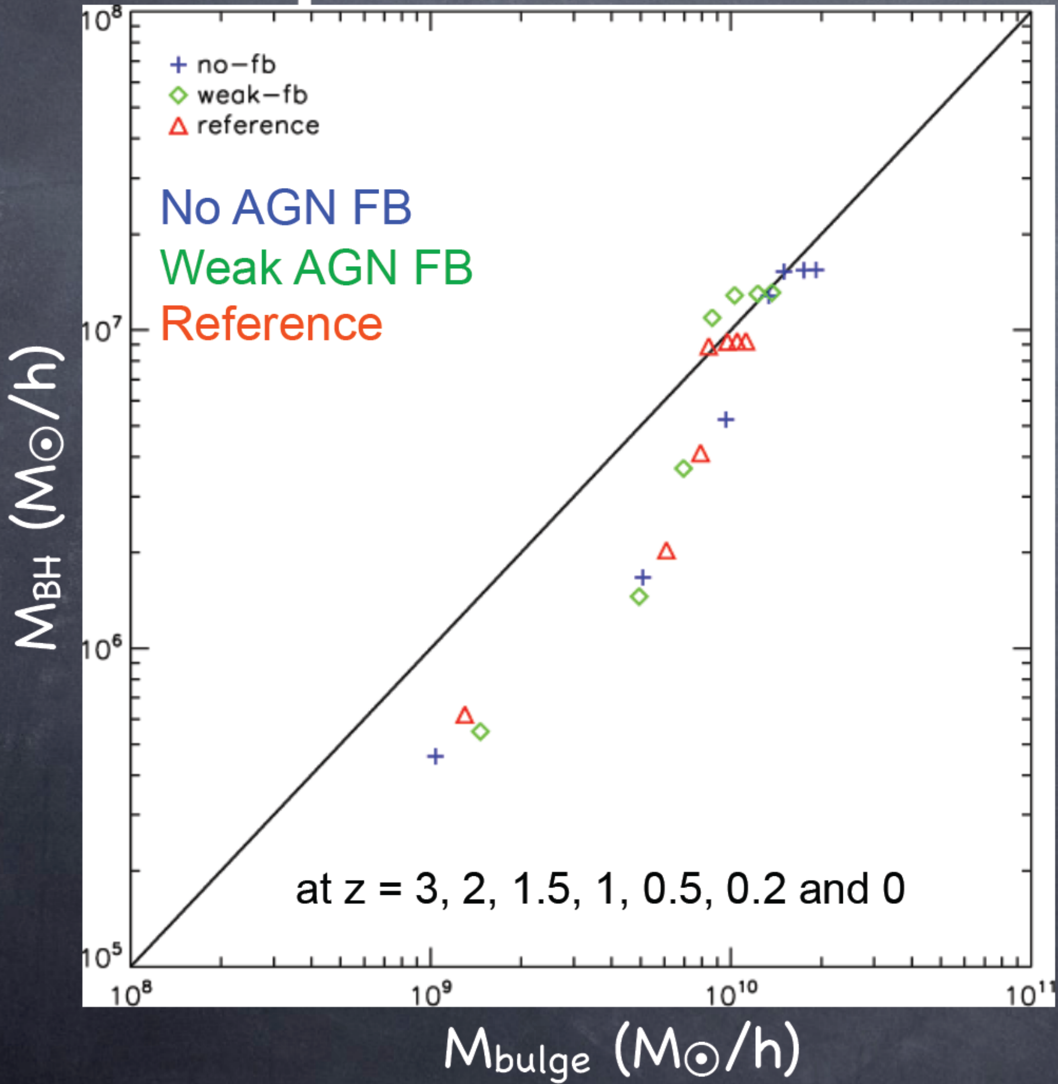


- Starburst phase で $\dot{M}_{\rm BH} \propto \dot{M}_{\rm bulge}$ となるようなプロセスが存在すれば（この場合は radiation drag）$M_{BH}$-$M_{bulge}$ 関係は quasar mode FB がなくても自然に成り立つ

Okamoto+'07

# Turbulent-Supported Obscuring Torus

Wada & Norman, 2002, ApJ, 566, L21

SN feedback による遮蔽トーラス形成と乱流粘性発生

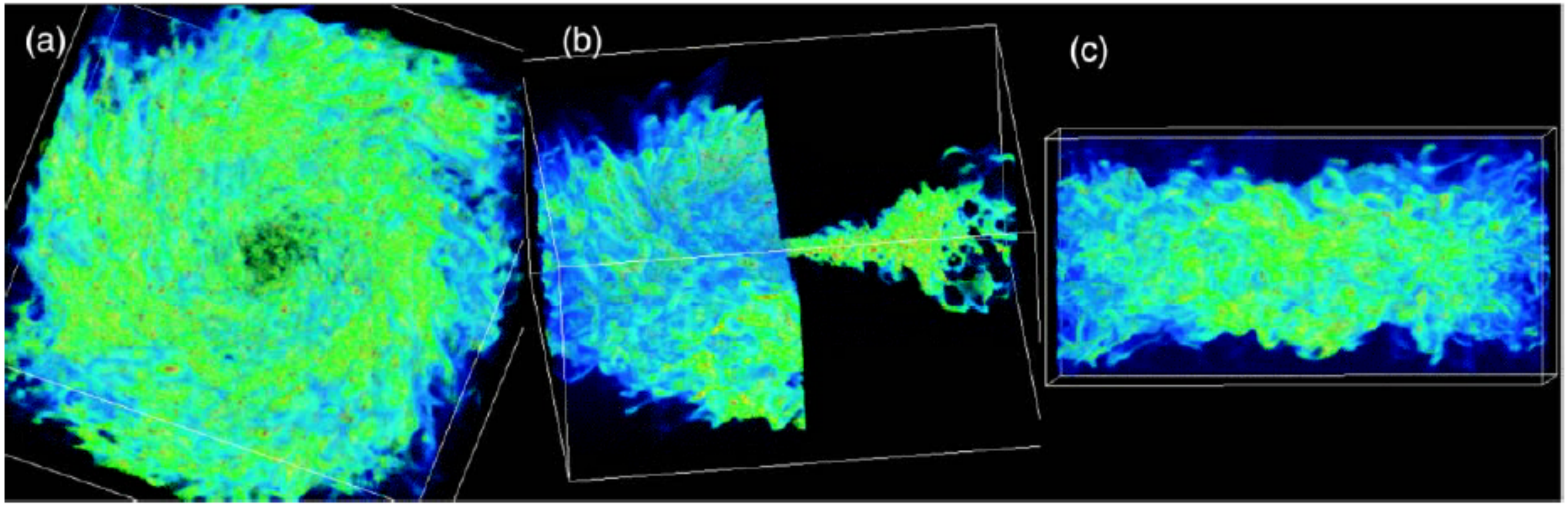


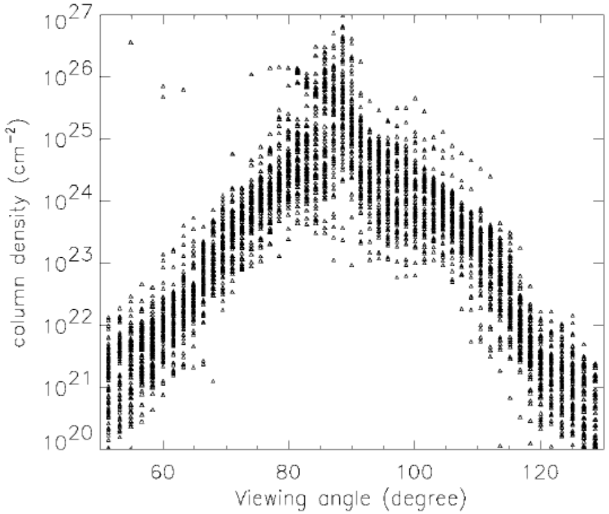


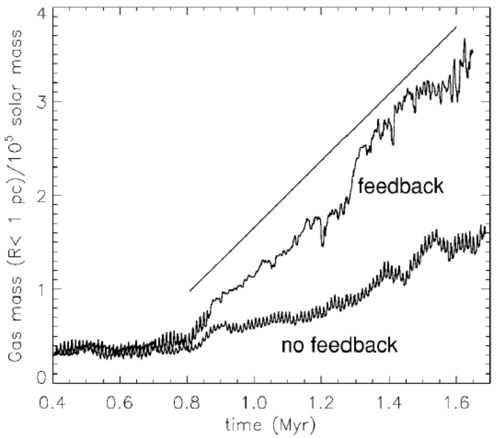


FIG. 3.—Time evolution of the gas mass inside $R < 1$ pc for two models (with and without energy feedback). Solid line represents the mass accretion rate 0.3 $M_\odot$ yr$^{-1}$.

# Coevolution of Supermassive Black Holes and Circumnuclear Disks

Kawakatu &Wada, 2008, ApJ, 681, 73

100pc → 1pc

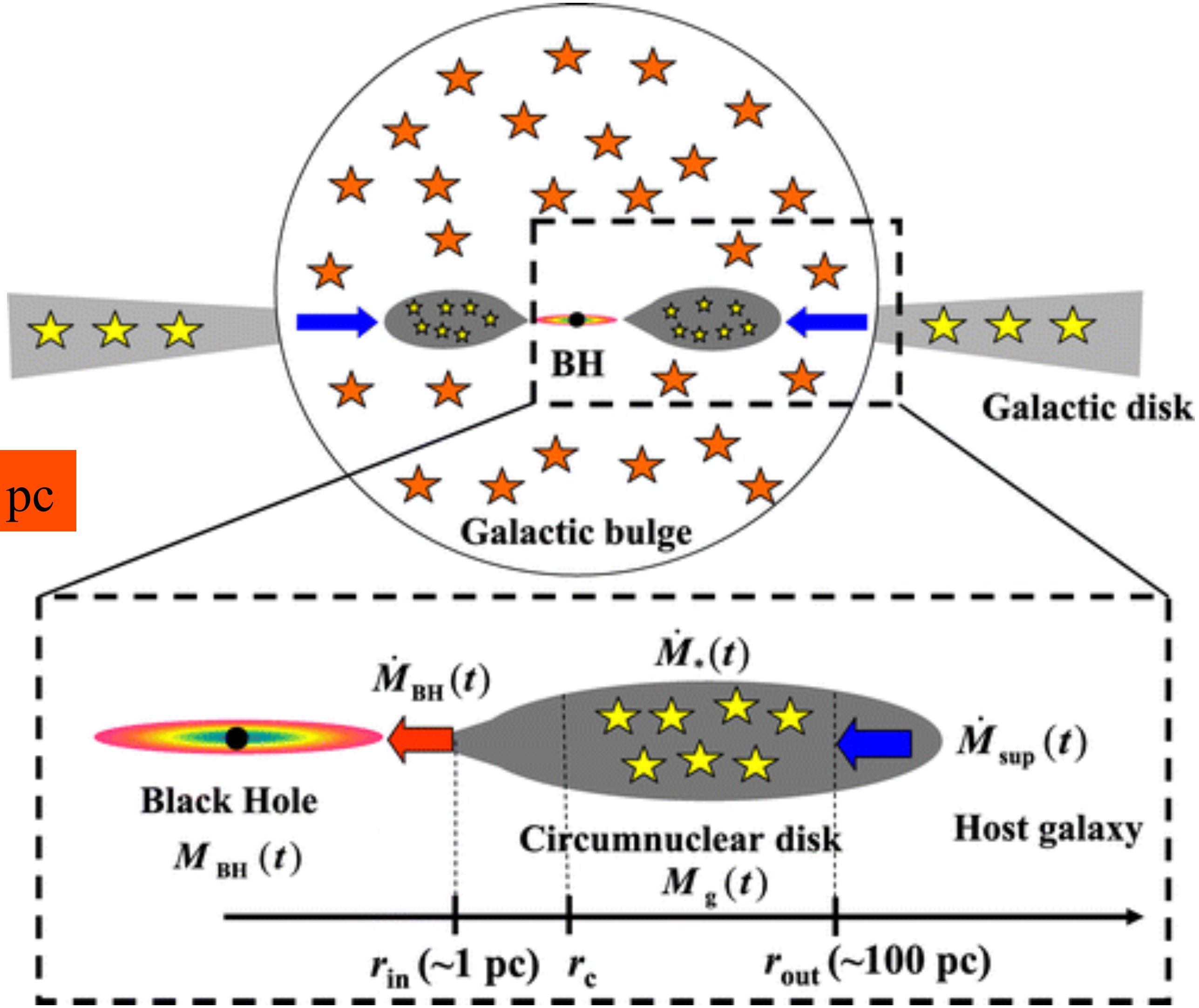


*SN-induced turbulence drives mass accretion*

# Rees Diagram (1984)

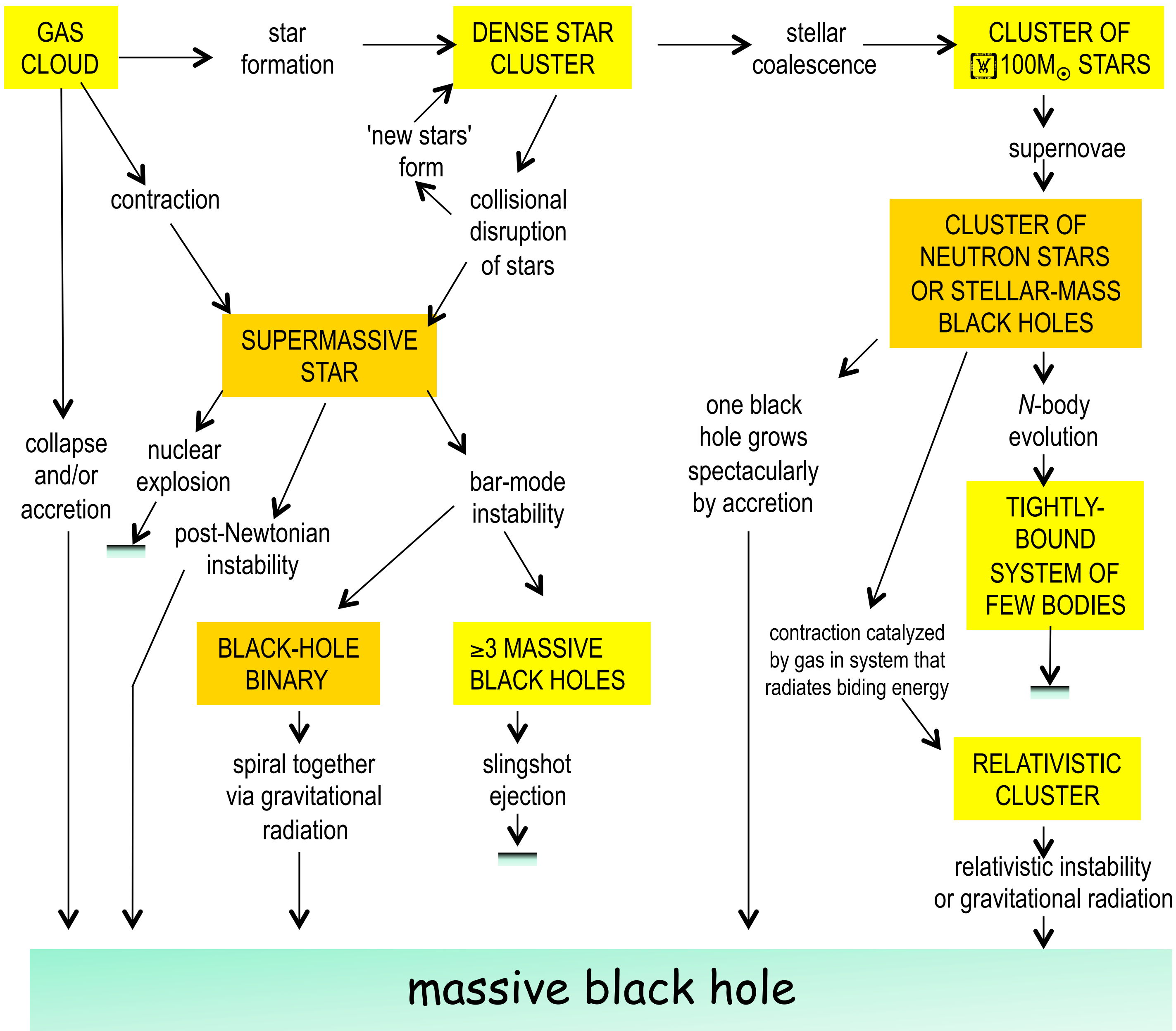

# Growth of Pop III BHs through Gas Accretion

Mass accretion rate is insufficient via radiative feedback
Pop III BHs cannot grow into niniquasars

Alvarez, Wise, Abel, 2009, ApJ 701, L133

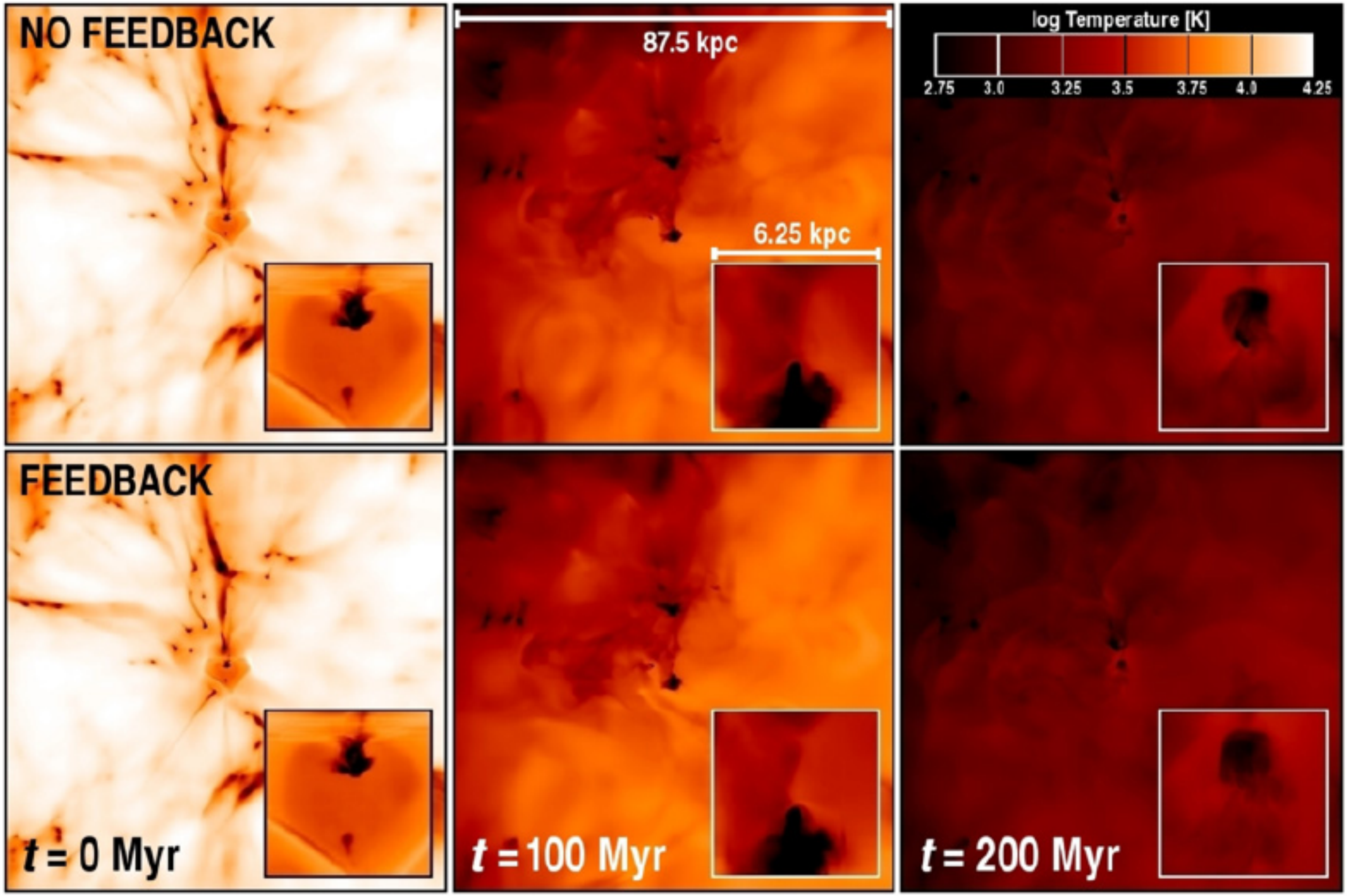

# Rapid (≈$10^5$yr) Formation of Subparsec Core of $10^8 M_\odot$ in Major Merger

N-body+SPH (GASOLINE) $10^5$-$10^6$particles

Mayer+10,
nature, 466, 1082

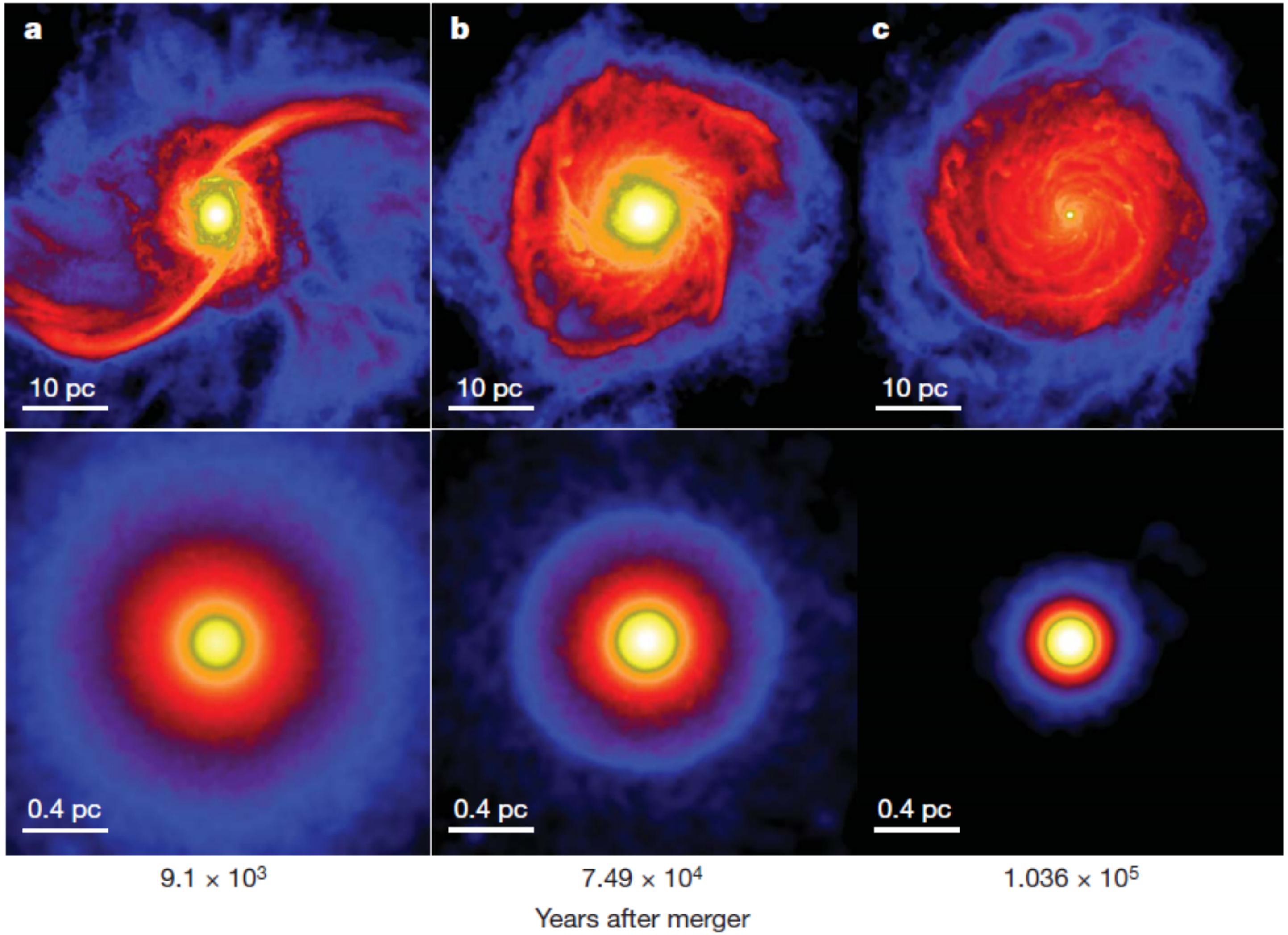

# Successive Merger of Multiple Massive Black Holes in a Primordial Galaxy

Tanikawa & Umemura 2010, ApJL submitted

## MBH 10体系のシミュレーション

Infall by dynamical friction

⇓

a binary MBH + an interacting BH

⇓

Binary hardening by slingshot
(three-body reaction)

⇓

Merger by gravitational wave
(4-6体が合体)

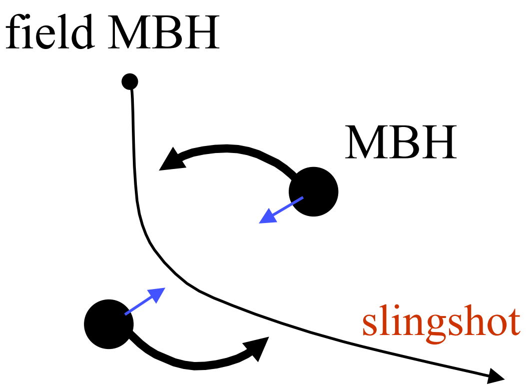


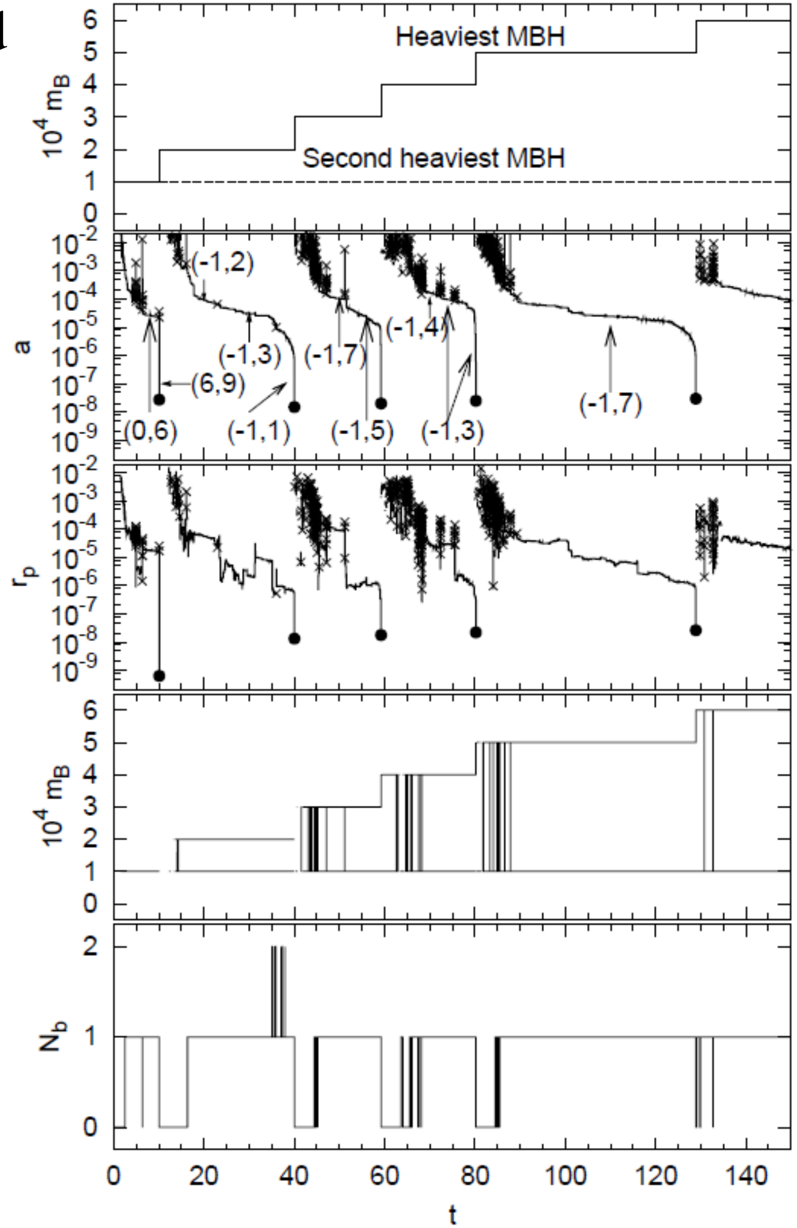

# Cosmological Rees Diagram

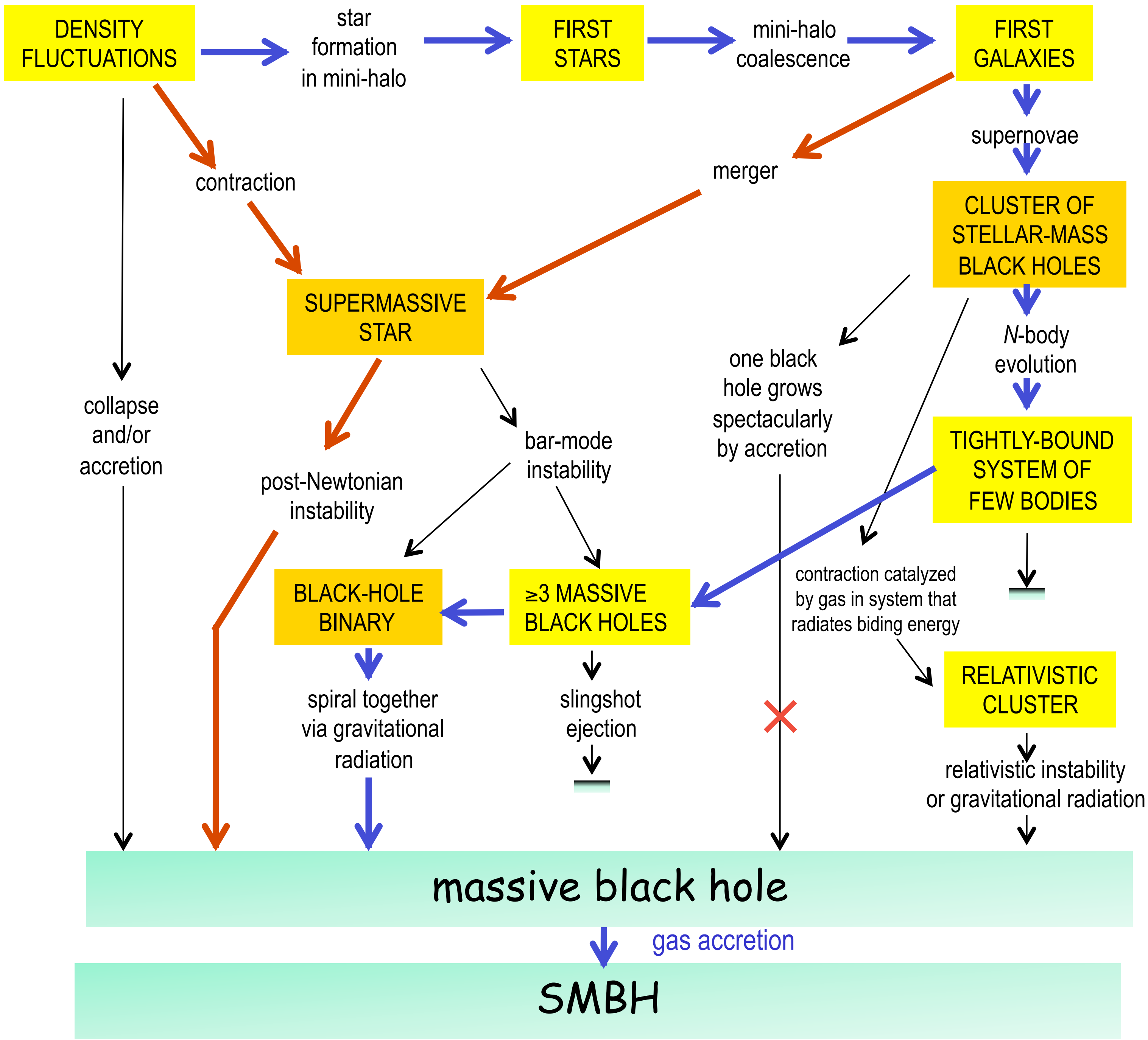

# CDM銀河形成論への挑戦

階層的銀河形成とSMBH形成とのconsistency

・銀河のbuilding block がMBHを持っているなら，原始銀河には複数のMBHがあるはず。

しかし，複数のAGN/MBHをもつ証拠は極めて少ない。

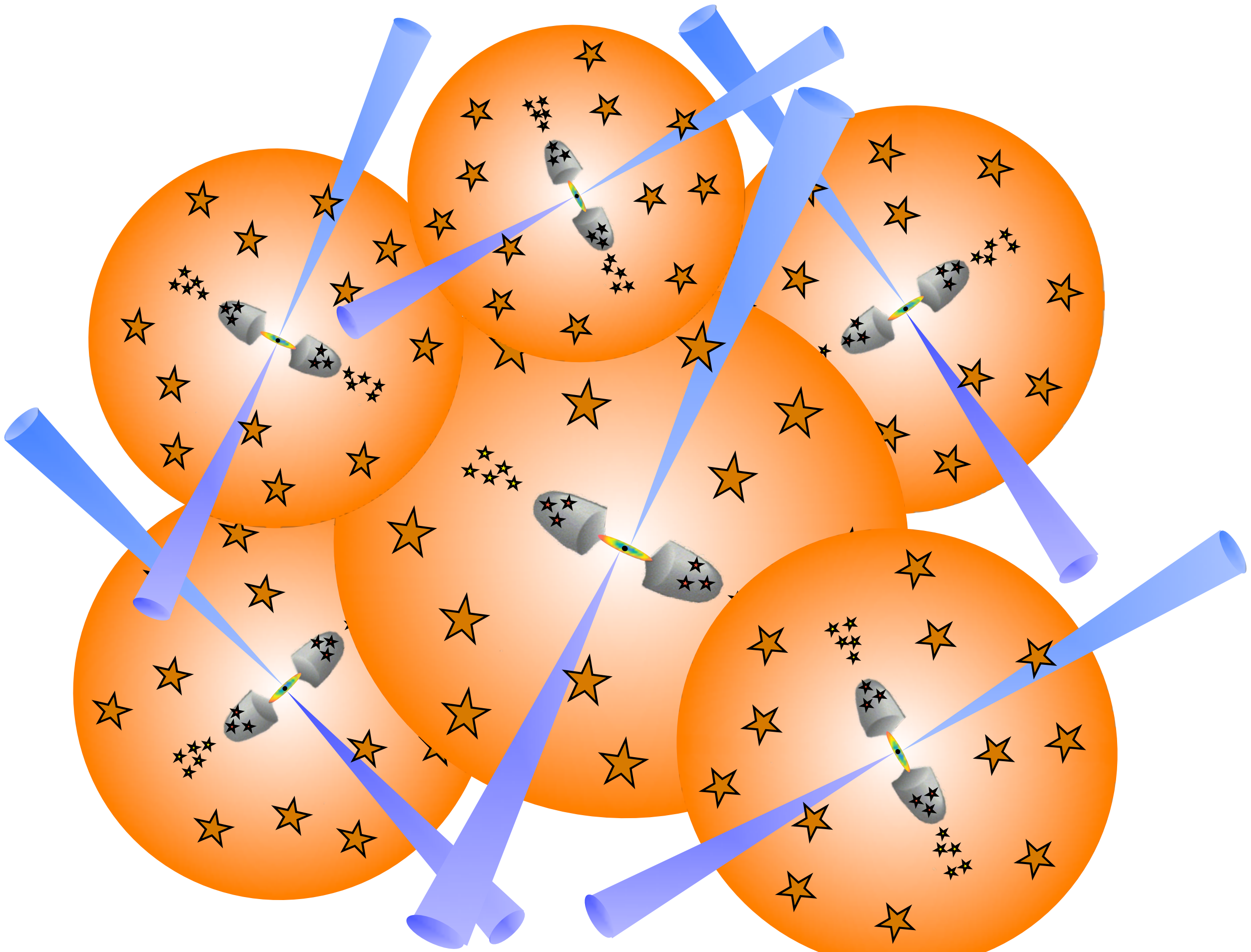

U: 銀河形成は物理になりましたか

H: まだちょっと早い